universität wien

MASTERARBEIT

Titel der Masterarbeit

„Isolation, oxidative folding and ion-channel modulation of plant cyclotides“

verfasst von

Martin Auer, BSc

angestrebter akademischer Grad

Master of Science (MSc)

Wien, 2013

Studienkennzahl lt. Studienblatt:	A 066 863
Studienrichtung lt. Studienblatt:	Masterstudium Biologische Chemie
Betreut von:	Ao. Univ. Prof. Dr. Hannes Todt

Acknowledgement

First of all I would like to thank Dr. Christian Gruber and Prof. Hannes Todt for supervising my thesis and for the possibility to conduct this work in their groups.

A special thank goes to Roland Hellinger and Johannes Köhbach, PhD students in Dr. Gruber's group, for help, advice and all explanations concerning the isolation and oxidative folding of cyclotides, and to Vaibhavkumar Gawali, PhD student in Prof. Todt's group, for the explanations and advice concerning the electrophysiology part of this work.

Furthermore I want to thank all the members of Dr. Gruber's research group for the friendly and motivating working atmosphere.

I also would like to thank my family for the valuable support and motivation.

Table of contents

List of Figures and Tables

List of Figures

List of Tables

Abbreviations

ACN	acetonitrile
AEP:	asparaginyl endopeptidase
APC	antibody presenting cell
ATP	adenosine triphosphate
BCE	before common era
BSA	bovine serum albumin
CCK:	cyclic cystine knot
cpm:	counts per minute
CTPP:	C-terminal propeptide
cO2	cycloviolacin O2
Da:	Daltons
ddH_2O:	double distilled water
DMEM:	Dulbecco´s Modified Eagle Medium
DMSO	dimethylsulfoxide
DTT	dithiothreitol
ER:	endoplasmic reticulum
EtOH:	ethanol
FBS:	fetal bovine serum
GSH	ox. glutathione
GSSG	red. glutathione
GFP:	green fluorescent protein

HEK:	human embryonic kidney 293 (cells)
HPLC	High performance liquid chromatography
kB1	kalata B1
Kv1.3	voltage gated potassium channel 1.3
MALDI-TOF/TOF:	Matrix Assisted Laser Desorption Ionization – Time of Flight
MeOH	methanol
MHC	major histocompatibility complex
MS:	mass spectrometry
N	peptide with native disulfides
NTPP:	N-terminal propeptide
NTR:	N-terminal repeat
PBS:	phosphate buffered saline
PDI:	protein disulfide isomerase
R	reduced peptide
TCR	T-cell receptor
TFA:	trifluoroacetic acid
TFE	trifluorethanol
TRP	tryptophan
VO	*Viola odorata*
0SS	reduced peptide without disulfide bonds
1SS	peptide containing one disulfide bond
2SS	peptide containing two disulfide bonds
3SS	peptide containing three disulfide bonds

1. Introduction

For over 2 millennia, humans utilized nature as a source for medicinal products. The earliest record dates back at around 2600 B.C. and it documented the use of plant-derived substances in Mesopotamia for the treatment of diseases (Newman and Cragg, 2013). Beside products from animals and microbes, plants are an important source of natural products. The World Health Organisation (WHO) estimated that 65% of the world population relies on plant derived medicines for their primary health care (Newman and Cragg, 2013).

Nowadays, a lot of the natural products are still in use for the treatment of several diseases. Scientists today try to discover and characterize the active compound(s) and mode of action of traditionally used medicinal plants (Koehn and Carter, 2005).

With the implementation of new techniques like high throughput screening (HTS) or combinatorial chemistry, the emphasis in the pharmaceutical industry shifted away from natural product discovery (Koehn and Carter, 2005). Researchers focused on small organic compounds in synthetic chemical libraries. Furthermore, research in molecular biology and cellular biology led to a higher amount of molecular targets and prompted shorter drug discovery timelines (Newman and Cragg, 2013).

Nevertheless, natural products still play a crucial role in drug discovery as one of the biggest resources of pharmacological lead compounds. This can be confirmed by the fact that the biggest part of New Chemical Entities (NCE) admitted every year to the pharmaceutical market still consists of natural products or derivatives therefrom, which is shown in Figure 1. (Newman and Cragg, 2007)

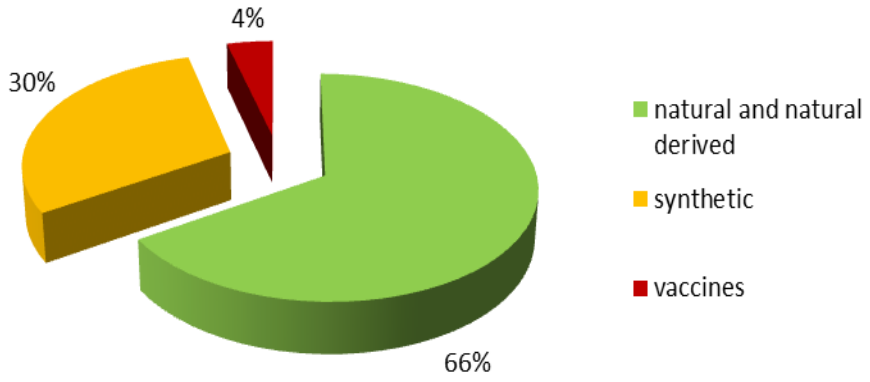

Fig.1: All new chemical entities from 1981 to 2006. As shown on this chart, 66% of all NCE admitted in the last 25 years are natural products or natural-derived products, 30% are produced by total synthesis and 4 % are vaccines (Newman and Cragg, 2007).

A special importance in the group of natural products plays bioactive natural peptides. Many natural peptides reveal different pharmacological effects, which makes them potential active compounds for pharmaceutical applications.

1.1 Bioactive peptides

Bioactive peptides are defined as peptides with hormone- or drug like activity that modulate physiological functions for example through binding to a specific receptor of a target cell surface. These peptides can for example be classified, according to their function, as antimicrobial, antithrombotic, antihypertensive, opioid, immunomodulatory, mineral binding and antioxidative (Sharma et al., 2012).

Bioactive peptides can be found in many, if not in all organisms. Large peptide sources are for example venoms from spiders, scorpions, snakes and marine animal's, in particular cone-snails (Vetter and Lewis, 2012). The venoms of cone-snails have been extensively studied in the past. The best known bioactive peptides from these venoms are the so called conotoxins (Vetter and Lewis, 2012). These are a group of peptides containing 10 to 30 amino acids and a high cysteine amount is characteristic for these toxins. The disulfide bridges between these cysteines are responsible for their structure and thereby for their activity. So far almost 100 conotoxins have been characterized and there are estimated 50,000 active peptides to be discovered (Gruber et al., 2010). Table 1 summarizes bioactive peptides and their activities from natural sources.

Table 1: Bioactive peptides from natural sources

Source	Peptide Class	Estimated Number of Peptides	Activity/Targets
Bacteria, plants, animals (invertebrates, vertebrates) humans	Anit-microbial peptides (AMPs), defensins	– [1]	Immunity, anti-microbial, insecticidal, antifungal, enzyme inhibitors
Animals/venom toxins	Bees, wasps and ants	Hundreds to thousands [2]	Haemolytic, anti-microbial, cytolytic, receptor/G-protein interface/receptomimetic (*e.g.*, mastoparan)
	Cone-snails, Conotoxins	50,000	Anti-pain (ion-channels, acetylcholine receptor), neurotensin R, entdothelin R, adreno R, 5-HT R, OT/AVP R, and many more
	Scorpions	100,000	Ion-channels, cytolytic
	Snakes	Many thousands	Neurotoxins; muscarinic-, □-adrenergic- and neurotensin R
	Spiders	1.5 – 16 million	Ion channels, cytolytic
Plants	Cyclotides	>19,000-59,000	Insecticidal, anti-HIV, cytotoxic, uterotonic, neurotensin R

[1]So far the number wasn´t determined, but because of the wide distribution and the high diversity, this group is one of the biggest. [2]Not many peptides have been characterized so far (Gruber et al., 2010).

Although the group of natural bioactive peptides is very large, only few have been released to the market and are available for pharmaceutical treatment. One of these approved drugs is ziconotide, a derivate of conopeptide MVIIA marketed under the name Prialt® and used as strong pain drug by blocking a calcium ion channel (Pope and Deer, 2013).

In addition to animal venoms as a rich source of bioactive peptides, plants are also a very important source for naturally- occurring peptides. As shown in Table 1, plants include 19,000 to 59,000 different active peptides which exist throughout the plant kingdom (Gruber et al., 2010). These peptides can divided into two groups, firstly the peptides in the extracellular space which play a crucial role in signalling and defence processes and secondly the peptides located inside the cell are associated with special physiological functions like development, growth and photosynthesis (Farrokhi et al., 2008).

Within the plant kingdom the group with the highest pharmaceutical potential is the so far less explored group of circular peptides, so-called cyclotides.

1.2 Cyclotides

Cyclotides, as mentioned above, are an abundant class of plant peptides containing a head-to-tail cyclic backbone and three highly conserved disulfide bonds, together known as cyclic cystine-knot (CCK) motif (Craik, 2011). The three disulfide bonds are formed as C_I-C_{IV}, C_{II}-C_V and C_{III}-C_{VI}. The disulfide bridges between $C_{I\text{-}IV}$ and $C_{II\text{-}V}$ build up the ring-shaped structure of the peptide, and the third disulfide-bond C_{III}-C_{VI} threads the ring (illustrated in Figure 2). Mainly two subfamilies of cyclotides have been described in the literature so far, Möbius and bracelet-type peptides. The classification depends on the presence or absence of a cis-Pro peptide bond in loop 5 (Figure 2). Möbius cyclotides contain a cis-proline residue in loop 5 that induces a local 180° twist in the peptide bond angle (Ireland et al., 2010). More than 70% of cyclotides are classified in the bracelet subfamily.

Cyclotides typically comprise about 28-31 amino acids in size, which leads to a typical mass range of 2500 – 4000 Da. The CCK motif confers them with remarkable stability. Compared to linear peptides they are stable against high temperatures and proteolytic degradation resulting in good oral bioactivity (Wong et al., 2012). Plant species from several families (Rubiaceae, Violaceae, Fabaceae, Solanaceae and Poaceae) express these peptides presumably for defence against insect pests, but they contain additional intrinsic bioactivities (Craik, 2011). Based on their stability and bioactivities, cyclotides are very interesting pharmaceutical templates with a significant potential as a scaffold for peptide-based drug design (Wang et al., 2009).

In Figure 2 representative cyclotide from Rubiaceae and Violaceae are illustrated. As mentioned above kalata B1 is a typical Möbius cyclotide and cycloviolacin O2 is a typical bracelet cyclotide.

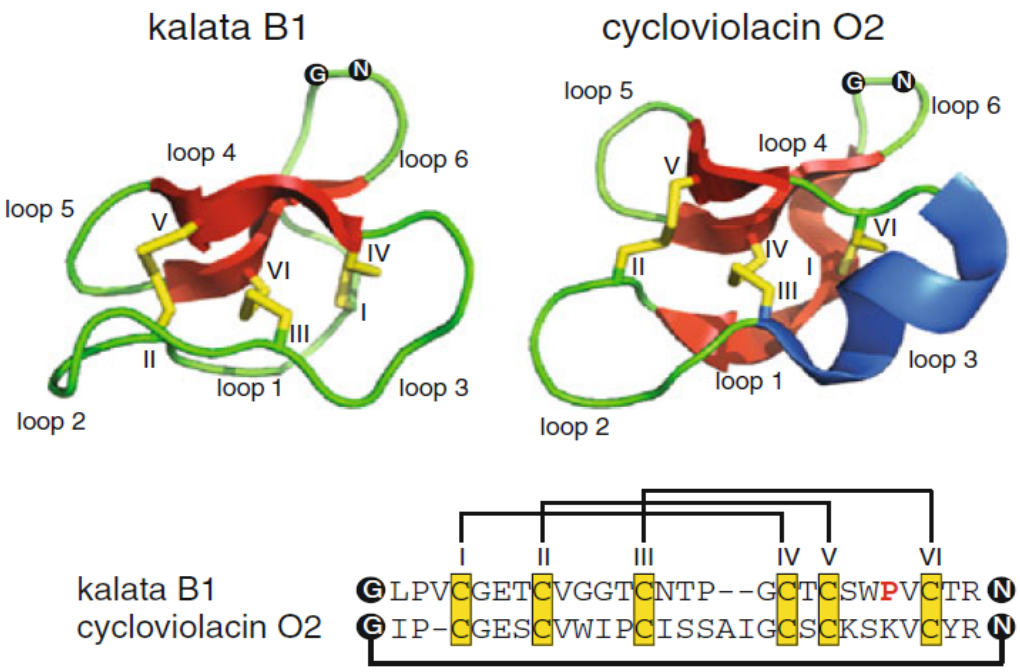

Fig.2.: Ribbon structure of the cyclotides kalata B1 and cycloviolacin O2. Kalata B1 belongs to the Möbius subfamily and can be found in the Rubiaceae plant *Oldenlandia affinis*. Cycloviolacin O2 belongs to the bracelet family and occurs in the Violaceae plant *Viola odorata*. The highly conserved disulfide bonds are marked in yellow and the cyclized backbone with black dots and a connecting line. Alpha helices are marked in blue and ß-sheets in red. The Figure was adapted from Hashempour et al. (2012).

1.2.1 Discovery of cyclotides

The discovery of cyclotides was based on ethnobotanical investigations of the Norwegian physician Lorents Gran in the 1970s (Gran, 1973). He was part of a Red Cross relief mission in the Republic of Congo and observed that indigenous woman used a tea from a plant called "kalata-kalata" to induce labour. Gran and his team identified the plant as *Oldenlandia affinis* and analysed this plant for its active uterotonic substances (Gran, 1973). Through his studies he identified the peptide kalata B1 as the active ingredient and hence he discovered the first cyclotide (Gerlach and Mondal, 2012).

However, it took until 1995 that researches determined the characteristic structure of kalata B1 and thereby initiated the interests in this new class of cyclic peptides (Saether et al., 1995).

So far, roughly 198 cyclotides have been discovered from 36 species in the Violaceae, Rubiaceae, Apocynaceae, Cucurbitaceae and Fabaceae plant families (Koehbach et al., 2013; Gerlach and Mondal, 2012). The missing phylogenetic link between Rubiaceae/Apocynaceae and Violaceae, suggest an independent evolution of cyclotides in different families (Gruber et al., 2008). The two major families which contain cyclotides are Rubiaceae and Violaceae.

While in every Violaceae species tested so far cyclotides were found, only 10% of tested Rubiaceae species contain cyclotides. Violaceae are family of flowering plants and comprises 23 genera and 800 species of cosmopolitan shrubs, herbs and rarely trees (Yance and Valentine, 1999). Furthermore, Violaceae plants are often used in the Traditional Chinese Medicine. Rubiaceae consist of 650 genera and 13,000 species and consist mostly of shrubs and small trees. It represents the fourth largest angiosperm family (Delprete et al., 2004). Rubiaceae can be found mostly in tropical and subtropical regions and is an important source of coffee, dyes and prescription medicines (Farnsworth, 1990). The distribution of cyclotides in Rubiaceae is compared to Violaceae more limited. But the amount of cyclotides in Rubiaceae remains still unclear, since only a small fraction of existing species have been analyzed for expression of cyclotides (Gruber et al., 2008; Gerlach and Mondal, 2012).

But also in other plant families for example Cucurbitaceae and Fabaceae, cyclotides can be found (Hernandez et al., 2000; Poth et al., 2011). Cucurbitaceae, also known as the melon and squash family, comprises 125 genera and 960 species. Some species are used in the Chinese folk medicine. So far two cyclotides were isolated from *Momordica cochinchinesnsis*, which inhibits trypsin activity (Felizmenio-Quimio et al., 2001). In the family of Fabaceae, the family of legumes and the third largest family of angiosperms, 24 novel cyclotides were found (Poth et al., 2011). The plant *Clitoria ternatea* is used in the traditional healing systems to treat gonorrhoea, induce vomiting and as an antidote to animal bites. (Fantz, 1991)

So far only a fraction of the existing plant species was screened for cyclotides. But the fact that many of these species are used in the traditional medicine and if it is predict that the pharmaceutical active substances are cyclotides, then the number of cyclotides exists in the nature could be much higher than expected, making cyclotides to one of the largest protein families in the plant kingdom (Gruber et al., 2008).

If cyclotides are used in the future as pharmaceuticals, it is necessary to synthesis these peptides *in vitro*. For these it is a crucial step to understand the biosynthesis and folding of cyclotides.

1.2.2 Biosynthesis and folding of cyclotides

The biosynthesis has been studied extensively over the past years. It is certain that all cyclotides are encoded by multigene families and are produced from larger precursor proteins. These precursors can include one or more cyclotide domains and are composed from an endoplasmic reticulum signal (ER), an N-terminal propeptide (NTPD) with 46-68 variable

residues, an N-terminal repeat region (NTR), the cyclotide domain(s) and a C-terminal pro-peptide (CTPP) tail which is essential for cyclization (Gunasekera et al., 2006). Each cyclotide domain has 28 to 37 residues and is separated by the NTR which contains 25 amino acids and is well conserved within genes from the same species (Gillon et al., 2008; Saska et al., 2007).

After the transcription of the protein precursor and the translation via ribosomes the disulfide bonds are formed in the ER. The forming of the disulfide bonds requires a redox system, which consists of the ferredoxin/thioredoxin system, the NADP/thioredoxin system and the gluthathione/glutaredoxin system (Gunasekera et al., 2006). Furthermore it was shown that an enzyme called protein-disulfide isomerase (PDI) plays a crucial role in the formation of the disulfide bonds (Gruber et al., 2006; Gruber et al., 2007). After finishing the formation, the cyclotides move from the ER to the Golgi where the forward through the secretory system and end up in a vacuole. During that movement the NTPD and the NTR are cleaved of by a so far unknown mechanism. The mechanism of cyclisation is yet not fully understood, but seems to be assured that an enzyme called asparaginyl endopeptidase (AEP) play an essential role (Saska et al., 2007). Because of the proteolytic activity as well as the transpeptidation activity of this enzyme it can excise the C-terminal pro-peptide tail and ligate the N- and the C-termini which are since the formation of the disulfide bonds in a close proximity.

For the cyclisation two high conserved amino acids are essential, the glycine (G) at position 1 which is important as a recognition site for the AEP and an asparagine (N) at the end of the cyclotide (Conlan et al., 2010). The AEP will bind to the asparagine followed by a nucleophilic attack from the amino group of the glycine, the cutting of the C-terminal pro-peptide and the ligation of the N and C- termini resulting in a new peptide bond (Figure 3) (Gunasekera et al., 2006; Gillon et al., 2008).

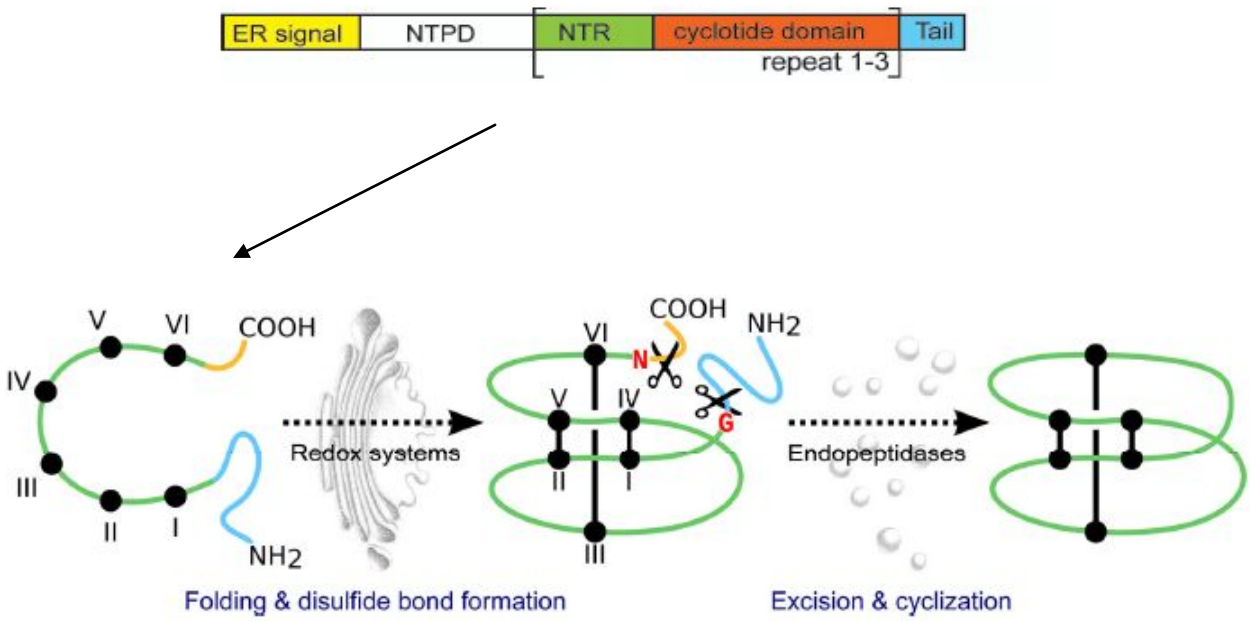

Fig.3: Summary of the biosynthesis of cyclotides in plants. The biosynthesis starts with the transcription of the precursor gene and the translation, followed by the formation of the disulfide bonds in the ER and the forwarding through the secretory system. After the cutting from the NTPD and the NTR by an unknown mechanism, the C-terminal pro peptide tail is cut off by the enzyme AEP which also catalyse the ligation of the C-terminus with the N-terminus (Qin et al., 2011 and Gunasekera et al., 2006).

One of the most important steps during the biosynthesis of cyclotides is the folding. The characteristic structure of cyclotides resulting from the disulfide bond formation and cyclization are essential for their bioactivity. Therefore it is of interest to understand the complex mechanism of cyclotide folding.

As mentioned above, folding of cyclotides in plants presumably requires an enzyme called protein disulfide isomerase (PDI) (Gruber et al., 2007). This enzyme increased the yield of correct folded kalata B1 at physiological pH significantly, compared to folding without the enzyme (Gruber et al., 2007). Different papers have been published about cyclotide folding so far and it was shown that the *in vitro* folding can be very efficient by using the optimal chemical conditions (Aboye et al., 2011; Gunasekera et al., 2009; Aboye et al., 2008; Wong et al., 2011). While the folding of Möbius cyclotides is far advanced, the folding of bracelet cyclotides remain still problematic and it is not possible to fold them with a satisfying yield. It was also shown that Möbius and bracelet cyclotides needs dramatically different folding conditions in vitro to fold in the native structure. This is based on different folding pathways of these two subfamilies because of the interaction of specific residues within the intercysteine loops 2 and 6 (Figure 4) (Aboye et al., 2011).

Also important for the cyclotide folding is the circumstance that in contrast to globular proteins which usually have their hydrophobic residues embedded within the core of the molecule, cyclotides have a large number of hydrophobic residues on their surface which has a major influence on the folding. That is why the addition of hydrophobic solvent to the folding puffers increased the yield of correct folded cyclotides (Aboye et al., 2011). Möbius cyclotides can be fold *in vitro* in aqueous buffer containing a hydrophobic solvent, for example isopropanol, which seems to stabilize the hydrophobic surface and redox agents, for example reduced glutathione. Bracelet cyclotides need complex folding conditions. The highest yield achieved for a bracelet cyclotide was almost 50% correct folded cycloviolacin O_2 (Aboye et al.,2011; Gunasekera et al., 2009; Aboye et al., 2008; Wong et al., 2011).

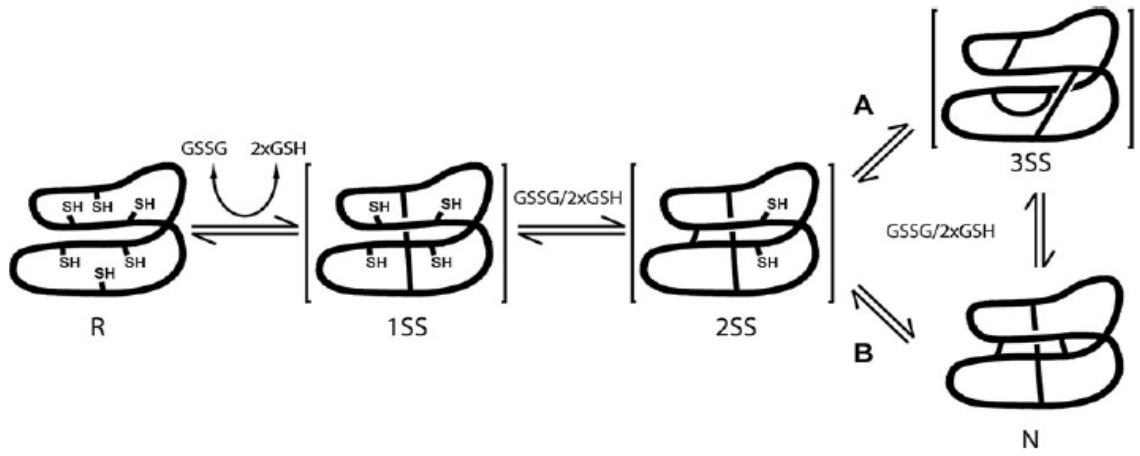

Fig.4: Folding pathways of cyclotides. In this figure two different folding pathways are shown. Fully reduced cyclotides fold over a 1 SS and 2 SS species to a 3 SS species. Depending on the folding buffer the cyclotide can fold via a nonnative 3SS species which can directly flip to the native one or directly after the 2SS species to the native 3 SS cyclotide. Möbius cyclotides favored pathway A, while bracelet use mostly pathway B (Aboye et al., 2011).

1.2.3 Bioactivity of cyclotides

Many bioactive peptides are limited in their use as pharmaceuticals because of their low stability and bioavailability under physiological conditions. The high stability in plasma and against gastrointestinal proteases, retained activity upon oral administration, the presence of hydrophobic patches on the surface and the several bioactivities makes cyclotides to ideal candidates for drug development studies (Daly et al., 2009). As allude above, cyclotides were discovered because of their uterotonic activity. In the last decade, many different bioactivities are reported such as, antitumor, anti-HIV and insecticidal to mention only few (Ireland, 2008; Jennings et al., 2005). In Figure 5 a summary of the different bioactivities of cyclotides are shown. Presumably the insecticidal activity is the main function of cyclotides in plants and

serves as a protection against pests (Jennings et al., 2005). For the majority of the different bioactivities, the mechanism-of-action is largely unknown. However it is evident that cyclotides can interact with membranes and form pores (Wang et al., 2012). While the mechanism behind the anti-HIV activity is unclear, the cytotoxic and antitumor activity of the cyclotide cycloviolacin O2 is well known. Cycloviolacin O2 causes rapid disruption of the lipid bilayers followed by leakage of the contents from whole cells (Gerlach and Mondal, 2012).

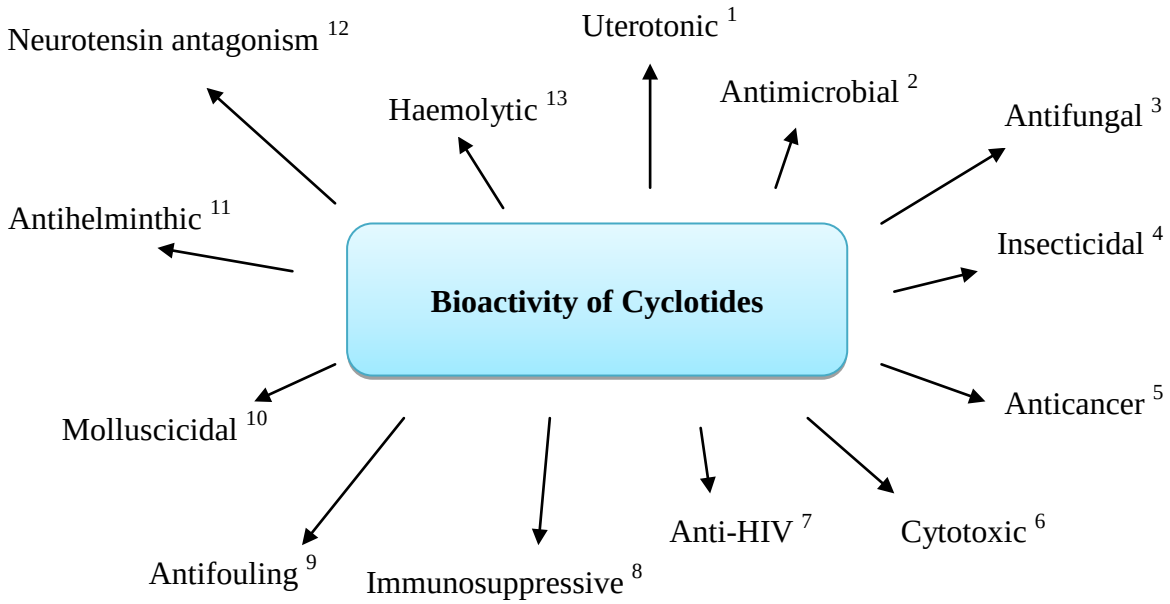

Fig.5: Bioactivity of cyclotides. [1](Gran, 1973), [2](Tam et al.,1999), [3](Tam et al.,1999), [4](Jennings et al., 2005), [5](Lindholm et al., 2002; Göransson et al.,2004 and Gerlach et al., 2010), [6](Gerlach and Mondal, 2012), [7](Ireland, 2008), [8](Gründemann et al., 2012), [9](Göransson et al., 2004), [10](Plan et al., 2008), [11](Colgrave et al., 2008), [12](Witherup et al., 1994), [13](Ireland, 2006).

In this thesis, I will place the focus on the immunosuppressive properties of cyclotides; hence this bioactivity is explained in the next chapter more precisely.

1.2.4 Immunosuppressive properties of cyclotides

The immune system of the human body is essential for surviving and for the defense against pathogens and tumor cells. To avoid self-recognition the immune system has some mechanisms which are continuously under surveillance. These mechanisms check the receptor of T-cells whether they have a low avidity to self-antigens (positive selection) or a high avidity to the body´s own cells (negative selection) (Wang et al., 2011). But in some cases the

immune system can overact against their own cells leading to autoimmune diseases such as multiple sclerosis and rheumatoid arthritis (RA). Around 5% of the population in Western countries develops an autoimmune disease during life, and these numbers are constantly increasing (Davidson and Diamond, 2011). There are many parameters involved in the development of an autoimmune disease like, gender, genetic background, environmental factors and malfunctioning lymphocyte development (Ermann and Fathman, 2001). One possible treatment for this malfunction is to reduce the activation or efficiency with immunosuppressive drugs like cyclosporine A, rapamycin or tacrolimus (Matsuda and Koyasu, 2000). Cyclosporine A is the treatment of choice by severe cases of autoimmune diseases as well as after organ transplantation to prevent allograft rejection. It is a non-ribosomal undecapeptide and was initially isolated from a fungus. Although it is widely-used, cyclosporine A has many and sometimes severe side effects (de Mattos et al., 2000). This lack of a safe and effective immunosuppressive treatment makes it necessary to develop new assured and safe immunosuppressive drugs (Gründemann et al., 2012).

On a molecular level, auto-reactive T-cells play an important role in disease development and progression, that is why many immunosuppressive drugs act on these cells (Yin et al., 2012).

T-cells or T lymphocytes are a special group of white blood cells, which plays a crucial role in the cell mediated immunity. Together with the B lymphocytes they build the acquired immunity. T-cells are formed in the bone marrow, followed by a migration to the thymes where they maturing. During the maturing in the thymes, which gives the cells the name, the lymphocytes are positively or negatively selected as described above and undergo gene rearrangement to determine a broad antigen receptor repertoire (Nemazee, 2006). Furthermore they build up MHC receptors on their surface. These receptors are known under the name T-cell-receptors (TCR) and distinguish the T-cells from other lymphocytes like B cells or natural killer cells (NK cells). In contrast to the antibodies, T cells can only recognize foreign substances when there antigen is presented via the MHC from an antigen presenting cell (APC) like dendritic cells or macrophages (Schütt and Bröker, 2009).

To trigger the appropriate immune response, T-cells are activated by the binding of the peptide presenting major histocompatibility complex (MHC) molecules on antigen presenting cells (APCs) to the appropriate T-cell receptor complex. Pathogenic antigens can act as co-stimuli and further enhance the signal. The T-cell activations triggered various signalling cascades which lead for example to the release of Ca^{2+} from the endoplasmic reticulum into the cytosol. In the activated T-cell the potassium channels IKCa and Kv1.3 play an important

role by regulating the membrane potential of the activated T-cell and to maintain Ca^{2+} influx during the activation period, which depends on a balanced intramolecular ion level and membrane potential (Feske et al., 2012; Oh-hora, 2009).

Two recent papers analysed the immunosuppressive properties of plant cyclotides in vivo. They reported that a mutant from the cyclotide kalata B1, where the threonine at position 20 is exchanged with a lysine (T20K mutant), shows significant immunosuppressive activity. While the exact mechanism remains still unknown the cyclotide [T20K]kalata B1 inhibit the activation and thereby the proliferation of human T-lymphocytes by decreasing the expression of interleukin 2 surfaces receptors and also the secretion rate of the interleukin 2 cytokine. Moreover the treatment also leads to a reduction of IFN-γ and TNF-α production (Gründemann et al., 2013), both very important cytokines. Although these findings throw more light in the mechanism behind the immunosuppressive activity of cyclotides, the exact target of this cyclotide on the T-cells persist unknown (Gründemann et al., 2012).

One potent target could be the voltage gated potassium channel Kv1.3 in T cells. This channel is known for longer time that it plays an important role in the activation of T cells and the inhibition of this channel leads to a suppression of the immune system (Chandy et al., 1984)

The connection between [T20K]kalata B1 and the Kv1.3 channel is given by a recent paper, which describe a peptide, isolated from the venom of the Mexican scorpion *Vaejovis mexicanus smithi* called Vm24. This peptide also showed anti-proliferative activity on T-lymphocytes by blocking the Kv1.3 channel of human T-lymphocytes with very high specificity and it has like the cyclotide [T20K]kalata B1conserved cysteines (Gurrola et al., 2012).

In a further *in silico* study from Anna Weizinger (Institute of Pharmacy, University of Vienna), she analyzed the ability of four different cyclotides, i.e. cycloviolacin O1, cO12, cO2 and kalata B7, to bind on bacterial sodium channels and it was shown that these cyclotides can in the model block the channels (unpublished data). Because the pore of potassium channels is a little bit smaller than the pore of sodium channels it is not possible to translate this result to potassium channels. Nevertheless this simulation suggests that cyclotides can basically bind on ion channels. In Figure 6 a crystal structure of the binding is shown.

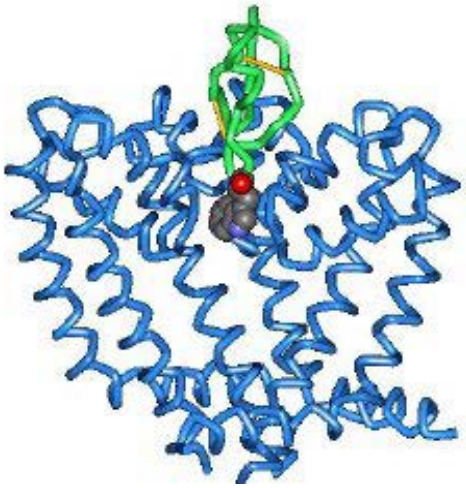

Fig.6: Cyclotide binding to sodium channels. In this crystal structure the pore of the bacterial sodium channel NavAb (blue) with the interaction of cycloviolacin O2 (green and the tryptophan is marked as spheres) is shown. In the model cyclotides can bind to ion channels (by courtesy of Weizinger Anna).

The determination if [T20K]kalata B1 can inhibit the human Kv1.3 channel is one aim of this thesis. To understand why ion channels are so important, a detailed description of ion channels is given in the following chapter.

1.3 Ion channels as targets for bioactive peptides

Ion channels are pore forming membrane proteins which allow charged particles, ions, to pass bio membranes. The transport is driven by the concentration gradient and the potential gradient. This passive transport is the major difference to the ion pumps, which pump ions against this gradient by using energy provided from ATP (Purves et al., 2004). Ion channels are located in the outer cell membrane as well as in membranes from cell organelles and are expressed in almost all living cells (Figure 7). During the sequencing of the human genome it was shown that it exist more than 400 putative ion channels in somatic cells (Bagal et al., 2012).

Ion channels are essential for the maintenance of the life essential functions. For example ion channels regulate the transport processes through bio membranes like the regulation of the acid- base balance or the osmotic activity (Purves et al., 2004). Furthermore they are essential for the maintenance of the resting membrane potential and generation of the action potentials in nerve and muscle cells. Approximately 1% of all humans gene encode for pore forming ion channels (Bagal et al., 2012).

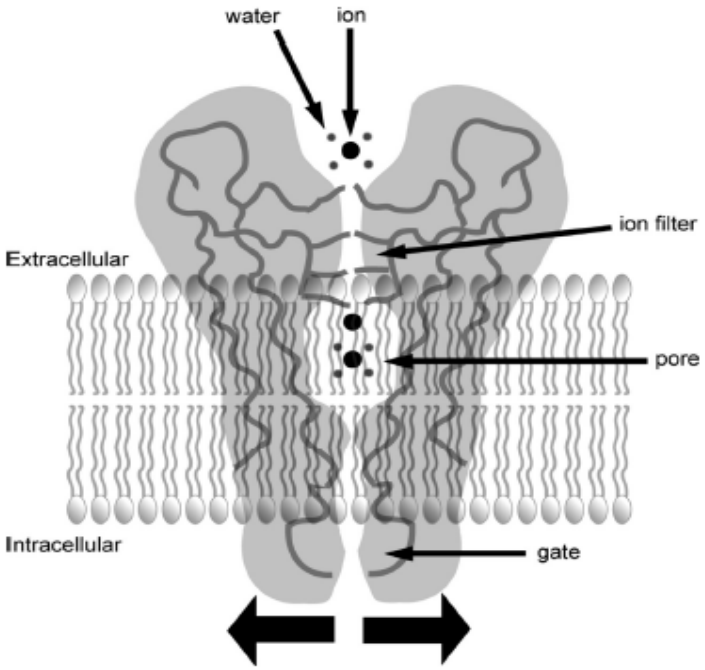

Fig.7: Basic structure of an ion channel. As it is shown in this figure, ion channels contain an extracellular part, intracellular part and a water filled pore region. Basically it is formed by several protein domains which vary enormously in sequence and topology. Depending of the channel, the pore region contains an ion filter which is highly sensitive for special ions (Bagal et al., 2012).

Ion channels can be very selective for certain types of ions as well as non-selective. One example for a non-selective channel is the TRP-channel (transient receptor potential channels) which has a similar selectivity for permeation of sodium, potassium and calcium ions. Selective channels are named by the ion which can pass through this channel. For example there are highly selective channels for positive charged ions like potassium, sodium, calcium and as well as for negative charged ions like chloride, nitrate and malate. Once the channel is open, the flux through the channel is a very rapid process. Thus up to almost 10^8 ions per second can permeate an ion channel (Purves et al., 2004).

There are three major mechanisms to regulate ion channels (see Figure 8). The first mechanism is the voltage gated ion channel. This type of channel is regulated by the membrane potential. For example, voltage dependent sodium channel in nerve cells or voltage dependent potassium channels (see also Section 1.3.2). The second type is the ligand-gated channel. In this type, a ligand binds extracellular or intracellular to the ion channel and that leads to a change of the conformation. An example for this type of channel is the acetylcholine receptor in nerve cells, which is essential for the forwarding of the action

potential between nerve cells or from nerve cells to muscle cells. And the third major type, which is not as abundant as the two mechanisms mentioned above, is the stress activated channel. This type of channel is activated as a response to an acute stress signal to the channel, for example a change in temperature (Purves et al., 2004).

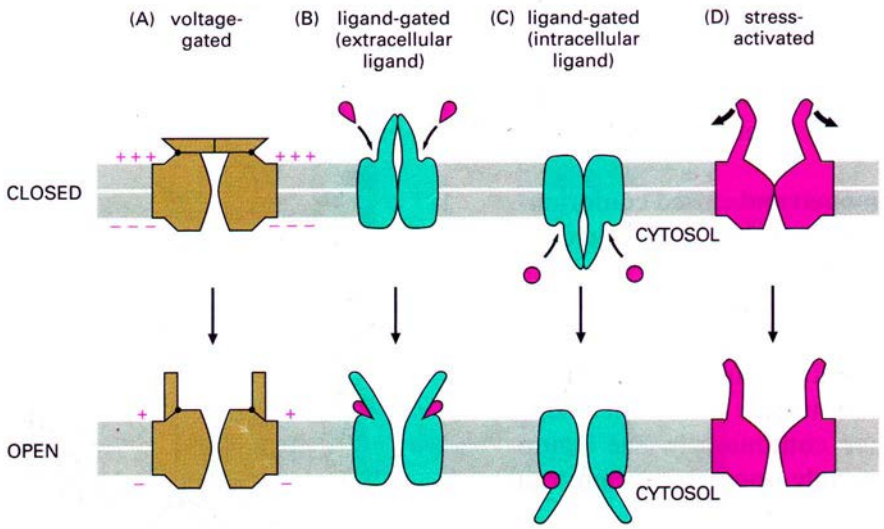

Fig.8: Gating of ion channels. In this figure the three major activation mechanisms of ion channels are shown. The first one is activated by a change in the action potential and therefore very important for the signalling pathway in nerve cells. The second type is a ligand – gated channel which is activated by the binding of a ligand, for example the acetylcholine receptor. The stress activated channel can be activated through a changing in the temperature or by applying pressure like pressure sensitive channels (Purves et al, 2004).

Because of the central functional role ion channels plays in human physiology it is obvious that deregulations of ion channels, caused for example by mutations in ion channels coding genes, leads to severe diseases. Therefore ion channels are an attractive therapeutic target.

1.3.1 Ion channels as therapeutic targets

As described previously, ion channels play an essential role in human physiology. Their function reaches from muscle regulation over cognition to the point of cell proliferation (Purves et al., 2004). Because of the crucial functional role and there localisation in the cell membrane as well as the widely distribution in the cell they are a highly potent class for drug discovery. So far more than 60 morbid changes in ion channels have been identified as human diseases linked to mutations in ion channels (see Table 2) (Bagal et al., 2012).

Table 2: Selected Ion channels caused diseases.

ion channel family	channel	G/L [1]	disease
K_{ir}	K_{ir} 1.1	L	Bartter´s syndrome
	K_{ir} 2.1	L	Andersen´s syndrome
	K_{ir} 6.2	L	congenital hyperinsulinism
		G	neonatal diabetes
	SUR2	L	dilated cardiomyopathy
K_v	K_v 1.1	L	episodic ataxia type 1
	KCNQ1	L	long QT syndrome
		G	short QT syndrome
	KCNQ2	L	benign neonatal febrile convulsions
	KCNQ4	L	nonsyndromic deafness
	hERG	L	long QT syndrome
		G	short QT syndrome
TRP	TRPP2		polycystic kidney disease
	TRPA1	G	familial episodic pain syndrome
	TRPC6	G	focal segmental glomerulosclerosis
CNG	CNGA1	L	retinitis pigmentosa
K_{Ca}	BK	G	epilepsy
Na_v	Na_v 1.1	G	epilepsy
		L	severe myoclonic epilepsy
	Na_v 1.5	G	long QT syndrome
	Na_v 1.6	L	cerebellar ataxia
	Na_v 1.7	G	erythromelalgia, paroxysmal extreme pain disorder
		L	congenital indifference to pain
	Na_v 2.1	G	benign familial neonatal seizures
Ca_v	Ca_v 1.2	G	timothy syndrome
	Ca_v 2.1	L	episodic ataxia type 2
glycine receptors	GLRA 1	L	stiff baby syndrome
GABA	$GABA_A$	L	juvenile myoclonic epilepsy
AChR	CHRNA4	L	autosomal dominant nocturnal frontal lobe epilepsy

[1]G/L: gain or loss of function (Bagal et al., 2012)

Unfortunately the big problem of ion channel as therapeutic targets is that so far only very few ion channels can be drugged successfully. Although alterations in ion channels are responsible for a great number of diseases, the majority of ion channel targeting drugs are approved only for a few diseases like cardiac, neurophysiology disorders and as local anesthetic drugs. Furthermore, in the last 10 years only very few novel drugs were approved, this is a likely consequence of clinical failures due to efficacy and safety issues and the

apparent difficulty in identifying clinical candidate across the ion channel family (Bagal et al., 2012). Because of this reasons there is a shortage of drugs modulating ion channels activity.

Therefore it is remarkable that in the last year assays, in which ligands can be screened against a wide range of ion channels, became available (Bagal et al., 2012). Furthermore the advanced progress in structural biology, which includes the ability to assemble crystal structures from the bound ligand on an ion channel, leads to a better understanding of the ligand binding process and hence ligand based drug development (Camerino et al., 2007). Accordingly, now is an exciting time for ion channel research and the next decade will bring significant changes in the ability to design safe and selective ion channel targeting drugs (Bagal et al., 2012).

Besides the discovery of classical organic molecules as drugs for ion channel related disorders, the venoms from a large number of animals such as snakes, scorpions, spiders, insects or sea-dwelling animals are a rich source of ion channel modulators (Camerino et al., 2007). The venoms are a mixture of toxic peptides and are produced for immobilization of prey as well as for the defense against predators (Bagal et al., 2012). Peptides toxins from this venoms act often as very selective and specific ion channel blockers on voltage regulated sodium, potassium and calcium channels as well as a few ligand gated ion channels (Camerino et al., 2007). A selection from some of these peptides is listed in Table 3.

Table 3: Some common ion channel targeting peptides, isolated from animal venoms

Peptide	Target channel	Source
Dendrotoxins [1]	Kv	Mamba snakes
Kaliotoxin [2]	Kv 1.3 and K_{Ca}	Scorpion Androctonus mauretanicus mauretanicus
Hongotoxin [3]	Kv 1	Central American Scorpion, Centruroides limbatus
Margatoxin [4]	Kv 1.3	Central American Bark, Scorpion *Centruroides margaritatus*
Conotoxin [5]	K; Na_v; Ca_v	Cone snail
Iberiotoxin [6]	K_{Ca}	Eastern Indian red scorpion, *Buthus tamulus*
Hetoropodatoxin [7]	Kv 4.2	giant crab spider, *Heteropoda venatoria*

References: [1](Katoh et al., 2000); [2](Korukottu et al., 2008); [3](Pragl et al., 2002); [4](Garcia-Calvo et al., 1993); [5](Terlau and Olivera 2004); [6](Galvez et al., 1990); [7](Sanguinetti et al., 1997)

The voltage gated potassium channels, which are the major group within ion channels, are an important pharmacological target for several disorders, like diabetes, ataxia, neurological abnormalities, epilepsy and autoimmune diseases (Choi B. H., 2010; Chandy et al., 2004; Camerino et al., 2007).

Voltage gated potassium channel are expressed in excitable cells like cardiac myocytes or nerve cells where they are crucial for the action potential as well as nonexcitable cells where they are thought to regulate hormone secretion. After opening of the channel by membrane depolarization, potassium will exit the cell because of the high concentration of potassium ions inside the cell compared to outside of the cell and thereby they repolarize the cell potential (Coghlan et al., 2001). The voltage gated potassium channels can divided into eight gene families, KCNA (Kv 1.1-8), KCNB (Kv 2.1-2), KCNC (Kv 3.1-4), KCND (Kv 4.1-3), KCNF (Kv 5.1), KCNG (Kv 6.1-4), KCNS (Kv 9.1-3), KCNV (Kv 8.1-3) (Camerino et al., 2007).

Many small molecules that are able to block voltage gated potassium channels are not selective or specific enough; therefore peptide toxins with a high selectivity and specificity (shown in Table 3) are very important for the determination of structure and function of these channels (Coghlan et al., 2001) and represent a novel class of molecules as potential drug leads.

In this thesis I will focus on analysis of naturally-occurring immunosuppressive plant peptides as modulators of the voltage gated Kv1.3, since many papers described the role of this channel in the T-cell activation and hence his role in autoimmune diseases (Cahalan et al., 2001; Chandy et al., 2004).

1.3.2 Potassium channel Kv1.3, its immunosuppressive properties and role in T-cell physiology

The Kv1.3 is a voltage depended potassium channel which is assembled of four identical subunits. Each subunit contains a hydrophobic core and six TM segments (S1-S6), a P-loop is located between the S5 and S6 and long hydrophilic N- and C- termini are prolonged into the cytoplasm (Calahan et al., 2001) (Figure 9).

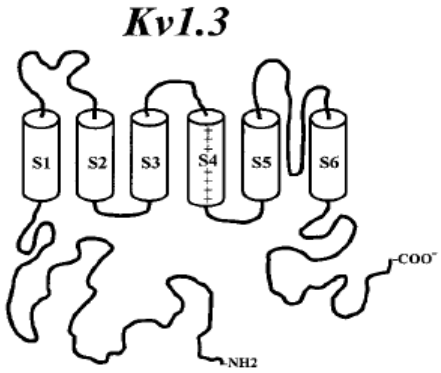

Fig.9: Structure of a Kv1.3 subunit. Kv1.3 consist of four identical subunits (S1- S6). Between S5 and S6 is a P-loop located and the long N- and C-termini are extended into the cytoplasm (Calahan et al., 2001).

As mentioned above, Kv1.3 is a voltage dependent ion channel, i.e a change in transmembrane voltage is required for opening and closing. It is reported that seven repeats of the motiv Arg-X-X-Arg, located on the S4, as well as residues in S2 and S3 are forming the voltage sensor of the channel. A change in the membrane potential leads to a movement of the charged residues in S4 and that leads to a conformational change of the channel including the opening of the gate (Calahan et al., 2001).

Previous studies indentified that Kv1.3 plays a major role in the activation of T lymphocytes and hence this channel is essential for a correct immune response (Chandy et al., 2004). To start a immune reaction, the T- and B-cells first have to migrate into the tissue, recognize a antigen, which is presented by an APC, produce and secrete signaling peptides like chemokines and antibodies, proliferation and differentiation. Some of these activities are controlled by Ca^{2+} signaling and the Kv1.3 plays a crucial role in the activation of Ca^{2+} channels, Ca^{2+} singaling and therefore in the activation of T-cells (Calahan et al., 2001).

After the activation event (see also 1.2.4), tyrosine kinases and phospholipase C (PLC) is being activated, which leads to the generation of inositol (1,4,5)-trisphosphate (IP_3). IP_3 triggers the release of Ca^{2+} from internal stores as well as the activation of the protein kinase C (PKC). The reduction of the internal Ca^{2+} stores leads to the activation of the Ca^{2+} release-activated Ca^{2+} channel (CRAC), which open through the activation and increased thereby the amount of Ca^{2+} in the cytosol. This Ca^{2+} and the PKC-dependent singaling pathways are necessary for the cell proliferation.

Kv1.3 and IKCa1 channels regulate the Ca^{2+} signaling by regulating the membrane potential (Chandy et al., 2004). Membrane hyperpolarization caused by the opening of Kv1.3 channels in response to membrane depolarization and the opening of IKCa1 channels through the

increased amount of Ca^{2+} in the cytosol are the driving force for Ca^{2+} entry by CRAC (Cahalan et al., 2001; Koo et al., 1997) . That is why a blockade of these potassium channels leads to a membrane depolarisation and thereby to the inhibition if Ca^{2+} influx which cause a inhibition of cytokine production as well as cell proliferation (Chandy et al., 1984). The role of Kv1.3 in the T-cell signaling cascade is summarized in Figure 10.

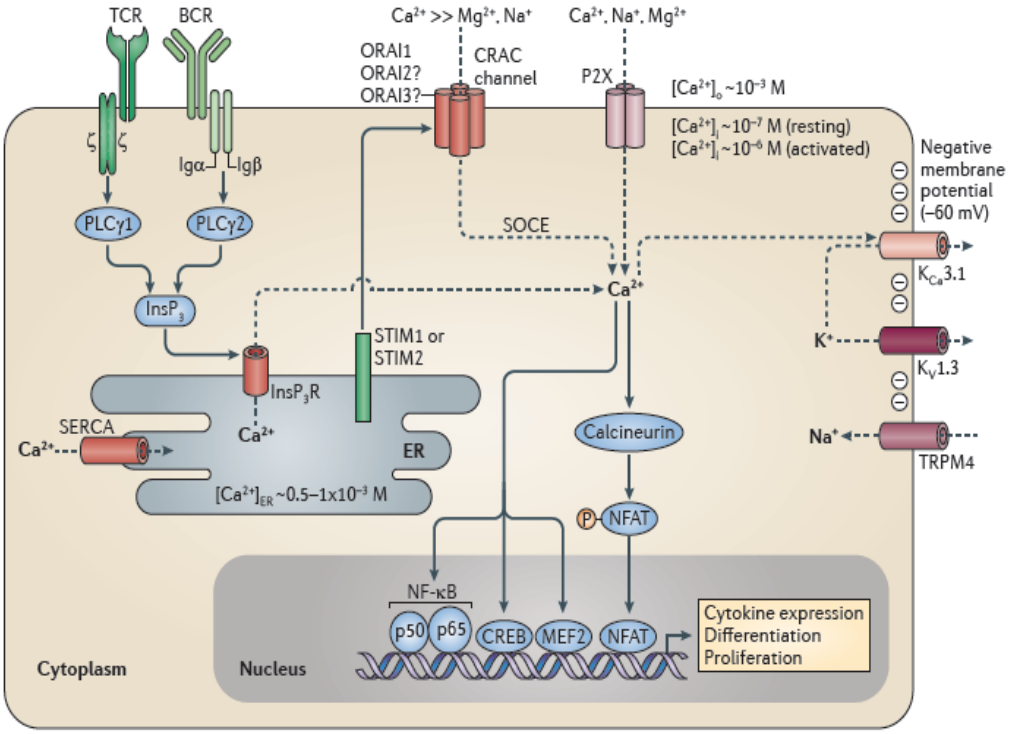

Fig.10: Ion channels regulating the activation of lymphocytes. Through the binding of the antigen to the T cell receptors (TCRs) the Ca^{2+} release-activated Ca^{2+} (CRAC) channels are activated. This is mediated through the activation of phospholipase Cy (PLCy), the production of inositol -1,4,5-trisphosphate ($InsP_3$) and the release of Ca^{2+} from endoplasmic reticulum (ER) Ca^{2+} stores. The following activation of stromal interacton molecule 1 (STIM1) and STIM2 results in the opening of ORAI1 CRAC channels and store-operated Ca^{2+} entry (SOCE). The Ca^{2+} influx through the CRAC channels leads to the activation of Ca^{2+} -dependent enzymes and transcription factors, like calcineurin and nuclear factor of activated T cells (NFAT). The Ca^{2+} influx in T-cells from outside depends on the gradient between the extracellular Ca^{2+} concentration and the intracellular Ca^{2+} concentration as well as on an electrical gradient established by two K^+ channels, Kv1.3 and $K_{Ca}3.1$ (Feske et al., 2012)

The expression of Kv1.3 and IKCa1 channels in T-cells is different and depends on the state of activation and differentiation. The number of Kv1.3 channels in resting T-cells is ~400 channels per cell. After activation the number increaseas very slightly to ~600 channels whereas the number of IKCa1 increase from 8 to 500 during activation. In resting T-cells, Kv1.3 is the dominant channel but during activation the channel phenotype changes, leading to the activation state in which the IKCa1 is the dominant channel. Hence a selective Kv1.3 blockade prevents activation without affecting preactivated cells. These cells can be inhibited by selevtice IKCa1 blockers (Pardo, 2004).

It is evident why Kv1.3 is very important for the activation of T-cells, thus we are interested to measure the interaction of potent immunosuppressive peptides with the Kv1.3. Therefore we utilize a method called patch chlamp technique which allows to study the modulation of single or multiple ion channels in cell's upon adminitration of, for example, cyclotides.

1.3.3 Analysis of ion channels via patch clamp technique

The patch clamp technique, allows the study of single and multiple ion channels in a wide spectrum of cells, especially excitable cells like neurons and cardiomyocytes. It was developed by Neher and Sakmann, two german physiologists, in the late 1970s (Neher and Sakmann, 1978). For this work they were awarded the Nobel Prize of Physiology and Medicine in 1991.

The principle of the measurements is to isolate a membrane patch from the cell and measure the current which flows through this patch. Therefore, a patch pipette is filled with the appropriate solution and the pipette is attached to on the electrode holder which is mounted on a micromanipulator. Afterwards the pipette is moved to the cell and pressed gently on the cell surface. Through applying suction, a connection between the membrane and the pipette is formed, the so called Gigaseal. At this point several configurations of the patch clamp technique are possible (Figure 11). These configurations are the whole-cell, outside-out and inside-out configuration. For the inside out recording, the pipette contains the extracellular solution whereas for the whole-cell and the outside-out recordings intracellular solution is used in the pipettes.

I used for my measurements the whole-cell method. The whole cell method is performed by opening the membrane which is patched by the pipette by applying strong suction and thereby establishing a contact between the cell interior and the internal solution of the pipette (Ogden and Stanfield 1994; Rycroft et al., 2006).

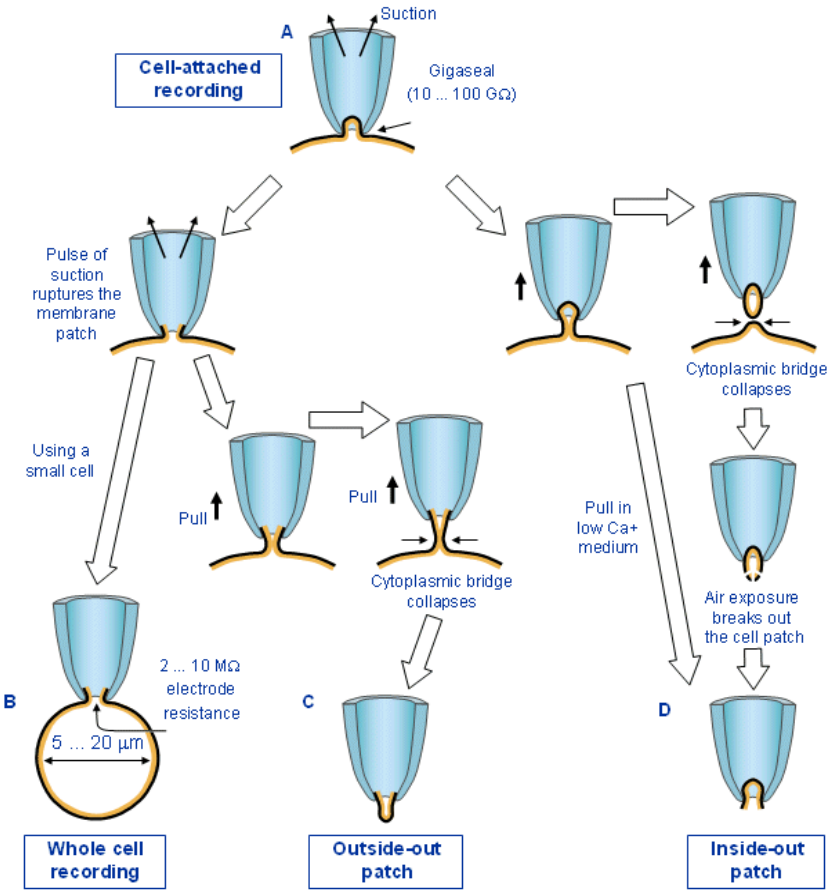

Fig.11: Diagram of four different patch clamp techniques. (a) Cell attached recording by formation of the gigaseal. (b) Gigaseal formation, followed by the application of strong suction to open the cell and achieve the whole cell mode. (c) For the outside-out technique the pipette has to withdraw a little bit after opening of the cell and for the inside-out measurements (d), the pipette has to pull out after attaching the cell (Malmivuo and Plonsey 1995).

The most important element in the patch clamp set up is the headstage with the feedback amplifier, which controls the membrane potential and can hold the potential on a steady level. This amplifier is a current to voltage converter and receive two inputs, one positive input from a certain potential whitch is set by the experimenter (V_{ref}) and one negative input from the pipette potential (V_p). If the voltage of these two inputs is not equal, then current will flow into the electrode. If there is a difference between the inputs, then the amplifier compensate that by passing current across the feedback resistor (R_f) that brings the cell content to the reference potential. This current from the amplifier is equal and opposite to the current which is produced from ions by crossing the membrane and represents the readout of the experiment (Rycroft et al., 2006).

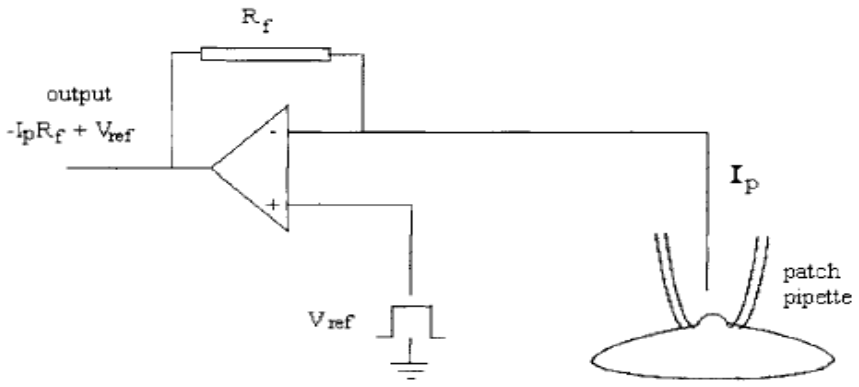

Fig.12: Illustration of the headstage current from the voltage amplifier. V_{ref} is the reference potential which is set by the experimenter. V_p is the pipette potential. R_f is the feedback resistor and I_p the current which flows through the pipette (Rycroft et al., 2006).

2. Aims of this study

Previously it was shown by our laboratory that certain cyclotides exhibit anti-proliferation activity on primary activated human T lymphocytes, but their mechanism of action and the target are still unknown (Gründemann et al., 2012, 2013). Similarly a recently identified scorpion peptide toxin showed also anti-proliferative activity on lymphocytes by blocking the Kv1.3 channel of human lymphocytes with very high specificity (Gurrola et al., 2012). It is also known that the Kv1.3 channel plays a crucial role in the activation of the T-cells and thereby it is a potential target for immunosuppressive drugs.

Therefore my main aim is to test cyclotides that contain similar 3D-fold to the scorpion venom peptide for the interaction with Kv1.3 channel of human lymphocytes. These measurements will be done by electrophysiological patch clamp analysis, which allows the study of multiple ion channels by measuring the changes from the membrane voltage. Our model will be purified human T-lymphocytes as well as tsA-201 cells which express the human Kv1.3 channel through transfection.

Since the availability of the cyclotides is limited and dependent the extraction from native plant material, the development of efficient strategies for chemical synthesis of cyclotides will be important if cyclotides ought to be used as pharmaceuticals in the future. In particular it is necessary that synthetic cyclotides are able to adopt their native disulfide conformation. Therefore my second aim is to optimize the synthetic yield of correctly-folded cyclotides under different oxidative-folding conditions. The progress in the folding process will be monitored and characterized by RP-HPLC and MALDI-TOF mass spectrometry.

3. Materials

- Dichloromethane (Roth)
- Methanol (Roth)
- ddH_2O
- DCM (Roth)
- TFA (Roth)
- Acetonitrile (Roth)
- a-Cyano-4-hydroxycinamicacid (Fluka analytics)
- C_{18} beads, Zeoprep 60 C18 40-63µm (Zeochem)
- Rotary evaporator
- freeze dryer, Christ alpha 2-4 LD plus
- HPLC, Dionex UltiMate 3000
- AB 4800 MALDI TOF/TOF analyzer
- 0.1 M NH4HCO3
- ox. Glutathione (Sigma-Aldrich)
- red. Glutathione (Sigma-Aldrich)
- Cystamine (Sigma-Aldrich)
- EDTA (Sigma-Aldrich)
- Tris (Sigma-Aldrich)
- BSA (Sigma-Aldrich)
- Brij 35 (Sigma-Aldrich)

- DMSO
- DTT (Sigma-Aldrich)
- ZipTip (Millipor)
- laminar flow (Thermo Scientific Hepa Safe)
- medium: RPMI with 10% FBS and 1% p/s (PAA, Austria)
- serum: Fetal Bovine Serum (FBS) (PAA, Austria)
- penicillin/streptomycin (PAA, Austria)
- freezing medium: FBS + 10% DMSO
- erythrocyte lysis buffer: per liter: 89.9 g NH_4Cl; 10.0g $KHCO_3$; 370 mg tetrasodium EDTA; pH 7.3
- competent E.coli cells DH5a
- LB medium
- ampicillin
- Plasmid DNA Purification (NucleoBond Xtra Midi Prep) (Macherey-Nagel)
- TurboFect Transfection
- serum free DMEM with high glucose
- GFP
- Trypsin (PAA)
- HEPES (Sigma-Aldrich)
- potassium fluoride (Sigma-Aldrich)
- EGTA (Sigma-Aldrich)
- Olympus IX 70 microscope
- Axon Instrument CU203BU Headstage

- Axon Instruments, Axopatch 200B
- Software -> Clampex Version 6.0.4; Axon Instruments
- Sutter Instrument CO Model P-97, Flamming Brown Micropipette puller

Table 4 summarizes the HPLC columns that were used during the isolation and purification of cyclotides.

Table 4: Schedule of all used HPLC columns.

Abbreviation	Full name, column dimensions, particle and pore size
semipreparative column	Kromasil, RP C_{18} 250 x 10.0 mm,
preparative column	Phenomenex Jupiter, RP C_{18}, 250 x 21.2 mm, 10µm
analytical column	Akzo Nobel, Kromasil 100-5 C_{18}, 250 x 4.6 mm
analyitcal folding column	Phenomenex, Aeris peptide, 3.6u XP-C_{18}, 150 x 2.1 mm

4. Methods

In this chapter, a detailed description of all experimental methods carried out during this thesis is given. It is organized, according to the two major projects of this work. First the isolation and purification of cyclotides, followed by the folding assays and secondly the electrophysiological patch clamp recording and preparation of the cells for these recordings.

4.1 Isolation of cyclotides from plant material

4.1.1 Extraction

First 500 g of plant material powder was extracted with 2500 ml of a 1:1 mixture of DCM: methanol in a 5 litre beaker covered with aluminium foil and kept for 48 h at room temperature. The mixture was stirred manually from time to time.

Afterwards the extraction mixture was filtered through a filter paper in a porcelain-vacuum-suction-filter and the plant powder was rinsed with the extraction solution. The filtrate was mixed 1:1 with distilled water, transferred to a separation funnel and shaken. This mixture was kept at room temperature until a phase separation was visible.

There should be two phases in the funnel, one from the DCM and one from the methanol/ddH_2O. The DCM was separated and the methanol/ddH_2O, which contains the protein, was purified with C_{18} material.

To do this, a glass sintered crucible was half filled with C_{18} material, connected to vacuum and activated with methanol. The C_{18} Material was then rinsed with ddH_2O containing 0.0045 % TFA. Because the methanol in the solution disturb the purification, it was necessary to dilute the methanol/ddH_2O Phase 1:3 with ddH_2O/0.0045% TFA. The C_{18} material was washed with 30% buffer B (buffer B = 90% AcN / 10% ddH_2O / 0.08% TFA) and eluted with 80 % B.

The acetonitrile in the 80% B fraction was removed via rotary evaporator and the remaining solution was frozen in a -80°C freezer and afterwards freeze dried. The remaining powder (crude extract) was stored at -20°C.

4.1.2 Isolation and purification of cO2 from Viola odorata

100 mg of the *Viola odorata* (VO) crude extract (3.1.2) was dissolved in 5 mL 50% B and diluted with Puffer A (H_2O / 0.1% TFA) to 25 ml. This comes up to a final concentration of 5% B. After filtering, the solution was loaded to the preparative HPLC column with 5.3 ml / min. The HPLC program is listed in Table 5.

Table 5: Program from the preparative HPLC of *V. odorata*.

Retention time (min)	Flow (ml/min)	% B
0	8	30
5	8	30
35	8	60
35.1	8	100
40	8	100
40.1	8	30
45	8	30
45.1	0.1	30
Fraction collection by time, every 90 sec. from 5.3 min. to 35 min.		

After the HPLC program was finished, every fraction was analysed via MALDI-TOF MS to determine the fraction which contains cO2. For that 0.5 µl of the sample was mixed with 3µl CHCA (in ACN) and 0.5 µl of that mixture was spotted on a MALDI-plate and analysed with the conditions in Table 6.

Table 6: MALDI – TOF – MS set up

MALDI – MS conditions	
Operating mode	MS reflector positive
Mass range (Da)	2000 – 4000
Focus mass	the monoisotopic mass of the cyclotide of interest
Shot/sub - spectrum	80
Total shots/spectrum	4800
Laser intensity	4000
Detector voltage multiplier	0.90

After freeze drying of the cO2 fraction, this fraction was dissolved in 5 mL buffer A and loaded on the semi preparative column and purified with the program in Table 7.

Table 7: Gradient setup for the semi preparative HPLC of *V. odorata*

Retention time (min)	Flow (ml/min)	% B
0	3	5
5	3	35
45	3	55
45.1	3	100
50	3	100
50.1	3	5
55	3	5
55.1	0.1	5
Fraction collection by time, every 75 sec. from 5 minutes to 45 min.		

Afterwards the fraction with the cO2 was determined as described above and freeze dried. The third purification step consists of an isocratic HPLC on the semi preparative column with 36% buffer B. The peaks were collected manual. Afterwards the peaks were checked via MALDI as described above. After the isocratic purification, cO2 was purely present in one fraction. This fraction was checked again with an analytical HPLC (Table 8), freeze dried and stored at -80°C.

Table 8: Gradient setup for the analytical HPLC.

Retention time (min)	Flow (ml/min)	% B
0	1	5
5	1	30
35	1	60
35.1	1	100
40	1	100
40.1	1	5
45	1	5
45.1	0.01	5
Injection volume: 10µl		**column oven: 30°C**

4.2 Oxidative folding of cyclotides

4.2.1 Reduction of native cyclotides

1 mg of the freeze dried cyclotide was dissolved in 500 µl of 0.1 M NH_4HCO_3 pH 8.5, mixed with 50 µl of 0.1 M DTT (final concentration of DTT in the reaction mix = 10 mM) and heated at 60°C for 30 min. Afterwards the reaction was quenched with 25 µl of diluted. TFA (~25%). After the reduction the reaction mix was loaded on the semiprep column and purified isocratic with 36% B to remove the DTT and in case of not completely reduced protein, the non-reduced protein. The peaks were collected manual and checked on the MALDI-TOF MS to identify the fraction that contained the reduced cyclotide. The reduced cyclotide fraction was freeze dried and stored at -80°C.

4.2.2 Folding of cO2 and vigno 10

The bracelet cyclotide vigno10 was provided from a friendly research group. It was chemical synthesized. First the provided vigno 10 was pooled, reduced and purified with the semiprep column and the program shown in Table 9.

Table 9: Gradient setup for the purification of vigno10

Retention time (min)	Flow (ml/min)	% B
0	3	5
5	3	20
65	3	40
65.5	3	55
72	3	100
72.5	3	100
80	3	5
80.1	0.01	5
Fraction collection by time, every 120 sec. and start at min. 5		

After the identification of the fraction with the vigno 10 via MALDI-TOF MS, this fraction was freeze dried and reduced as described in 3.2.2. The cO2 was isolated from fresh plant material (3.1) and reduced (3.2.2).

The folding experiments of cO2 and vigno 10 were carried out parallel with the same buffers. First, the freeze dried reduced cyclotides were dissolved in 100µl buffer A and the

concentration was measured via nanodrop at 280 nm. The experiments were carried out with a protein concentration of 20 µM in the final folding reaction mix. Each approach had an amount of 350 µl. The folding buffer was pipetted into an 1.5 ml Eppendorf reaction tube and mixed with the required amount of reduced protein. Afterwards the redox equivalent, dissolved in the respective buffer, was added. After a short mix the reaction time started. After the time points 2´ - 5´- 10´- 20´ - 30` - 1h – 2h – 4 h – 8h – 24h – 48h and 72h an aliquot of 25 µl was taken and stopped with TFA. After 24h and 48h new redox equivalent was added (the redox equivalent was always prepared fresh). Exceptions are the buffers 9 – 11. Here the first aliquot was taken after 5 min, after 5 d and 7 d a sample was taken as well and after 72 h and 5 d new redox equivalent was added. The different folding buffers are shown in Table 10.

Table 10: Folding conditions of cO2 and vigno10.

	Buffer	Additives	Redox equivalent (mM)	pH
1	0.1 M NH_4HCO_3	35% DMSO; 6% Brij 35	GSH/GSSG (2/0.1)	8.2
2	0.1 M Tris/HCl	35% DMSO; 6% Brij 35; 1 mM EDTA	GSH/cystamine (2/2)	8.5
3	0.1 M NH_4HCO_3	65 % isopropanol	GSH/GSSG (2/0.1)	8.2
4	0.1 M NH_4HCO_3	75 % isopropanol	GSH/GSSG (2/0.1)	8.2
5	0.1 M NH_4HCO_3	85 % isopropanol	GSH/GSSG (2/0.1)	8.2
6	0.1 M NH_4HCO_3	95 % isopropanol	GSH/GSSG (2/0.1)	8.2
7	0.1 M Tris/HCl	BSA (150 mg/ml); 1 mM EDTA	-	7,5
8	0.1 M Tris/HCl	150 mg/ml BSA/Dextran 70 1:1; 1mM EDTA	GSH/GSSG (2/1)	7,5
9	50 mM Na_2HPO_4	10% from each ACN/TFE/ DMSO; 1M GuHCl	-	7.0
10	50 mM Na_2HPO_4	10% from each ACN/TFE/ DMSO; 1 M GuHCl	GSH/GSSG (2/0.1)	7.0
11	50 mM Na_2HPO_4	10% from each ACN/TFE/ DMSO; 1 M GuHCl	Cysteine/Cystine (10/1)	7.0

DMSO -> dimethyl sulfoxide; GSH -> reduced glutathione ; GSSG -> ox. glutathione; BSA -> bovine serum albumin; ACN -> acetonitrile; TFE -> trifluoroethanol; GuHCl -> guanidine HCl

After the collection of the aliquots, these samples were analysed by HPLC with the analytical folding column and the program shown in Table 11.

Table 11: Gradient setup for the analytical HPLC for the folding samples.

Retention time (min)	Flow (ml/min)	% B
0	0.3	5
27.5	0.3	60
32	0.3	90
33	0.3	90
37.1	0.3	5
45	0.3	5
45.1	0.3	5
Injection volume: 10µl		**column oven: 30°C**

Furthermore all samples were analysed with MALDI-TOF MS as described in 3.1.3. In case the folding samples contain DMSO, it was necessary to remove DMSO before the samples could be analysed. For this the samples from the buffer 1-2 and 9-11 were prepared with ZipTip™. The ZipTip was first equilibrate with 10 µl of 100% buffer B and then washed two times with 10 µl of buffer A. Afterwards the sample was aspirate and dispense three to seven times with a volume of 10 µl and washed two times with 10 µl of 5% MeOH. At the end the sample was eluted in 4µl 80% buffer B.

4.2.3 Folding of [T20K]kalata B1

The KB1 mutant [T20K] was synthesized by Roland Hellinger, a PhD student in the group of Dr. Gruber. First the [T20K]kalata B1 was analysed with the analytical column to analyse its purity and to confirm its fully reduced state (program see Table 8). The folding was accomplished as described in 3.2.3 with the buffers shown in Table 12 and with sampling during the time point from 2’ to 72 h.

Table 12: Folding conditions for [T20K]kalata B1.

	Buffer	Additives	Redox equivalent (mM)	pH
1	0.1 M NH_4HCO_3	35% DMSO; 6% Brij 35; 1 mM EDTA	GSH/cystamine (2/2)	8.2
2	0.1 M NH_4HCO_3	50% isopropanol	GSH/GSSG (2/2)	8.2
3	0.1 M NH_4HCO_3	65% isopropanol	GSH/GSSG (2/2)	8.2
4	0.1 M NH_4HCO_3	75% isopropanol	GSH/GSSG (2/2)	8.2
5	0.1 M NH_4HCO_3	85% isopropanol	GSH/GSSG (2/2)	8.2
6	0.1 M NH_4HCO_3	95% isopropanol	GSH/GSSG (2/2)	8.2

4.3 Cell culture

4.3.1 Isolation of human T-cells

Human peripheral lymphocytes were isolated from the blood of healthy adult donors obtained from the Blood Transfusion Centre (University Medical Center, Freiburg, Germany). To isolate the T cells, the venous blood was transferred to 50 ml centrifuge tubes and centrifuged 5 min with 1000 rpm at 4°C. The supernatant was discarded and to each pellet, 2 ml of lysis buffer was added. After an incubation time of 2 min, the lysis was stopped with the addition of FBS. The cell suspension was pooled in a few tubes and centrifuged again at the same conditions. The lysis was repeated once. The final white pellet containing the T-cells was resuspended in 7-10 ml of freezing medium (dependent of the size of the pellet), transferred in cryo tubes and stored at -80°C.

4.3.2 Thawing cells from -80°C

To thaw and cultivate frozen cells, the cells were defrosted at room temperature and transferred in a 15 ml centrifuge tube, mixed with 10 ml medium and centrifuge for 3 minutes with 1000 rpm at room temperature. After discarding the supernatant, the pellet was resuspended in 3 ml medium, transferred to a petri dish and incubated at 37°C and 5% CO_2.

4.3.3 Handling of Jurkat cells

The Jurkat cells were defrosted as described in 3.3.3. Except that the cells were resuspended in 15 ml medium and transferred in a cell culture flask. Every day the medium was changed. For this the cells were transferred in a centrifuge tube and centrifuged for 3 minutes with 1000 rpm at room temperature. The supernatant was discarded and the pellet resuspended in 1 ml fresh medium. In the meantime 15 ml fresh medium were put in a cell culture flask. Afterwards 50 – 200 µl of cells were transferred to the culture flask.

4.3.4 Transfection of tsA-201 cells

To measure the human Kv1.3 channel in tsA-201 cells, these cells were before transfected with the plasmid pRC/CMV 5.5 kb containing human Kv 1.3 DNA. The plasmid was a gift

from Alexandra Koschak (Medical University Vienna). The used plasmid is shown in Figure 13.

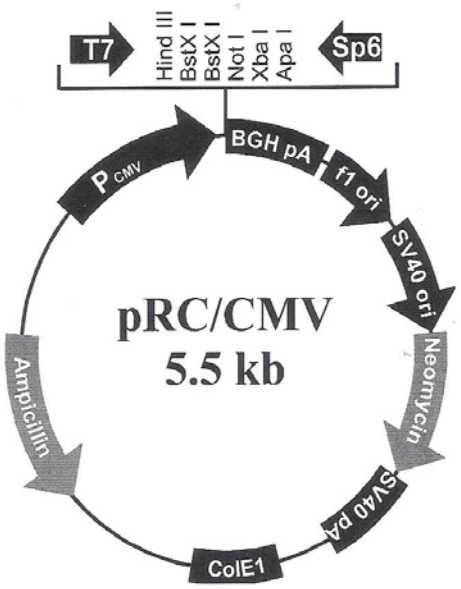

Fig.13: Plasmid with human Kv 1.3 DNA for transfection of tsA201 – cells.

For the transfection of tsA-201 cells the TurboFect Transfection method from Thermo Scientific was used. First the medium and serum free DMEM with high glucose was warmed to 37°C. In the meantime tsA-cells with a 70-80% confluence was selected and the old medium was replaced with fresh warm medium and incubated for at least 10 min at 37°C and 5% CO_2. Afterwards 100 µl of serum free DMEM with high glucose was mixed with the plasmid of interest (conc. 1.5 µg/µl). Then 5 µl of TurboFect was added and vortexed for 1 sec. After adding 1 µl of GFP solution with a concentration of 0.02 µg/µl, the mixture was incubated at room temperature for 10 min. Afterwards the mixture was added gently to the seeded cells and incubated over night at 37°C and 5% CO_2.

On the next day the transfection efficiency was checked by UV-treatment (green fluorescence) with the microscope and by positive transfection split on 2-3 new dishes. For this the medium was removed and the cells washed with 1 ml PBS. After wards the cells were trypsinized with 1 ml Trypsin. After stopping the trypsinization with 1 ml medium the cells were centrifuged at 900 rpm for 4 min and resuspended, depending on the size of the pellet, in 1-4 ml and spread out on 1-4 dishes (1 ml per dish). After the incubation of 2 h in the incubator the functional expression using Patch clamp test was checked.

4.4 Patch Clamp recordings

4.4.1 Preparation of the cells

Three different cells were used for the patch clamp recordings, human T-cells, Jurkat cells and transfected tsA-201 cells. The preparation from the T-cells and Jurkat cells is a little bit different as from the tsA-201 cells. From the T-cells and the Jurkat cells (see also Sections 4.3.1. and 4.3.3) 3-5 ml cell suspension was centrifuged with 1000 rpm for 3 min. The supernatant was removed and the pellet was resuspended in 2 ml warm (37°C) extracellular solution (shown in Table 13). Afterwards the extracellular solution with the cells were transferred in a petri dish and immediately analysed via patch clamp. In contrast to the T-cells, the tsA-201 cells are adherent. The transfected cells were put out from the incubator, the medium was changed with 1ml extracellular solution and the cells were ready for the patch clamp measurements.

Table 13: Composition of the extracellular and intracellular solution for the patch clamp recordings.

extracellular solution		intracellular solution	
145 mM	NaCl	140 mM	KF
5 mM	KCl	2 mM	$MgCl_2$
1 mM	$MgCl_2$	1mM	CaCl2
2.5 mM	$CaCl_2$	10 mM	HEPES
5.5 mM	Glucose	11 mM	EGTA
10 mM	HEPES		
suppl. with 0.1 mg/ml BSA			
pH 7.35 with NaOH		pH 7.22 with KOH	

4.4.2 Manufacture of the pipettes

For the patch clamp recordings borosilicate and aluminium silicate pipettes were used. The aluminium silicate pipettes were used very rarely, only in cases when with the borosilicate pipettes no satisfying results were achieved. For pulling the pipettes the Sutter Instrument CO Model P-97 micropipette puller was used.

4.4.3 Formation of a gigaseal and whole cell recording

The formation of the gigaseal, which is the connection between the cellmembrane and the pipette, was observed with an Olympus IX 70 microscope. After pulling the pipettes, the pipettes were fire polished with a lighter (only in case of borosilicate), filled with intracellular solution (Table 13) and were stuck on the electrode of the head stage. The pipette pulling result in pipettes with a resistant of 1.2 – 3.5 MΩ, depending on the glass type and the pulling method. Afterwards a slight positive pressure was applied to the inside of the pipette to keep the pipette tip free of contamination. Then an appropriate cell was chosen and centred it to the middle of the visual field. After moving the pipette slowly to the cell and touching the solution, the pipette offset was adjusted immediately. After setting the pipette offset, the pipette resistance and the value of the pipette offset was noted. Afterwards the pipette was slowly moved again till the pipette touched the cell. Contact of the cell was indicated by a rise in pipette resistance. When the pipette resistance reached 10 mega ohm the holding potential was reduced to minus 60 mV and slightly suction was applied to the pipette. In some cases, seal formation occurred immediately or it took some while and more suction to happen. A gigaseal was indicated by a high pipette resistance starting at 500 MΩ to 1-2 GΩ. After formation of a high resistance seal, the artefacts from the pipettes were reduced and short time suction was applied to open the cell. This process could take some time and was not every time successful. Once the cell was open the holding potential was further reduced to minus 80 mV, the whole cell mode was activated and the artefacts were reduced by setting the capacity and the series resistant.

Afterwards two different protocols were measured, the IV and the pulse protocol. First the IV protocol was measured, to analyse the maximum current, followed by the pulse protocol. The IV protocol decreased the depolarizing voltage steps from -80 mV to +40 mV in 20 mV steps and in the pulse protocol the Kv1.3 currents were elicited by depolarizing the voltage steps of 200 ms from the holding potential -80 mV to +40 mV at 15 sec intervals.

4.4.4 Analysis of potent blockers

The blocker, dissolved in extracellular solution was applied with a perfusion system from Axon Instruments. Before starting with the patch clamp recordings, the perfusion system was washed with dest. water and one chamber was filled with the extracellular solution and each blocker was filled in a chamber. Then the tip of the perfusion system was centred so that it

was very close to the cell which was measured. After formation of the gigaseal and opening of the cell, the perfusion system with the extracellular solution was turned on immediately. After the measurement of the IV protocol, to see the maximal current, the pulse protocol was started and after getting a stabile current the drug was washed in via the perfusion system. When a stable block was achieved, then the perfusion system was changed to bath solution to wash out the peptide.

5. Results

In this chapter the results from the conducted experiments are presented. I will start with describing the isolation and purification of cyclotides from plant material, followed by the oxidative folding of cyclotides and the results from the electrophysiological determination of the ion channel modulation from [T20K]kalata B1.

5.1 Isolation, purification and oxidative folding of cyclotides

The oxidative folding of cyclotides is from vitally importance, because thereby it is possibly to avoid the labour-intensive cyclotide extraction from plant material. But so far the whole oxidative folding procedure is still not fully understood. Therefore several research groups try to discovery the mechanism behind the folding and the influence of certain residues which plays a role in the oxidative folding (Aboye et al., 2008; Gunasekera et al., 2009; Wong et al., 2011).

In this study, the oxidative folding of the synthesised bracelet cyclotide vigno 10 in comparison to cycloviolacin O2, a bracelet cyclotide isolated from *V. odorata* as well as the folding of the immunosuppressive Möbius cyclotide [T20K]kalata B1 was studied.

To have sufficient material for the folding experiments, cO2 was isolated and purified from *Viola odorata* as described in Section 4.1. The purified cO2 and the synthesised vigno 10 and [T20K]kalata B1 were reduced and analysed by MALDI-MS and RP-HPLC to confirm their high purity (>95%) as well as the completely oxidation of three native cysteine residues, which is indicated by a mass shift of 6 Da on MALDI-MS (Supplementary Data 1, Appendix). The reduction of the disulfide bonds leads to a decreased hydrophobicity and thereby to a significantly earlier elution of the peptides from the RP-HPLC column.

For the initial folding studies, buffers which show the highest yields in the study of Hashempour et al. 2012 were analysed for both cyclotides (Table 10). Furthermore the study of Aboye et al. 2008 shows the highest yield for cO2 so far, i.e. ~ 50%, this folding condition served as a standard condition during the experiment (Table 10). A previous study also shows that high concentration of isopropanol favour the folding of bracelet cyclotides (Wong et al., 2011).

The refolded samples were analysed by RP-HPLC and MALDI-MS. The RP-HPLC results are shown in Figure 14-17. Furthermore the yield was determined by measuring the area under the curve of the peaks and the folding yields were plotted against the incubation time (Supplementary data 3, Appendix).

As it is shown in Table 14, the standard DMSO/detergent buffer (=35% DMSO/6% Brij 35 in Tris pH 8.5) leads to the highest yield for cO2, 26.6%. In the aqueous isopropanol buffers the cyclotide cO2 folded with a much smaller yield, especially the yield was decreasing with higher isopropanol concentration. For the cyclotide vigno 10, the observations are similar, whereas the highest yield was observed in the standard DMSO/detergent buffer, 4.1%, vigno 10 folded in the isopropanol buffers with lower efficiency (Supplementary data 3, Appendix).

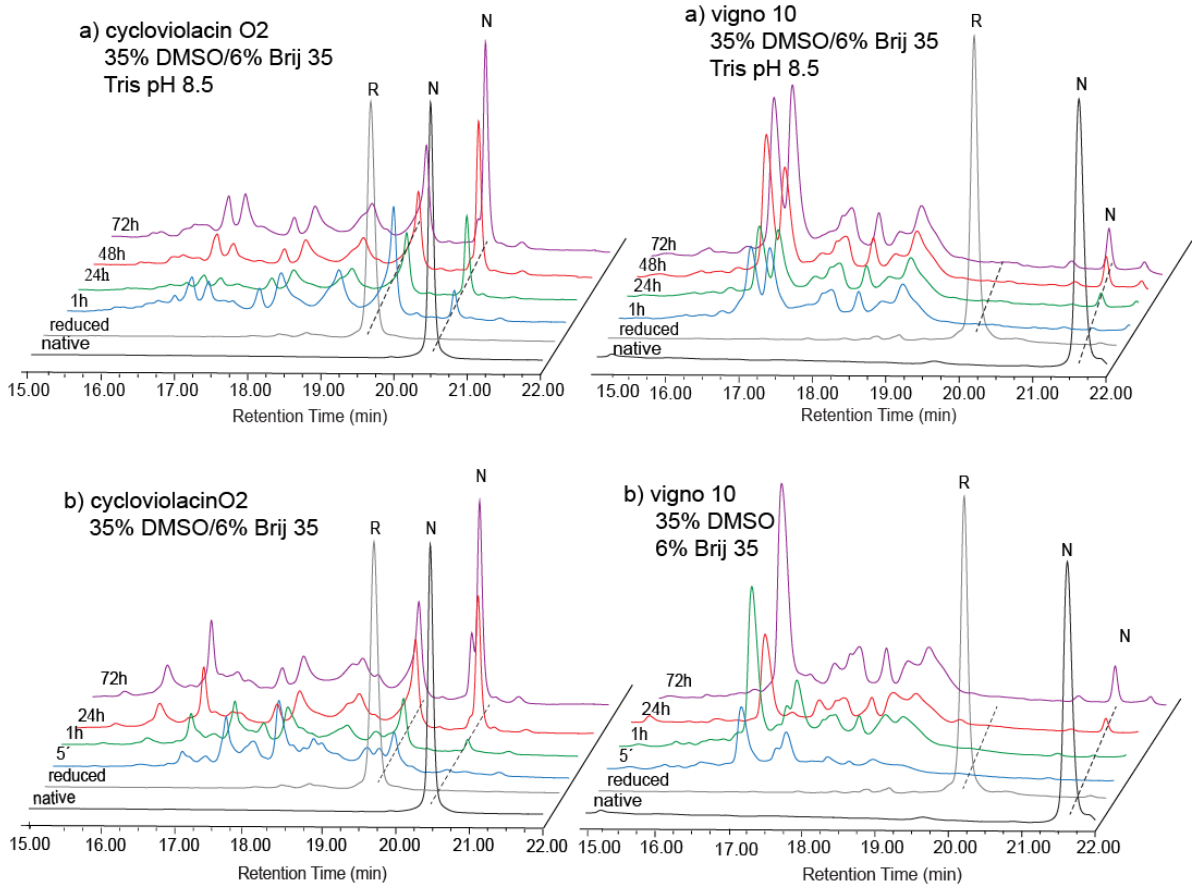

Fig. 14: Refolding of cO2 and vigno 10 with the DMSO/detergent buffers. All experiments were conducted at 20°C. The buffer contains 0.1M NH_4HCO_2 pH 8.2 and GSH/GSSG as a redox pair, except condition b. this buffer contains Tris/HCl pH 8.5

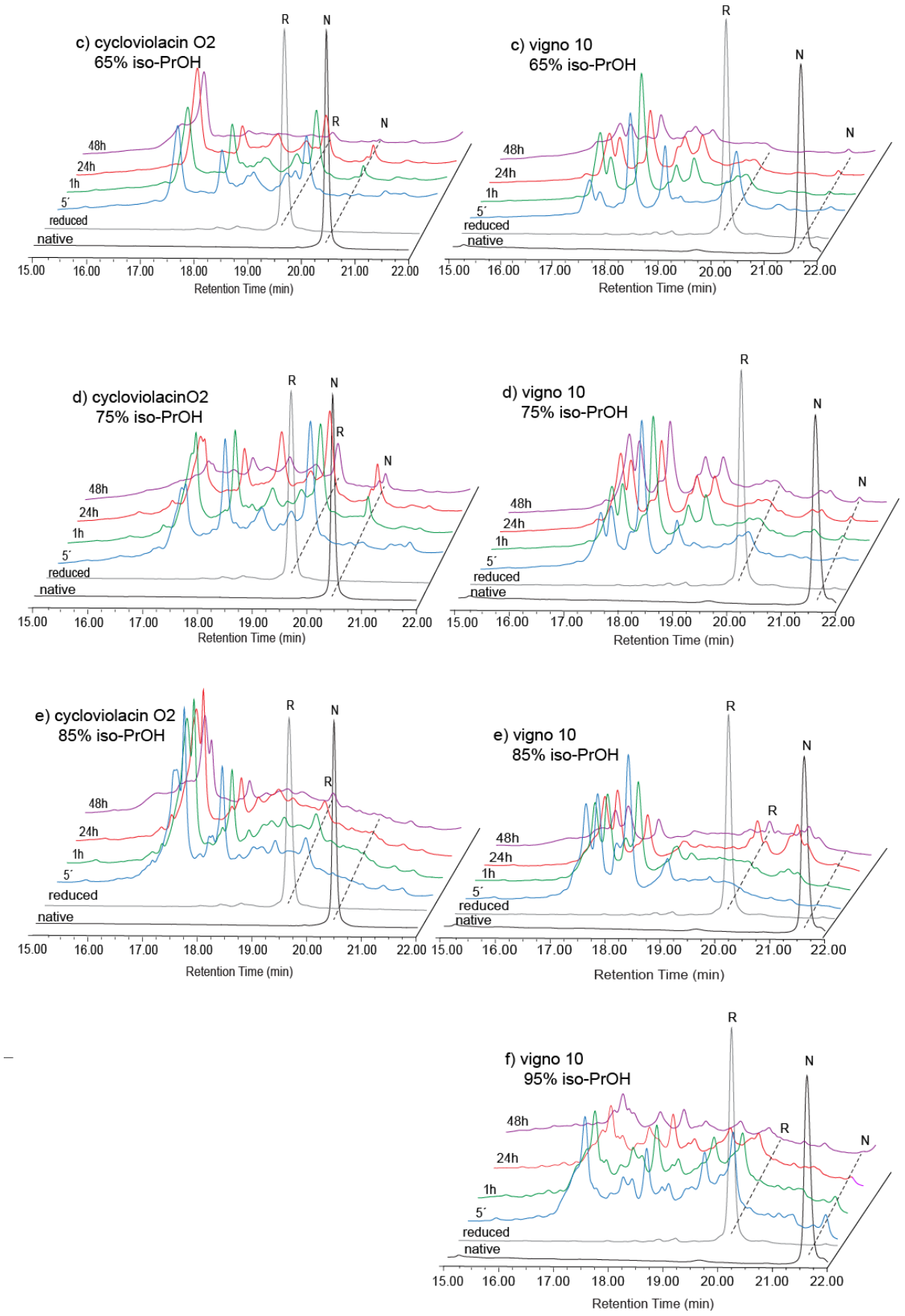

Fig. 15: Refolding of cO2 and vigno 10 with buffer containing isopropanol. The RP-HPLC traces from different time-points are presented. All experiments were conducted at 20°C. The buffer contains 0.1 M NH_4HCO_2 pH 8.2 and GSH/GSSG.

As shown in Table 14, the folding yield of vigno 10 in the initial folding studies was not satisfying. Also the yield of native cO2 was not higher than 26%. That is why a second round of folding studies was carried out. Based on the previous study on oxidative folding of cysteine-rich peptides (Buczek et al., 2006) buffers containing a high concentration on BSA and Dextran 70 were used for further folding studies (Table 10).

The procedure was the same as in the initial folding study and is described in detail in 4.2.During the analysis of the folding samples which contains high concentration of BSA, two problems occurred: (i) BSA precipitated in the HPLC column, which led to high pressure error in the HPLC device. (ii) During the analysis from the first folding samples, before the BSA accumulated in the column, it was observed that a small part from the BSA was eluted from the column with the same retention time as the native cyclotides which led to a huge peak in the HPLC spectra. Because of these two reasons it was not possible to analyse the folding samples from the second folding experiment accurately. Hence we performed another folding trial. The folding conditions in the third experiment were based on the previous study from Reinwarth et al., 2013 and are shown in Table 10.

The folding buffers differ substantially from the other conditions. It contains acetonitrile as well as trifluorethanol and DMSO in a Na_2HPO_4 buffer with different concentrations of redox equivalent, in the following abbreviated with ADT.

The results of the RP-HPLC are presented in Figure 16. For the cyclotide vigno 10, the ADT buffer didn’t work at all. The yield of the native peptide is almost zero, but the amount of different intermediates is quite high. For the cO2 it worked better, the highest yield was achieved with the addition of cysteine/cystine, 7.34%, but still, it is much smaller than the yield reached with the standard DMSO/detergent buffer.

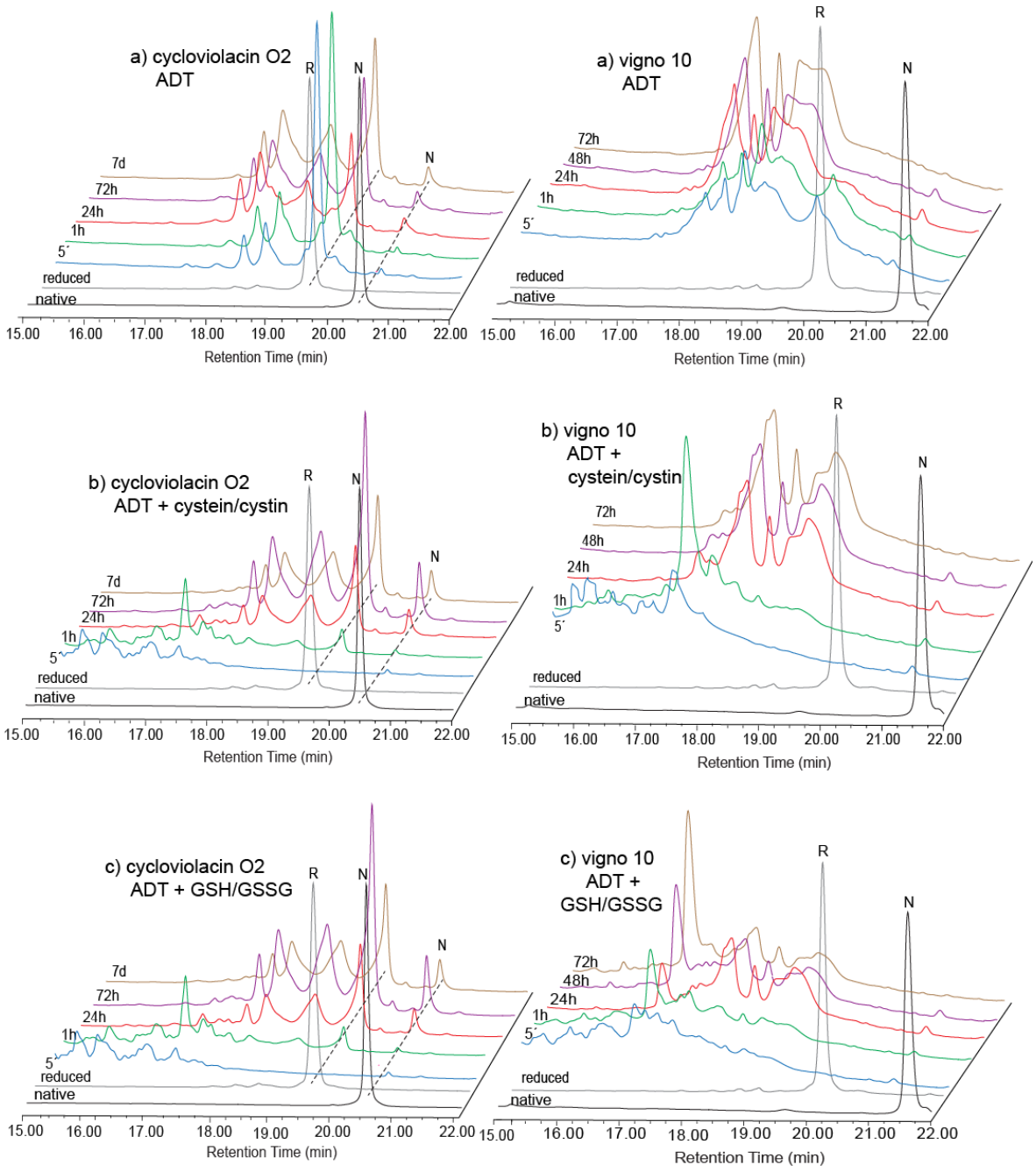

Fig. 16: Refolding of cO2 and vigno 10. The RP-HPLC traces from different time-points are presented. All experiments were conducted at 20°C. The buffer contains 50mM Na_2HPO_4 pH 7.0. a) This buffer contains no redox equivalent. b) Buffer containing cysteine/cystine (10/1 mM). c) Buffer containing GSH/GSSG (2/0.1 mM).

In addition to the folding experiments of cO2 and vigno10, the folding conditions of the kalata B1 mutant [T20K] were also optimized. Six different conditions were tried as it is shown in Table 10 (see also Aboye et al., 2011).

After the folding process which is described in detail in 4.2.3, the samples were analysed with RP-HPLC and the traces are shown in Figure 17. As it was expected for this Möbius cyclotide, it folded with a very high yield in alcoholic conditions. All buffers, except the 95%

isopropanol buffer, led to yields higher than 85% of native folded peptide. The best result, i.e. ~95% native folded peptide, was achieved with 65% isopropanol in 0.1 M NH_4HCO_3 buffer with a pH 8.2. The buffer containing 95% isopropanol shows no appreciable yield.

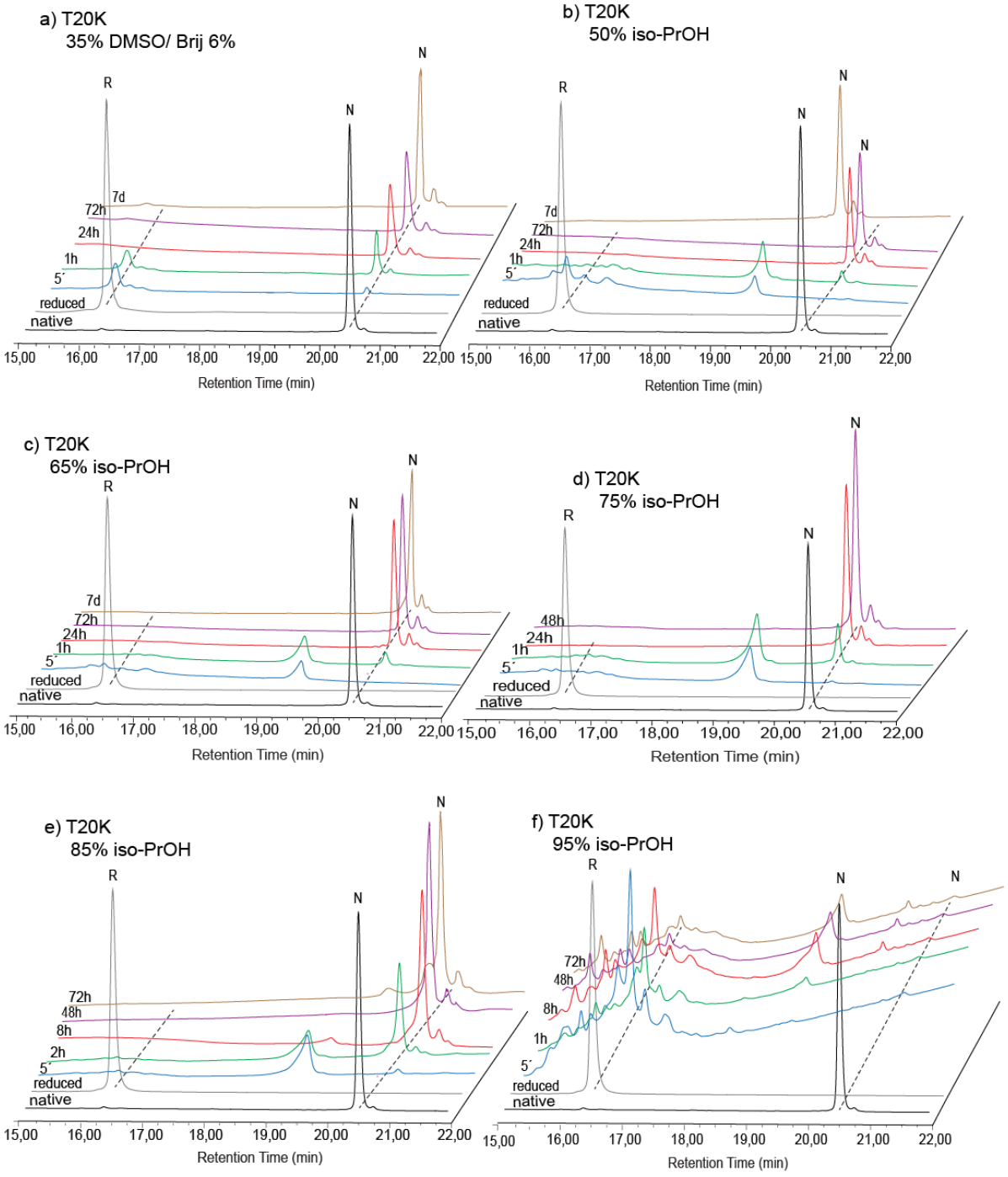

Fig.17: Refolding of [T20K]kalata B1. The RP-HPLC traces from different time-points are presented. All experiments were conducted at 20°C. The buffer contains 0.1 M NH_4HCO_2 pH 8.2 and GSH/GSSG as a redox pair.

The final yields and the folding kinetics of all folding experiments are presented in Table 14 and in graphical form in the Supplementary Data 3, Appendix.

Table 14: Summary of the folding results and kinetics

Cyclotide [1]	Buffer [2]	Yield (%) [3]	Folding kinetics ^4k_n (h^{-1})	$t_{1/2}$ (h)
cO2	35% DMSO/6% Brij35	21.60	0.125	5.54
	35% DMSO/6% Brij35; Tris pH 8.5 [5]	26.59	0.133	5.22
	65% isopropanol	6.07	1.026	0.68
	75% isopropanol	7.03	2.358	0.29
	85% isopropanol	1.24	1.208	0.57
	ADT [6]	3.01	0.139	5.00
	ADT + GSH	5.56	0.167	4.15
	ADT + Cystein [7]	7.34	0.797	0.87
vigno 10	35% DMSO/6% Brij35	3.29	0.097	7.18
	35% DMSO/6% Brij35; Tris pH 8.5 [5]	4.1	0.021	32.52
	65% isopropanol	1.05	2.353	0.29
	75% isopropanol	0.77	2.978	0.23
	85% isopropanol	0.8	5.681	0.12
	95% isopropanol	0.65	5.119	0.14
	ADT [6]	0	- [h]	-
	ADT + GSH	0.17	-	-
	ADT + Cystein [7]	0.16	-	-
[T20K] kalata B1	35% DMSO / 6% Brij35 / 1 mM EDTA	87.85	0.714	0.97
	50% isopropanol	90.2	0.241	2.87
	65% isopropanol	94.96	0.184	3.77
	75% isopropanol	92.59	0.227	3.06
	85% isopropanol	92.18	0.448	1.55
	95% isopropanol	0.83	-	-

[1] All folding experiments were carried out with a peptide concentration of 20 µM at 20°C and after 24 h and 48 h new redox equivalent was added.
[2] All buffers were prepared in 0.1 M NH_4HCO_3; pH 8.2; with GSH/GSSG (2/0.1 mM) exceptions are indicated otherwise and the ADT buffers contain 50 mM Na_2HPO_4 instead of the 0.1 M NH_4HCO_3
[3] Yield after 72 h at 20°C was; determined by automatic peak integration using Chromeleon software 6.8
[4] Rate constant of native folded peptide (k_n) and folding half-time of observed folding yields determined by single exponential fit using GraphPad Prism 5
[5] buffer containing GSH/cystamine (2/2 mM)
[6] buffer containing no redox equivalent
[7] buffer containing cysteine/cystine (10/1 mM)
[8] not determined

To summarise these results, the folding conditions of three different cyclotides were optimized. In detail two representative bracelet cyclotides, cO2 and vigno 10 and one representative Möbius cyclotide [T20K]kalata B1 were used for the experiments. Whereas the Möbius cyclotide folded very fast and with a high yield, the folding of the bracelet cyclotides was more complex and achieved only a moderate yield. These results agree with previous publications (Gunasekera et al., 2009; Aboye et al., 2008; Aboye et al., 2011).

In the supplementary data 4, Appendix, a table with the disulfide species at certain time points from each cyclotide is shown. It is visible, that during the folding of cO2 after 2 min only 3SS species existed, while during the folding of [T20K]kalata B1 1SS and 2 SS species dominated the folding and after 1h the first 3SS species was visible.

5.2 Ion channel modulation of [T20K]kalata B1

The voltage gated potassium channel Kv1.3 plays an important role in the activation of T lymphocytes; hence an inactivation of this channel leads to a weak immune response. In previous publications a few Kv1.3 blockers were described as potent immunosuppressive drugs (Kalman et al., 1998; Varga et al., 2012 and Gurrola et al., 2012). Gründemann et al. showed in his work, that [T20K]kalata B1 has immunosuppressive properties. Hence one of the aims in this study was to analyse if the peptide [T20K]kalata B1 can block the potassium channel Kv1.3 by using electrophysiological patch clamp technique. TsA201cells, were transiently transfected with the human Kv1.3 DNA (see also 4.3.4) and investigated by the patch clamp technique in the whole cell mode. First of all it was analysed if the TsA201 cells produce stable and reproducible results. For this the cell was perfused with the extracellular solution to simulate the mechanical forces which act on the cell during the measurements and to calculate the normal run-down of the current. The results are shown in Figure 18.

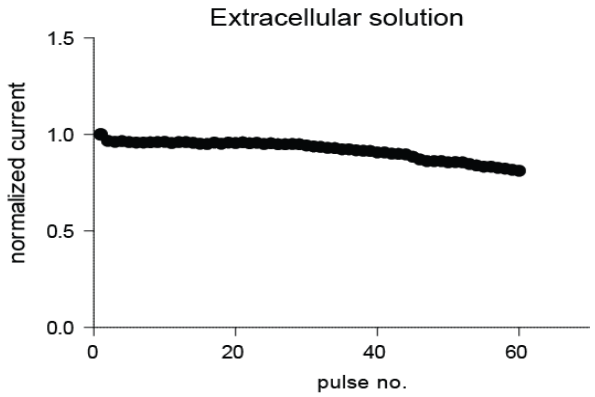

Fig. 18: Control measurements of Kv1.3 with extracellular solution. Whole-cell Kv1.3 currents were elicited by 200ms step depolarization to + 40 mV from a holding potential of -80mV and intervals of 15 sec and the peak outward currents were normalized to the peak outward current elicited by the first pules in the train. Shown is the reduction of the current from a typical cell within the first 35 pulses. This reduction is 12.22 % ± 4,35%; P ≤ 0.05 (N = 3).

In order to verify the proper function of the perfusion system, the measurements started with the analysis of fluoxetine, which is a reversible blocker of Kv1.3 (Choi et al., 1999). For this, tsA cells were transfected with human Kv1.3 DNA and GFP via the TurboFect Transfection method from Thermo Scientific (detail description 4.3.4). After checking the transfection efficiency, the cells were analysed as described in Section 4.4. In Figure 19 the amount of current from a transfected cell compared to an untransfected cell is shown and in Figure 20 the result of the fluoxetine measurements. As it is presented in Figure 19, the native outward currents elicited by the applied clamp protocol are very small (< 1nA) compared to the transfected cells (> 10 nA), and they lack the slow decay phase following activation, which are typical for Kv1.3 channels. This confirms that the outward currents in transfected cells are mainly carried by Kv1.3 channels.

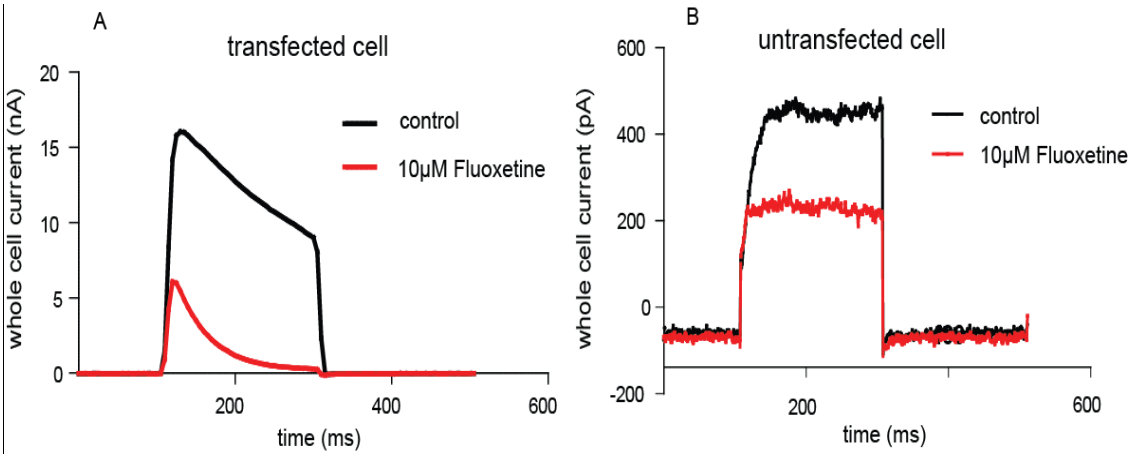

Fig. 19: Comparison of transfacted and untransfected cells. Whole-cell Kv1.3 currents were elicited by 200 ms step depolarization to + 40 mV from a holding potential of -80 mV and intervals of 15 sec. Flx = fluoxetine. A, Kv1.3 currents from a transfected cell obtained in the absence and presence of 10 µM fluoxetine. B, shown is native outward currents in untransfected cells. Peak outward currents were normalized to the peak outward current elicited by the first pulse in the train.

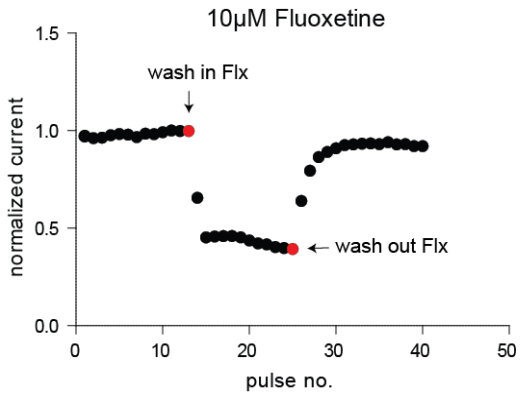

Fig. 20: Inhibition of Kv1.3 by fluoxetine. Whole-cell Kv1.3 currents were elicited by 200 ms step depolarization to + 40 mV from a holding potential of -80 mV and intervals of 15 sec. Flx = fluoxetine. Shown is the fast block after the wash in and the completely recovery after the wash out of 10 µM fluoxetine. The amount of block is 61.23% ± 2.69%; ($P \leq 0.05$; N = 3) Peak outward currents were normalized to the peak outward current elicited by the first pulse in the train.

As it is shown in Figure 20 the fluoxetine block is rapid and completely reversible and 10 µM fluoxetine showed a ~61% block of the current, consistent with a previous report (Choi et al., 1999).

Afterwards, the ion channel modulation of the peptide [T20K]kalata B1 was analysed. Therefore the peptide was applied at a concentration of 2 µM; the results are shown in Figure 21. The application of [T20K]kalata B1 was followed by a slow, continuous decline of the outward currents.

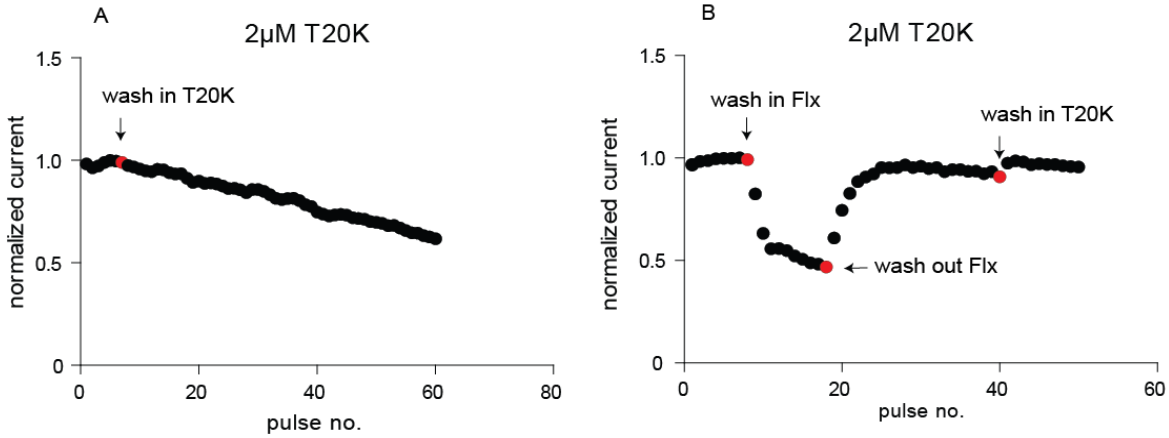

Fig. 21: Effect of 2 µM [T20K]kalata B1 on Kv1.3. Whole-cell Kv1.3 currents were elicited by 200 ms step depolarization to + 40 mV from a holding potential of -80 mV and intervals of 15 sec. Peak outward currents were normalized to the peak outward current elicited by the first pulse in the train. Flx = fluoxetine. In both figures the normalised current of one typical cell is shown. A, the wash in of 2µM T20K is shown. From the wash in till the pulse 35, the current was reduced around 19.30% ± 3.92%; ($P \leq 0.05$; N = 4). B, The effect of 2µM T20K after wash in and wash out of fluoxetine is shown.

As mentioned above, Gründemann et al. showed that the kalata B1 mutant [T20K] has immunosuppressive properties. But furthermore, he identified a mutant which has similar general characteristics but showed no immunosuppressive activity at all. In this mutant the valine at position 10 is exchanged by a lysine. Because of the similar characteristics but the opposite immunosuppressive activity, this mutant served as a good negative control. The result of the effect from [V10K] on Kv1.3 is shown in Figure 22 (Gründemann et al., 2013).

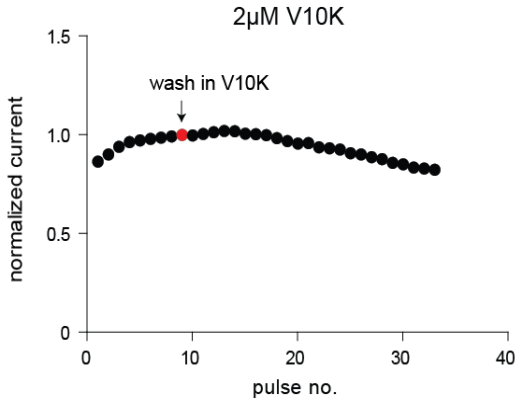

Fig. 22: Effect of 2 µM [V10K]kalata B1 on Kv1.3. Whole-cell Kv1.3 currents were elicited by 200 ms step depolarization to + 40 mV from a holding potential of -80 mV and intervals of 15 sec. Peak outward currents were normalized to the peak outward current elicited by the first pulse in the train. Shown is the trace from one typical cell. From the start of the wash in till the pulse 35 the current was reduced by 15.70% ± 4.57%; ($P \leq 0.05$; $N = 3$)

As it is shown in figures 21-22, [T20K]kalata B1 shows no significant block of the Kv1.3 channel. The result in Figure 18 shows that the spontaneous loss of current (“run down”) in our experimental configuration is around 12%. The measurements with 2µM [T20K]kalata B1 show a very slow decline of the current by 19.3% which is compared to the run-down in Figure 18 not significant ($P = 0.1025$) and 2 µM [V10K] reduce the current by 15.7%, this is also not significant ($P = 0.4887$). To confirm these results, the measurements were repeated with 4 µM. The results are shown in Figure 23.

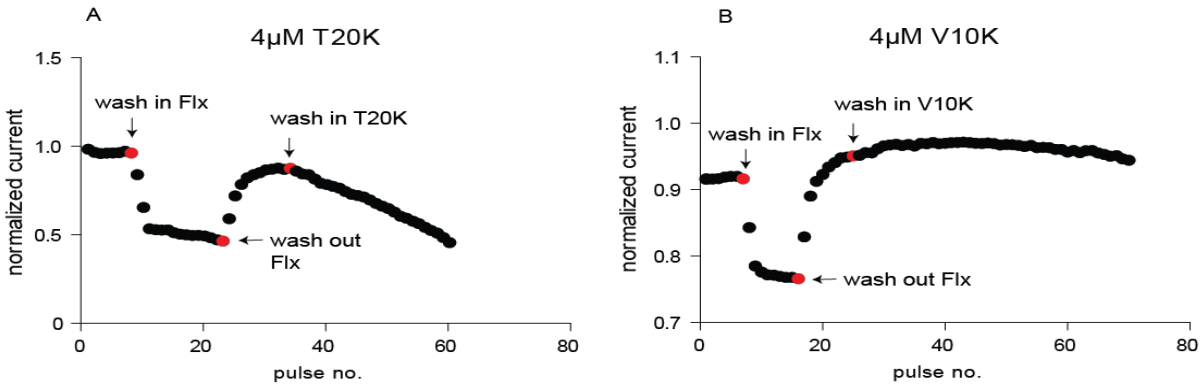

Fig. 23: Effect of 4 µM [T20K]kalata B1 and 4 µM [V10K]kalata B1 on Kv1.3. Whole-cell Kv1.3 currents were elicited by 200 ms step depolarization to + 40 mV from a holding potential of -80 mV and intervals of 15 sec. Peak outward currents were normalized to the peak outward current elicited by the first pulse in the train. Flx = fluoxetine. In both figures data from one typical cell is shown. A, the effect of 4 µM [T20K]kalata B1 is shown. From the point of wash in till the pulse 60 the current was reduced by 52.10% ± 8.50%; ($P \leq 0.05$; N = 6). B, the effect of 4 µM [V10K] on the Kv1.3 is shown. The current between the wash in and the pulse 60 was reduced by 2.41% ± 2.81%; (P = not significant; N = 4).

The slow decrease in outward current during application of T20K, which is a significant reduction (P = 0.0013) may be caused by a slowly developing block of Kv1.3 channels. Alternatively, T20K may give rise to damage of the cell membrane which may reduce ionic current either by alteration of the lipid environment of the channel or by inducing membrane leakage which eventually leads to loss of current clamp. In the latter case the current reduction produced by T20K would be irreversible upon washout of the drug.

To analyse the effect of removal of the drug, 4 µM [T20K] kalata B1 was applied until the current had declined by 20%. Thereafter washout of the drug was started. The result of a series of three experiments is shown in Figure 24.

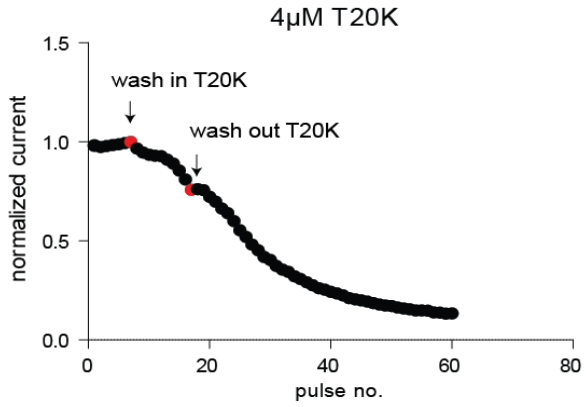

Fig.24: Effect of intermediate wash out of 4 µM [T20K] kalata B1 in Kv1.3. Whole-cell Kv1.3 currents were elicited by 200 ms step depolarization to + 40 mV from a holding potential of -80mV and intervals of 15 sec. Peak outward currents were normalized to the peak outward current elicited by the first pulse in the train. Flx = fluoxetine.Shown is a typical one single cell trace. During this measurements from the wash in until the pulse number 40 the current had decreased by 71.17% ± 7.37% ; ($P \leq 0.05$; N = 3).

As it is seen in Figure 23 and 24, 4 µM [T20K]kalata B1 shows a stronger decrease of outward current than the concentration of 2 µM , but 4 µM [T20K]kalata B1 shows another difference. The wash in of 4 µM [T20K] kalata B1 was accompanied by a continuous increase in holding current after wash in; this is shown in Figure 25. This supports the notion that application of T20K was associated with a leakage of the membrane.

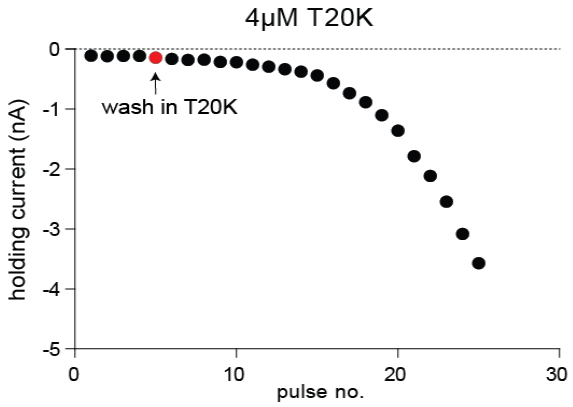

Fig. 25: Effect of 4 µM [T20K]kalata B1 on the holding current of one cell. Whole-cell Kv1.3 currents were elicited by 200 ms step depolarization to + 40 mV from a holding potential of -80 mV and intervals of 15 sec.

In a previous work it was also shown that [T20K]kalata B1 labelled with a fluorescein on the cysteine on position 5 has no cytotoxic effect like the native [T20K]kalata B1 (Hellinger et al., unpublished observations). To verify the hypotheses that the decreasing of the currents result from the cell toxicity of the [T20K]kalata B1 a fluorescein tagged [T20K]kalata B1 was analysed. The result is shown in Figure 26.

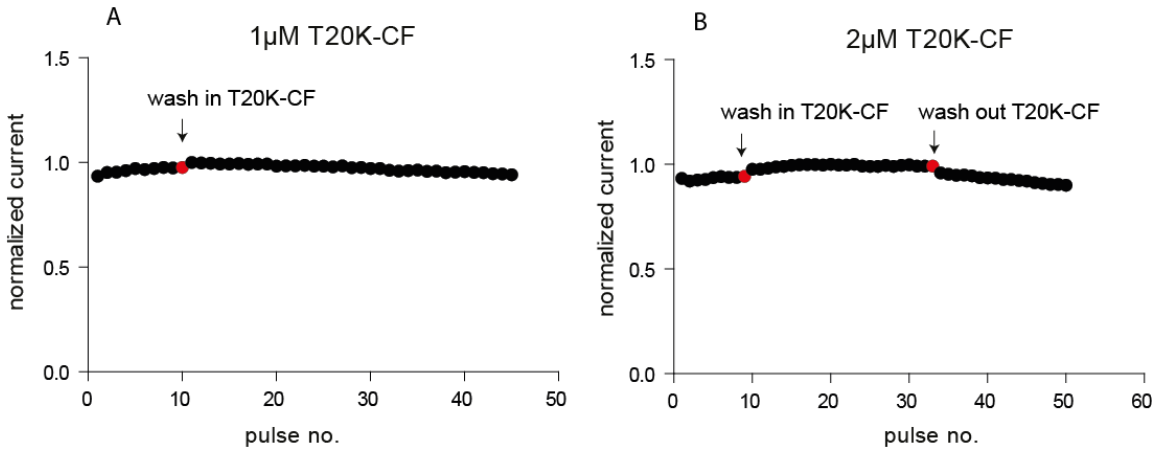

Fig. 26: Effect of 1 µM [T20K-5CF]kalata B1 and 2 µM [T20K-5CF]kalata B1 on Kv1.3. Whole-cell Kv1.3 currents were elicited by 200 ms step depolarization to + 40 mV from a holding potential of -80 mV and intervals of 15 sec. Peak outward currents were normalized to the peak outward current elicited by the first pulse in the train. Flx = fluoxetine. In both figures data from one typical cell is shown. A, the effect of 1 µM [T20K-5CF]kalata B1 is shown. From the point of wash in till the pulse 40 the current was reduced by 3.60% ± 3.63%; (P = not significant; N = 4). B, the effect of 2 µM [T20K-5CF]kalata B1 on the Kv1.3 is shown. The current between the wash in and the pulse 32 was increased by 3.48% ± 3.90%; (P = not significant; N = 4).

6. Discussion

6.1 Isolation, purification and oxidative folding of cyclotides

Since the availability of the cyclotides is limited and dependent on the extraction from native plant material, the development of efficient strategies for chemical synthesis and oxidative folding of cyclotides will be important if cyclotides ought to be used as pharmaceuticals in the future. Therefore several researchers try to determine and understand the mechanism of oxidative folding of cyclotides (Aboye et al., 2008; Gunasekara et al., 2009).

In this study the folding conditions of three different cyclotides, namely cycloviolacin O2, vigno 10 and [T20K]kalata B1, were optimized. Cycloviolacin O2 and vigno 10 are members of the bracelet subgroup and the kalata B1 mutant [T20K] is a classical Möbius cyclotide. The first step of an experiment with cyclotides is always the isolation and the purification of the certain peptide. The cycloviolacin O2, a representative from the bracelet cyclotide subgroup, was isolated from *Viola odorata* a plant from the Violaceae family and one of the best studied cyclotide containing plants whereas vigno 10 and [T20K]kalata B1 where chemical synthesised.

In general the isolation and purification of peptides from plants are limited by the sensitivity of some peptides against exposure to solvents, heat and enzymes. In the case of cyclotides this is not a problem because the CCK motif confers the cyclotides with a number of unique properties, like resistance against chemical, thermal and enzymatic degradation. During the isolation and purification of cyclotides, these properties as well as their typical late elution times on RP-HPLC are advantageous. The method used in this study is described in 4.1. With this method it is possible to extract cyclotides with high yields up to 1-2 g per kg of plant material (Ireland et al., 2010). To confirm the high purity (>95%) and the cysteine oxidation state, the native and reduced cO2 as well as the reduced vigno 10 and [T20K]kalata B1, were checked by MALDI-MS and RP-HPLC (Supplementary data 1, Appendix)

To reduce the disulfide bond which may have formed during the storage of the synthesised peptides and to reduce the native disulfide bonds in the isolated peptide, the cyclotides were incubated with DTT. The reduced peptides were then used for the folding experiments.

In previous folding studies (Hashempour et al.,2012; Aboye et al., 2008) buffers containing 0.1 M ammonium-bicarbonate buffer with high concentration of isopropanol showed the

highest yield for vigno 10 and a buffer containing Tris/HCl, DMSO, Brij 35 and EDTA achieved the highest yield for cO2 (~50% native peptide) so far. According to these publications, four different buffers with various isopropanol concentrations as well as two buffers containing DMSO, Brij 35 and different kinds of redox pairs were tested for both cyclotides (see also in Table 10). Furthermore, in the recent work of Wong et al. 2011, it was shown that high concentrations of isopropanol lead to a higher yield of folded bracelet cyclotides. In this report all buffers contained the redox agents reduced and oxidized glutathione or cystamine instead of the oxidized glutathione.

As listed in Table 14 folding of cycloviolacin O2 led to yields between ~1% and 27% of refolded native peptide. The refolding was favoured by the DMSO/detergent buffer whereas the buffers with different concentrations of isopropanol led to yields lower than 7%. This is consistently with previous studies where Aboye et al. studied the folding of cO2 and achieved a yield of ~50% at 4°C (Hashempour et al., 2012; Aboye et al., 2008). The folding of the second bracelet cyclotide, vigno 10, led to yields between 0.6 and 4% and as in the case of cO2, the isopropanol buffers led to a lower yield as the DMSO/detergent buffer. But the results doesn´t agree with the literature. It was shown in a previous study that vigno 10 folded in 75% isopropanol with 11.4% (Hashempour et al., 2012)., whereas the yield in this study is lower than 1%. This difference is surprising because the folding conditions were equal; 75% isopropanol in 0.1 M NH_4HCO_3 with a pH of 8.2 and a GSH/GSSG concentration of (2/0.1 mM). The temperature was also the same, 20°C. Only the reaction time was different, Hashempour et al. stopped the reaction after 24 h and in this study the reaction was stopped after 72 h. So it remains unclear, how to explain this difference.

The further folding conditions which were used based on the work of Buczek et al. (Buczek et al., 2006). In this previous work it was shown that albumin works as a redox-active crowding agent and thereby it could influence the kinetics and thermodynamics of forming disulfide bonds in cysteine rich peptides by providing an excluded volume effect. Furthermore it was shown that albumin accelerates the folding reactions at concentrations lower than it is need for the excluded volume effect and in lower mM concentration albumin was as affective as glutathione. Because of all these facts, two different buffers with albumin were carried out with cO2 and vigno 10 (Table 10). During the experiment it was observed that peptide precipitate by stopping the folding with TFA. After centrifugation and dissolving, the precipitate was analysed by MALDI-MS, and it was shown that no cyclotide precipitated

(data not shown). During the analysis via RP-HPLC the BSA in the sample accumulate and congest the column. So it was not possible do determine the yield of native folded peptide.

In the third experiment folding conditions were based on the work of Reinwarth et al. to refold cO2 and vigno 10 (Reinwarth et al., 2013). The buffer composition differs significantly from the other conditions (Table 10). It contains the organic solvent acetonitrile and DMSO as an oxidation agent and solvent, trifluoroethanol (TFE) as secondary structure stabilizing and solvating adjuvant; it can solubilize hydrophobic side chains and stabilize a-helices and guanidinium hydrochloride as aggregation disrupting and solvating additive. As it is shown in Table 14, the usage of this condition to refold cO2 resulted in a yield lower than 7%. The yield of the refolded vigno10 was extremely low or non-existent. This was surprisingly because Reinwarth achieved in his work yields >50% for peptides which folded in other buffers only with a very low yield. What is the difference between his peptides and my peptides? The major difference is the peptide concentration. Whereas I used in my folding experiments 20µM peptide concentration, Reinwarth used 10mg/ml. In a previous study the effect of higher peptide concentration on the folding yield was analysed (Wong et al., 2011) and it was shown that concentration higher than 100µM leads to precipitation. Also Reinwarth mentioned that during his work precipitation was a big problem which he solved with long sonication and addition of guanidinium hydrochloride as an aggregation disrupting additive. Unfortunately it was not possible to try the high concentration with cO2 and vigno10 because so much peptide was not available. A second reason could be the strong difference in the sequence of the peptides. The only similarity in the sequences of both peptides is the conserved cystine from the CCK; the remaining part is different (Reinwarth et al., 2013).

In addition to the folding of the bracelet cyclotides cO2 and vigno 10, we optimized the folding conditions for [T20K]kalata B1, which was used for the electrophysiological studies. Although several publications describe the folding of native kalata B1, it is possible that the mutant [T20K]kalata B1 requires slightly different folding conditions. Buffers containing five different conditions of isopropanol and one buffer with DMSO and Brij 35 was analysed (see Table 10). In every tested buffer, [T20K]kalata B1 folded with a yield higher than 88%; the only exception was the buffer with the highest isopropanol concentration; in this buffer the yield was lower than 1%. Generally, in the buffers containing isopropanol, an intermediate folding species was apparent which disappeared after 24 hours. The DMSO/Brij buffer showed no intermediate disulfide species (Figure 17). During the folding it was also observerd, that in samples with GSH or cysteine build some cyclotide – GSH/cysteine

complex. MALDI traces of this interaction from cO2 in the ADT (Acetonitril/DMSO/TFE) buffer with GSH are shown in the supplementary data 2, Appendix. In the first folding sample, after 5 minutes, 5 additional peaks are visible, each peak differ from the other in 307 Da which is exactle the mass of the reduced gluthathione. It seems that up to 4 molecules of GSH can bind to the cyclotide. During the folding the concentration of the cyclotide – GSH complex is declining and result after 48 hours in only two additional peaks which are barely detectable. These results suggest that during the folding several GSH and cysteine molecules bind to the cyclotide but with the time and maybe through oxidation they dissociate from the peptide.

As the results in this study shows, the oxidative folding of bracelet cyclotides seems to be fundamentally different from the folding of Möbius cyclotides. The folding of the Möbius [T20K]kalata B1 was characterised by one and two disulfide folding intermediate species; on the other hand the folding of the bracelet cyclotide cO2 is dominated by fully oxidised peptides (Supplementary Data 4, Appendix). .This is in agreement with the previous work of Aboye et al., 2008. In addition to the different folding pathways, the two subfamilies also require different folding conditions *in vitro* and it seems that the folding of bracelet cyclotides is sequence-dependent. A sequence comparison of the three cyclotides, which were analysed in this study, is shown in Table 15. It shows that the sequence of cO2 and vigno 10 differs only in 5 amino acids (Table 15), whereas the sequence of [T20K]kalata B1 has little similarity to bracelet cyclotides. The [T20K]kalata B1folded in a isopropanol buffer without any special co-solvent at high yields, while the cO2 and especially vigno 10 folded with very low yields. This leads to the assumption that bracelet cyclotides need more complex folding conditions with special co-solvents. In this study it is also shown that [T20K]kalata B1 folded in high yields in the special DMSO/Brij buffer which is optimized for the folding of cO2 (Table 14).

Table 15: Sequence comparison of cycloviolacin O2, vigno 10 and [T20K]kalata B1

cyclotide	amino acid sequence	mass (Da)	subfamily
cO2	G-IPCGESCVWIPCISSAIGCSCKSKVCYRN	3138.3	bracelet
vigno10	GTIPCGESCVWIPCISSVVGCSCKSKVCYKD	3226.2	bracelet
T20K	GLPVCGETCVGGTCNTP--GCTCSWPVCTRN	2843.9	Möbius
cysteine	I II III IV V VI		

One of the reasons of the different folding yields is the different structure of the subfamilies. A structure comparison between the Möbius cyclotide kalata B1 and the bracelet cyclotide cycloviolacin O2 is presented in Figure 2. One of the distinguish factors between the subfamilies is located in loop 5. This loop contains a cis-Pro bond which his highly conserved in Möbius cyclotides, resulting in a conceptual 180° twist in the backbone and is characteristic for this subfamily. Bracelet cyclotides often have two Lys residues in this loop instead. Aboye and collegues show that this difference in loop 5 is not the determining factor for the different oxidative folding properties. Folding of a hybrid Möbius/bracelet kalata B1-based (W19K/P20N/V21K) cyclotide was successful using folding conditions which are typical for Möbius cyclotides (Aboye et al., 2008). Gunasekera et al. show in their studies that a different loop 3 sequence is responsible for the need of co-solvents and detergents in the folding of bracelet cyclotides. In this loop a surface-exposed hydrophobic patch is located in bracelet cyclotides and this patch is stabilised by the presence of DMSO and the non-ionic detergent Brij 35 (Gunasekera et al., 2009).

Generally, successful folding of cyclotides depends on several parameters which can be summarized as follows: (i) prevention of aggregation, (ii) the maintenance of a proper redox potential and (iii) the use of a structure enhancing/stabilizing solvent system. Cyclotides favour aggregation because of the high number of ß sheets and hydrophobic patches (Wong et al., 2011). In this study, aggregation was not a problem because the protein concentration was fixed at 20 µM and at this concentration no aggregation occurs. The redox potential is needed for the oxidation of the cystine residues which is usually mediated by air oxygen, glutathione or DMSO (Wong et al., 2011). The correct building of the disulfide bridges is essential for the structure and therefore the biological activity of cyclotides that is why this step is very crucial. The problem with air oxygen is the very slow reaction rates, but the use of strong oxidation

agents can lead to significant sight reactions by incorrect bridging of cysteine residues (Gunasekera et al., 2008). To prevent such side reactions, mild oxidation agents like glutathione or cystamine was used; in some buffers in combination with the slightly oxidizing agent DMSO. Successful oxidative folding also depends on structural factors like proximity and accessibility of the cysteine residues (Wong et al., 2011). The proximity drives the kinetics of disulfide bridge formation between neighbouring cysteine residues, and distance of cysteines often leads to misfolded species. For example the misfolded cyclotide Cys I-II, III-IV, V-VI is the major side-product which is described in the work of Gunasekera et al. and Aboye et al. (Gunasekera et al., 2008; Aboye et al., 2008). However, for the formation of native disulfide bonds it is necessary that the cysteine residues come to a sufficient proximity. In a closed structure like the ring-structure of cyclotides, proximity is not the determining factor, because the closed backbone structure constrains the cysteine residues into close proximity. The determinants are more likely the loop entropy and enthalpy factors (Wong et al., 2011). An approach to reduce the amount of misfolded peptide is to maintain the redox potential system. This is very crucial because DMSO, a mild oxidant, alters the GSH:GSSH ratio and the redox system to an oxidizing environment (Wong et al., 2011), leading to an irreversible accumulation of “kinetically misfolded” products. In folding buffers containing DMSO, the addition of fresh GSH:GSSG at regular intervals restore the proper redox intervals during the folding reaction and thereby it reduce the amount of misfolded peptides (Wong et al., 2011). That is why in the folding studies of this work new redox agents were added to the folding approach after 24 and 48 hours. Furthermore the temperature and the pH, which affects the thiol-disulfide exchange reactions, are also factors which can increase the yield of native folded peptide.

The third parameter is the use of a structure enhancing solvent. The “closed” structure of cyclotides leads to a steric crowded interior during the oxidation of the cysteine residues (Wong et al., 2011). During the folding the cystine knot is located in the interior, whereas the hydrophobic side chains move to the exterior which is the reason for a hydrophobic nature of the peptides and that is why the native peptide elutes later from a RP-HPLC column than the reduced cyclotide (Aboye et al., 2008). This hydrophobic nature of cyclotides needs a hydrophobic co-solvent in the folding buffer like DMSO, ACN, TFE or isopropanol (Gunasekera et al., 2009). The reason for that is that the hydrophobic solvent can help to reduce the energy barrier for the formation of the hydrophobic surface, whereas water would prevent folding, it would repel hydrophobic side chains and force them into the interior.

After folding of cyclotides, the second aim of this work was to analyse whether the immunosupressive cyclotide [T20K]kalata B1 can interact with the potassium channel Kv1.3 which plays a crucial role in the activation of T- cells.

6.2 Ion channel modulation of [T20K]kalata B1

Ion channels play a crucial role for human physiology. For example they are necessary to maintain the membran potential as well as to regulate muscle contraction and cell proliferation (Bagal et al., 2013). This study focuses on the voltage gated potasssium channel Kv1.3 which is one of 76 human K^+ channels that regulates the membrane potential and Ca^{2+} signaling in human T-cells (Feske et al., 2012). Hence his major function is the activation of T-cells and therefore the regulation of an immune response. Its expression is increased 4- to 5-fold in activated T-cells compared to non activated T-cells. .

Because of the essentail role ion channels play in the human body, blockers of ion channels have significant therapeutic potential in the management of diseases affecting excitable and nonexcitable tissues (Camerrino et al., 2007). For example the proliferation of T-cells can be specifically and persistently inhibited by blockers of Kv1.3. This underlines the therapeutic potential of high-affinity and high specificity Kv1.3 inhibitors. In previous studies, several naturally-occurring peptides, especially from scorpion venom and sea anemones have been described to be effective blockers of the Kv1.3 channels (Panyi et al., 2006 and Gurrola et al., 2012). Furthermore, the peptide Vm24 which is described by Gurrola et al. as a selective Kv1.3 blocker shows a immunosupressive property and is like the immunosupressive cyclotide [T20K]kalata B1 a disulfide-rich peptide from a natural source. (Gurrola et al., 2012). The target of the [T20K]kalata B1 peptide remains unknown, but the structure similarity with the Vm24 suggest that it might block the Kv1.3 channel and that leads to the immunosupressive effect of [T20K]kalata B1 (Gründemann et al., 2013; Gurrola et al., 2012). As mentioned above, [T20K]kalata B1 is a mutant of the cyclotide kalata B1 where the threonine at position 20 is exchanged with a lysine. The posibility whether cyclotides can bind to ion channels was analysed by Anna Weizinger (University of Vienna, Institute of Pharmacy) using a modelling approach. She conclude that cyclotides can interact with ion channel, which is shown in a 3D structural model in Figure 6.

Therefore the aim of this thesis was to determine whether [T20K]kalata B1 blocks the Kv1.3 channel and thereby inhibits the proliferation of T-cells. The primary goal was to analyse this

hypothesis in native human T-cells, but these cells were very difficult to patch and it was not possible to reach a satisfying giga seal. Hence tsA-cells were used next which were transfected with a recombinant human Kv1.3. Inital control measuremnts were carried out with the standard blocker fluoxetine. Fluoxetine is an important antidepressant drug by inhibition of the reuptake of serotonin into the synaptic cleft. In addition to his pharmacological properties, it influence a variety of ion channels, including voltage-activated potassium channels. Fluoxitine is not a selective blocker of Kv1.3 but it is a good control for the purpose of our measurement . Fluoxetine was used in a concentration of 10 µM and showed a 61.23% ± 2.69% block (Figure 20) which is comparable whit the work of Choi et al. (1999).

After confirming the validity of the patch clamp set up by testing the blocker fluoxetine, [T20K]kalata B1 was analysed at a concentration of 2 µM. As shown in Figure 21, there is no significant effect after wash in of 2 µM [T20K]kalata B1. Although there is a small continuous declining of the current (19.3% ± 3.92%) this is not significantly higher than the run-down of the current shown in Figure 18 (P = not significant). In Figure 18 the current also declined with 12.22% ± 4.35% when the cell was perfused with extracellular solution. This leads to the result that the declined current with 2 µM [T20K]kalata B1is rather run-down or non-specific than a slow block. In addition to finding that the kalata B1 mutant [T20K]kalata B1 has immunosuppressive properties, Gründemann et al. also identified a mutant which showed no immunosuppressive activity (Gründemann et al., 2013). In this mutant the valine at position 10 is exchanged through a lysine (mutant [V10K]). This mutant served as a negative control in our measurements and was tested in the same concentrations as [T20K]kalata B1. A wash in of 2 µM [V10K] showed the same results as 2 µM [T20K]kalata B1 (Figure 22), the current is declining with 15.70% ± 4.57% (P = not significant). That confirms the result discussed above and allows us to conclude that with 2 µM [T20K]kalata B1 no block, not even a slow block is observable. Gründemann et al. showed in his work that a concentration of 1.8 µM [T20K]kalata B1 leads to a 20% reduction of activated T-cells. If Kv1.3 was the target of [T20K]kalata B1 then it should be at least a small block of the current visible (Gründemann et al., 2013).

After measuring 2 µM of [T20K]kalata B1 the concentration was increased to 4 µM (Figure 23). This time [T20K]kalata B1 showed also a continuous decline of the current, but more steep than with 2 µM [T20Kkalata B1 (52.10% ± 8.5%; which is a significant reduced compared to the run-down, $P \leq 0.05$), whereas 4 µM of [V10K] showed no significant decline

of the current (2.41% ± 2.81%) (Figure 23). It was also shown that the wash-in of 4 µM [T20K]kalata B1 was accompanied by a continuous increase of the holding current (Figure 25). The continuous decrease of the current could be explain with the decline of the holding current at the same time, which suggests that the peptide interacts with the membrane and disrupt it by forming pores. The slow disruption of the membrane led to additional pores in the membrane where ions cross the cell wall, which disturbs the membrane potential and hence affects the measurements of the potassium channels leading to the increasing holding current. The ability of cyclotides to form pores in cell membrane is described in several papers (Sando et al., 2011; Cascales et al., 2011; Burman et al., 2011; Wang et al., 2012; Henriques et al., 2011). It was suggested that kalata B1 can enter the cell and it is classified in a new family of cell penetrating peptides (Cascales et al., 2011). In a previous study it was shown that the bioactivity of kalata B1 is dependent on the lipid composition of target cell membranes and furthermore that the anti-HIV activity of kalata B1 is the result of its ability to target and disrupt the membrane of HIV particles (Henriques et al., 2011). In general it is considered that the cell membrane plays an essential role in several different bioactivities of cyclotides (Wang et al., 2012). Sando et al., suggest in their work that the pore formation mechanism can be explained by four consecutive steps (Sando et al., 2011). First step is the binding of kalata B1 to the membrane surface which is controlled by hydrophobic interactions and facilitated by phosphoethanolamine phospholipids. The second step includes the oligomerization of the peptide and step 3 comprises the insertion into the hydrophobic core. The last step is the pore formation as the embedded peptides span the two layers of the membrane. The pore formation mechanism of cyclotides is shown in Figure 27. Maybe the ability of forming pores plays also a role in the immunosuppressive property of cyclotides. To determine this, further analyses are necessary.

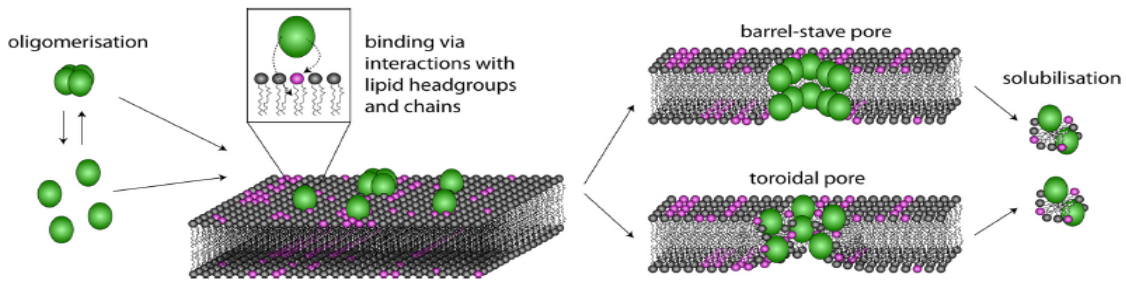

Fig.27: Pore formation mechanism of cyclotides. Cycotides can bind to the membrane as monomers or oligomers by ineraction with the lipid headgroups. After a treshold concentration of cyclotides has been reached, cyclotides permeate the membrane either via a barrel-stave pore or a toroidal pore. In high concentration cyclotides can also solubilizes the membrane (Wang et al., 2012).

A second possibility to analyse if the continuous decline is a block or just a non-specific event was to wash the peptide out after a couple of pulses as shown in Figure 24. The peptide 4 µM [T20K]kalata B1 was washed in for a few pulses and then washed out with extracellular solution. If [T20K]kalata B1 was a blocker then it would be expected that the current is decreasing no further and it should remain stable during the wash out. However, as seen in the Figure 24, the current, despite the wash out, further decreased (71.17% ± 7.37%).

As it was shown in a previous study (Hellinger et al., unpublished observations) a fluorescein tagged [T20K]kalata B1 result in a non-cytotoxic peptide. The fluorescein label on the cysteine on position 5 change the general charge of the peptide, hence it cannot interact with the cell membrane anymore. Because of the less cell toxicity the labeled peptide is a good control if the decreasing current is a result of the leakage of the membrane. As it is shown in figure 26 there is no change in the current with 1µM and with 2µM the current was slightly increased, which confirm the previous results.

To sum up, the active mutant [T20K]kalata B1 showed at a concentration of 2 µM the same effect as the inactive mutant [V10K], and no block of the Kv1.3 was observed. The concentration of 4 µM [T20K]kalata B1 showed a continuous slow decrease of the current which can be explained by the decrease of the holding current and the cytotoxicity of the peptide; 4 µM [V10K] showed no decline of the current and the holding potential, and this can be explained with the lower cytotoxicity of [V10K] compared to [T20K]kalata B1 (Hellinger et al., unpublished observations). Furthermore it was not possible to determine a dose-response relationship, since 2 µM and 4 µM of the peptide indicated toxic effects. Also the intermediate wash out showed not the typical blocker effect. That allows us to conclude that [T20K]kalata B1 is not a blocker for the voltage gated potassium channel Kv1.3.

7. Conclusion and Outlook

In this study the folding conditions for three cyclotides, namely cycloviolacin O2, vigno 10 and the kalata B1 mutant [T20K], was optimized with the aim to improve their *in vitro* folding yields. It is also known that [T20Kkalata B1 has an immunosuppressive effect, but the target remains still unknown. One possible target is the voltage gated potassium channel Kv1.3 which plays an important role in the T-cell activation. Hence we analysed whether [T20K]kalata B1 can block this ion channel.

Different folding conditions were carried out and it was shown that without the use of an organic co-solvent, like DMSO and Brij 35 the oxidative folding yield of bracelet cyclotides decreased to < 5%, whereas the Möbius cyclotide [T20K]kalata B1 folded in isopropanol buffers without any second co-solvent with high yields. The result of this study shows that the oxidative folding of bracelet cyclotides is still challenging and likely needs to be optimized on a case-by-case basis in the future. In particular the formation of the three disulfide bonds, which build the cystine knot, is the crucial step in the oxidative folding of cyclotides. Because of the sequence diversity between the bracelet cyclotides, in future it will be necessary to tune the folding conditions individually for each bracelet cyclotide.

The electrophysiological analysis of [T20K]kalata B1 comes to the result, that the voltage gated potassium channel Kv1.3 is not a target for the cyclotide [T20K]kalata B1. It was shown that [T20K]kalata B1 doesn’t decrease the voltage of this channel. Rather it seems to interact with the membrane and leads to a formation of pores. Hence it was not possible to determine a dose-response curve. The target of [T20K]kalata B1 still remains unknown and further analyses will be necessary to determine the mechanism of the immunosuppressive effect of [T20K]kalata B1.

8. References

Aboye, T. L., Clark, R. J., Burman, R., Roig, M. B., Craik, D. J., and Göransson, U., 2011. Interlocking disulfides in circular proteins: Toward efficient oxidative folding of cyclotides. Antioxidants & Redox Signaling 14: 77-86.

Aboye, T. L., Clark, R. J., Craik, D. J. and Göransson, U., 2008. Ultra-stable peptide scaffolds for protein engineering-synthesis and folding of the circular cystine knotted cyclotide cycloviolacin O2. ChemBioChem 9: 103-113

Bagal, S. K., Brown, A. D., Cox, P. J., Omoto, K., Owen, R. M., Pryde, D. C., Sidders, B., Skerratt, S.E., Stevens, E. B., Storer, R. I. and Swain, N. A., 2013. Ion channels as therapeutic targets: a drug discovery perspective. Journal of Medicinal Chemistry 56: 593-624.Buczek, O., Green, B. R., Bulaj, G., 2006. Albumin is a redox-active crowding agent that promotes oxidative folding of cysteine-rich peptides. Peptide Science 88:, 8-19

Burman, R., Strömstedt, A.A., Malmsten, M. and Göransson, U., 2011. Cyclotide-membrane interactions: Defining factors of membrane binding, depletion and disruption. Biochimica et Biophysica Acta 1808: 2665-2673

Cahalan, M. D. and Chandy, K. G., 1997. Ion channels in the immune system as targets for immunosuppression. Current Opinion in Biotechnology 8: 749-756

Cahalan, M. D., Chandy, K. G., DeCoursey, T. E. and Gupta, S., 1985. A voltage-gated potassium channel in human T-lymphocytes. Journal of Physiology 385: 197-237

Cahalan, M. D., Wulff, H. and Chandy, G., 2001. Molecular properties and physiological roles of ion channels in the immune system. Journal of Clinical Immunology 21: 235-52

Camerino, D. C., Tricarico, D. and Desaphy, J-F, 2007. Ion channel pharmacology. The Journal of the American Society for Experimental NeuroTherapeutics 4: 184-198

Cascales, L., Henriques, S.T., Kerr, M.C., Huang, Y.H., Sweet, M.J., Daly, N.L. and Craik, D.J., 2011. Identification and characterization of a new family of cell-penetrating peptides. Journal of Biological Chemistry 286: 36932-36943

Chandy, K. G., DeCoursey, T. E., Cahalan, M. D., McLaughlin, C. and Gupta, S., 1984. Voltage-gated potassium channels are required for human T lymphocyte activation. Journal of Experimental Medicine 160: 369-85

Chandy, K. G., Wulff, H., Beeton, C., Pennington, M., Gutman, G. A. and Cahalan, M. D, 2004. K+ channels as targets for specific immunomodulation. Trends in Pharmacological Sciences 25: 280-9

Choi, B. H. and Hahn, S. J., 2010 Kv1.3: a potential pharmacological target for diabetes. Acta Pharmacologica Sinica 31: 1031-1035

Choi, J. S., Hahn, S. J., Rhie, D. J., Yoon, S. H., Jo, Y. H. and Kim, M. S., 1999. Mechanism of fluoxetine block of cloned voltage-activated potassium channel Kv1.3. Journal of Pharmacology and Experimental Therapeutics 291: 1-6

Coghlan, M. J., Carroll, W. A. and Gopalakrishnan, M., 2001. Recent developments in the biology and medicinal chemistry of potassium channel modulators: Update from decade of progress. Journal of Medicinal Chemistry 44: 1627-53

Colgrave, M. L., Kotze, A. C., Ireland, D. C., Wang, C K. and Craik, D. J., 2008. The anthelmintic activity of the cyclotides: natural variants with enhanced activity. Chembiochem 9: 1939-45

Conlan, B. F., Gillon, A. D., Craik, D. J. and Anderson, M. A., 2010. Circular proteins and mechanisms of cyclization. Biopolymers 94: 573-583.

Cragg, G. M. and Newman, D. J., 2013. Natural products: A continuing source of novel drug leads. Biochimica et Biophysica Acta 1830: 3670-3695

Craik, D. J., 2011. The folding of disulfide-rich proteins. Antioxidants & Redox Signaling 14, 61-4

Daly, N. L., Rosengren, K. J. and Craik, D. J., 2009. Discovery, structure and biological activities of cyclotides. Advanced Drug Delivery Reviews 61: 918-930

Davidson, A. and Diamond, B., 2001. Autoimmune diseases. New England Journal of Medicine. 345: 340-350

de Mattos, A.M., Olyaei, A.J. and Bennett, W.M., 2000. Nephrotoxicity of immunosuppressice drugs: Long-term conseauences and challenges for the future. American Journal of Kidney Diseases 35: 333-346

Delprete, P.G., Smith, N.P., Heald, S.V., Henderson, A., Mori, S.A. and Stevenson, D.W., 2004. Flowering plant families of the american tropics. New York Botanical Garden Press: 328-33

Ermann, J. and Fathman, C.G., 2001. Autoimmune diseases: genes, bugs and failed regulation. Nature Immunology 2: 759-761

Fantz, P. R., 1991. Ethnobotany of Clitoria (Leguminosae). Economic Botany 45: 511-520

Farnsworth, N. R., 1990. The role of ethnopharmacology in drug development. Ciba Foundation symposium 154: 2-11.

Farrokhi, N., Whitelegge, J. P. and Brusslan, J. A., 2008. Plant peptides and peptidomics. Plant Biotechnology Journal 6: 105-134

Felizmenio-Quimio, M.E., Daly, N.L. and Craik, D.J., 2001. Circular proteins in plants: solution structure of a novel macrocyclic trypsin inhibitors from *Mormordica cochinchinensis*. Journal Biological Chemistry 276: 22875-82.

Feske, S., Skolnik, E.Y., Prakriya, M., 2012. Ion channels and transporters in lymphocytes function and immunity. Nature reviews. Immunology 12: 532-547

Galvez, A., Gimenez-Gallego, G., Reuben, J. P., Roy-Contancin, L., Feigenbaum, P., Kaczorowski, G. J. and Garcia, M. L., 1990. Purification and characterization of a unique, potent, peptidyl probe for the high conductance calcium-activated potassium channel from venom of the scorpion Buthus tamulus. Journal of Biological Chemistry 265: 11083-90

Garcia-Calvo, M., Leonard, R. J., Novick, J., Stevens, S. P., Schmalhofer, W., Kaczorowski, G. J. and Garcia, M. L., 1993. Purification, characterization, and biosynthesis of margatoxin, a component of Centruroides margaritatus venom that selectively inhibits voltage-depentent potassium channels. Journal of Biological Chemistry 268: 18866-74

Gerlach, S. L. and Mondal, D., 2012. The bountiful biological activities of cyclotides. Chronicles of Young Scientists Issue 3: 169-177

Gerlach, S. L., Rathinakumar, R., Chakravarty, G., Göransson, U., Wimley, W. C., Darwin, S. P., and Mondal, D., 2010. Anticancer and chemosensitizing abilities of cycloviolacin O2 from Viola odorata and psyle cyclotides from Psychotria leptothyrsa. Biopolymers 94: 617-25.

Gillon, A. D., Saska, I., Jennings, C. V., Guarino, R. F., Craik, D. J., and Anderson, M. A., 2008. Biosynthesis of circular proteins in plants. The Plant Journal 53: 505-515

Göransson, U., Sjögren, M., Svangard, E., Claeson, P. and Bohlin, L., 2004. Reversible antifouling effect of the cyclotide cycloviolacin O2 against barnacles. Journal of Natural Products 67: 1287-90

Gran, L., 1973.On the effect of a polypeptide isolated from "Kalata-Kalata" (Oldenlandia affinis DC) on the oestrogen dominated uterus. Acta Pharmacologica et Toxicologica 33: 400–408

Gruber, C. W., Cernazar, M., Clark, R. J., Horibe, T., Renda, R.F., Anderson, M. A., and Craik, D. J., 2007. A novel plant protein-disulfid isomerase involved in the oxidative folding of cystine knot defense proteins. Journal of Biological Chemistry 282: 20435-20446

Gruber, C. W., Elliott, A. G., Ireland, D. C., Delprete, P. G., Dessein, S., Goransson, U., Trabi, M., Wang, C. K., Kinghorn, A. B., Robbrecht, E. and Craik, D. J., 2008. Distribution and Evolution of Circular Miniproteins in Flowering Plants. The Plant Cell 20: 2471-2483.

Gruber, C. W., Muttenthaler, M., and Freissmuth, M., 2010. Ligand-Based peptide design and combinatorial peptide libraries to target G Protein-coupled receptors. Current Pharmaceutical Design 16: 3071-3088

Gründemann, C., Koehbach, J., Huber, R., Gruber, C. W., 2012. Do plant cyclotides have potential as immunosuppressant peptides? Journal of Natural Products 75: 167-174

Gründemann, C., Thell, K., Lengen, K., Garcis-Käufer, M., Huang, Y. H., Huber, R., Craik, D.J., Schabbauer, G. and Gruber, C. W., 2013. Cyclotides suppress human T-lymphocyte proliferation by an interleukin 2-depentent mechanism. Public Library of Science ONE 8(6): e68016

Gunasekera, S., Daly, N. L., Anderson, M. A. And Craik, D. J., 2006. Chemical synthesis and biosynthesis of the cyclotide family of circular proteins. IUBMB Life 58, 515-24

Gunasekera, S., Daly, N. L., Clark, R. J., and Craik, D. J., 2009. Dissecting the oxidative folding of circular cystine knot miniproteins. Antioxidants & Redox Signaling11, 971-980

Gurrola, G. B., Hernandez-Lopez, R. A., Rodriguez de la Vega, R. C., Varga, Z., Batista, C. V. F., Salas-Castillo, S. P., Panji, G., del Rio-Portilla, F. and Possani, L. D., 2012. Structure, function, and chemical synthesis of Vaejovis mexicanus peptide 24: A novel potent blocker of Kv1.3 potassium channels of human T lymphocytes. Biochemistry 51, 4049-61

Hashempour, H., Koehbach, J., Daly, N. L., Ghassempour, A. and Gruber, C.W., 2012. Characterizing circular peptides in mixtures: sequence fragment assembly of cyclotides from a violet plant by MALDI-TOF/TOF mass spectrometry. Amino Acids 44, 581-95

Henriques, S.T., Huang, Y.H., Rosengren, K.J., Franquelim, H.G., Carvalho, F.A., Johnson, A., Sonza, S., Tachedjian, G., Castanho, M.A.R.B., Daly, N.L. and Craik, D.J., 2011. Decoding the membrane activity of the cyclotide kalata B1. Journal of Biological Chemistry 286: 24231-24241

Hernandez, J., Gagnon. J., Chiche, L., Nguyen, T., Andrieu, J. and Heitz, A., 2000. Squash trypsin inhibitors from *Momordica cochinchinensis* exhibit an atypical macrocyclic structure. Biochemistry 39: 5722-30

Ireland, D. C., Clark, R. J., Daly, N. L. and Craik, D. J., 2010. Isolation, Sequencing, and Structure – Activity Relationships of Cyclotides. Journal of Natural Products 73, 1610-1622

Ireland, D. C., Colgrave, M. L. and Craik, D. J., 2006. A novel suite of cyclotides from Viola odorata: sequence variation and the implications for structure, function and stability. Biochemical Journal 400, 1-12

Ireland, D. C., Wang, C. K., Wilson, J. A., Gustafson, K. R. and Craik, D. J., 2008. Cyclotides as natural anti-HIV agents. Biopolymers 90, 51-60

Jennings, C. V., Rosengren, K J., Daly, N. L., Plan, M., Stevens, J., Scanlon, M. J., Waine, C., Norman, D. G., Anderson, M. A. and Craik, D. J., 2005. Isolation, solution structure, and insecticidal activity of kalata B2, a circular protein with a twist: do Möbius strips exist in nature? Biochemistry 44, 851-60

Kalman, K., Pennington, M. W., Lanigan, M. D., Nguyen, A., Rauer, H., Mahnir, V., Paschetto, K., Kem, W. R., Grissmer, S., Gutman, G. A., Christian, E. P., Cahalan, M. D., Norton, R. S. and

Chandy, K. G., 1998. shK-Dap22, a potent Kv1.3-specific immunosuppressive polypeptide. Journal of Biological Chemistry 273(49), 32697-707

Katoh, E., Nishio, H., Inui, T., Nishiuchi, Y., Kimura, T., Sakakibara, S. and Yamazaki, T., 2000. Structural basis for the biological activity of dendrotoxin-I, a potent potassium channel blocker. Biopolymers 54: 44-57

Koehn, F. E. and Carter, G. T., 2005. The evolving role of natural products in drug discovery. Nature Reviews in Drug Discovery 4: 206-220.

Koo, G. C., Blake, J. T., Talento, A., Nguyen, M., Lin, S., Sirotina, A., Shah, K., Mulvany, K., Don Hora, Jr., Cunningham, P., Wunderler, D. L., McManus, O. B., Slaughter, R., Bugianesi, R., Felix, J., Garcia, M., Williamson, J., Kaczorowski, G., Sigal, N. H., Springer, M. S. and Feeney, W., 1997. Blockade of the voltage- gated potassium channel Kv1.3 inhibits immune resposnes in vivo. Journal of Immunology 158: 5120-8

Korukottu, J., Schneider, R., Vijayan, V., Lange, A., Pongs, O., Becker, S., Baldus, M. and Zwecjstetter, M., 2008. High-resolution 3D structure determination of kaliotoxin by solid-state NMR spectroscopy. Public Library of Science One 3: e2359

Lindholm, P., Göranssin, U., Johansson, S., Claeson, P., Gullbo, J., Larsson, R., Bohlin, L. and Backlund, A., 2002. Cyclotides: a novel type of cytotoxic agents. Molecular Cancer Therapeutics 1: 365-9

Malmivuo, J., Plonsey, R., 1995. Bioelectromagnetism. Oxford University Press, New York. p.250-284

Matsuda, S. and Koyasu, S., 2000. Mechanisms of action of cyclosporine. Immunopharmacology 47: 119-125

Neher, E., Sakmann, B., Steinbach, J.H., 1978. The extracellular patch clamp: a method for resolving currents through individual open channels in biological membranes. European journal of physiology 375: 219-28

Nemazee, D., 2006. Receptor editing in lymphocyte development and central tolerance. Nature Reviews in Immunology 6: 728-740

Newman, D. J. and Cragg, G. M., 2007. Natural products as sources of new drugs over the last 25 years. Journal of Natural Products 70: 461-477.

Ogden, D. and Stanfield, P., 1994. Patch clamp techniques for single channel and whole-cell recording. Microelectrode Techniques: The Plymouth Workshop Handbook. Company of Biologists Ltd., Cambridge, UK, p. 53.

Oh-hora, M., 2009. Calcium signaling in the development and function of T-lineage cells. Immunology Review 231: 210-224

Panyi, G., Possani, L. D., Rodríguez de la Vega, R. C., Gaspar, R., and Varga, Z., 2006. K+ channel blockers: novel tools to inhibit T cell activation leading to specific immunosuppression. Current Pharmaceutical Design 12: 2199-220

Pardo, L.A., 2004. Voltage-gated potassium channels in cell proliferation. Physiology 19: 285-92

Plan, M R., Saska, I., Cagauan, A. G., Craik, D. J., 2008. Backbone cyclised peptides from plants show molluscicidal activity against the rice pest Pomacea canaliculata (golden apple snail). Journal of Agricultural and Food Chemistry. 56: 5237-41

Pope, J. E. and Deer, T. R., 2013. Ziconotide: a clinical update and pharmacologic review. Expert Opinion Pharmacotherapy 14: 957-66

Poth, A.G., Colgrave, M.L., Philip, R., Kerenga, B., Daly, N.L., and Anderson, M.A., 2011. Discovery of cyclotides in the Fabaceae plant family provides new insights into the cyclization, evolution, and distribution of circular proteins. ACS Chemical Biology 6: 345-5

Pragl, B., Koschak, A., Trieb, M., Obermair, G., Kaufmann, W. A., Gerster, U., Blanc, E., Hahn, C., Prinz, H., Schütz, G., Darbon, H., Gruber, H. J. and Knaus, H. G., 2002. Synthesis, characterization, and application of cy-dye- and alexa-dye-labeled hongotoxin(1) analogues. The first high affinity fluorescence probes for voltage gated K+ channels. Bioconjugate Chemistry 13: 416-25

Purves, W. K, Sadava. D., Orians, G. H. and Heller, H. C., 2004. Biologie, 7.Auflage. Spektrum Akademischer Verlag.

Qin, Q., McCallum, E. J., Kaas, Q., Suda, J., Saska, I., Craik, D. J. and Mylne, J. S., 2010. Identification of candidates for cyclotide biosynthesis and cyclisation by expressed sequence tag analysis of Oldenlandia affinis. BMC Genomics 11: 111-120

Reinwarth, M., Glotzbach, B., Tomaszowski, M., Fabritz, S., Avrutina, O. and Kolmar, H., 2013. Oxidative folding of peptides with cystine-knot architectures: Kinetic studies and optimization of folding conditions. ChemBioChem 14: 137-146

Rycraft, B., Halliday, F. C. and Gibb, A., 2006. Patch Clamping. Cell Biology. Elsevier Science (USA): p.395-403

Saether, O., Craik, D. J., Campbell, I. D., Sletten, K., Juul, J. and Norman, D. G., 1995. Elucidation of the primary and three-dimensional structure of the uterotonic polypeptide kalata B1. Biochemistry 34: 4147-58

Sando, L., Henriques, S.T., Foley, F., Simonsen, S.M., Daly, N.L., Hall, K.N., Gustafson, K.R., Aguilar, M.I. and Craik, D.J, 2011. A synthetic mirror image of kalata B1 reveals that cyclotide activity is independent of a protein receptor. ChemBioChem 12: 2456-2462

Sanguinetti, M. C., Johnson, J. H., Hammerland, L. G., Kelbaugh, P. R., Volkmann, R. A., Saccomano, N. A. and Mueller, A. L., 1997. Heteropodatoxins: peptides isolated from spider venom that block Kv4.2 potassium channels. Molecular Pharmacology 51: 491-8

Saska, I., Gillon, A. D., Hatsugai, N., Dietzgen, R. G., Hara-Nishimura, I., Anderson, M. A., and Craik, D. J., 2007. An asparaginyl endopeptidase mediates in vivo protein backbone cyclization. Journal of Natural Products 282: 29721-29728

Schütt, C., Bröker, B., 2009. Grundwissen Immunologie.. Spektrum Akademischer Verlag. 2.Auflage: 10-70

Sharma, S., Singh, R. and Rana, S., 2012. Bioactive Peptides: A Review. International Journal of Bioautomation 15: 223-250

Smith-Garvin, J. E., Koretzky, G. A. and Jordan, M. S., 2009. T cell activation. Annual Reviews in Immunology 27: 591-619

Tam, J. P., Lu, Y. A., Yang, J. L. And Chiu, K. W., 1999. An unusual structural motif of antimicrobial peptides containing end-to-end macrocycle and cystine.knot disulfides. Proceedings of the National Academy of Scienses U.S.A. 96: 8913-8918

Terlau, H. and Olivera, B. M., 2004. Conus venoms: a rich source of novel ion-channel-targeted peptides. Physiology Reviews 84: 41-68

Varga, Z., Gurrola-Briones, G., Papp, F., Rodriguez de la Vega, R. C., Pedraza-Alva, G., Tajhya, R. B., Gaspar, R., Cardenas, L., Rosenstein, Y., Beeton, C., Possani, L., D. and Panyi, G., 2012. Vm24, a natural immunosuppressive peptide, potently and selectively blocks Kv1.3 potassium channels of human T cells. Molecular Pharmacology 82: 372-382

Vetter, I. and Lewis, R.J., 2012. Therapeutic potential of cone snail venom peptides (conopeptides). Current Topics in Medicinal Chemistry 12: 1546-52

Wang, C. K., Colgrave, M. L., Ireland, D. C., Kaas, Q. and Craik, D. J., 2009. Despite a conserved cystine knot motif, different cyclotides have different membrane binding modes. Biophysical Journal 97: 1471-1481

Wang, C.K., Wacklin, H.P. and Craik, D.J., 2012. Cyclotides insert into lipid bilayers to form membrane pores and destabilize the membrane through hydrophobic and phosphoethanolamine-specific interactions. Journal of Biological Chemistry 52: 43884-43898

Wang, R., Xie, H., Huang, Z., Ma, J., Fang, X., Ding, Y and Sun, Z., 2011. Transcription factor network regulating CD(+)CD8(+) thymocyte survival. Critical reviews in immunology 31: 447-58

Witherup, K. M., Bogusky, M. J., Anderson, P. S., Ramjit, H., Ransom, R. W., Wood, T. and Sardana, M., 1994. Cyclopsychotride A, a biologically active, 31-residue cyclic peptide isolated from Psychotria longipes. Journal of Natural Products 57: 1619-25

Wong, C. T. T., Taichi, M., Nishio, H., Nishiuchi, Y., and Tam, J. P., 2011. Optimal oxidative folding of the novel antimicrobial cyclotide from Hedyotis biflora requires high alcohol concentrations. Biochemistry 50: 7275-7283

Yance, D. and Valentine, A., 1999. Herbal Medicine, Healing and Cancer. Keats Publishing Chicago

Yin, Y., Li, Y. and Mariuzza, R.A., 2012. Structural basis for self-recognition by autoimmune T-cell receptors. Immunological Reviews 250: 32-48

9. Appendices

9.1 Supplementary Data

9.2 Abstract

9.3 Zusammenfassung

9.4 Curriculum vitae

9.1 Supplementary Data:

1.) Isolation and purification of plant cyclotides.

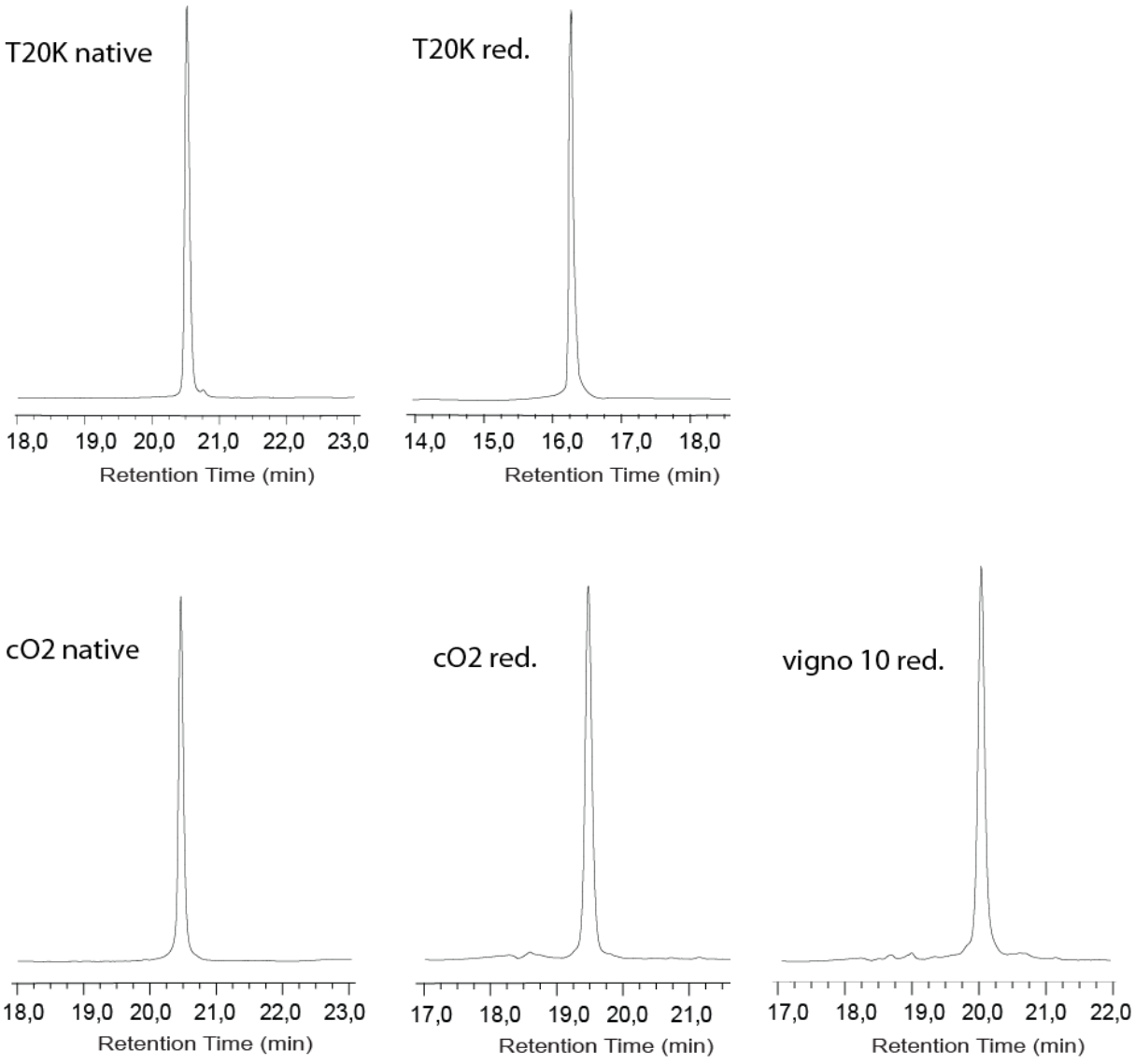

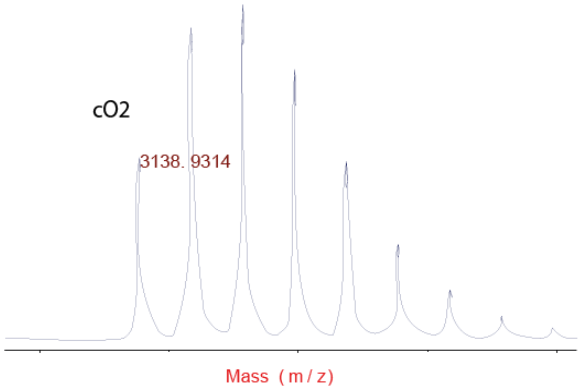
cO2
3138. 9314
Mass (m/z)

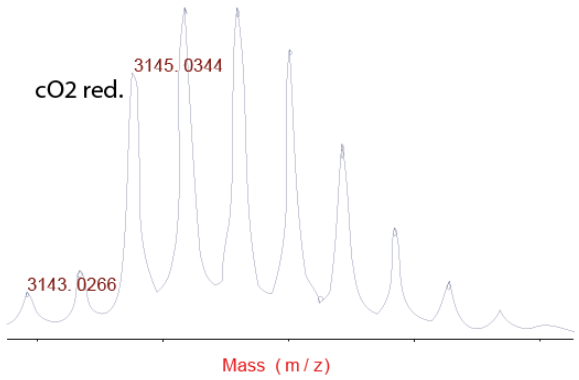
cO2 red.
3145. 0344
3143. 0266
Mass (m/z)

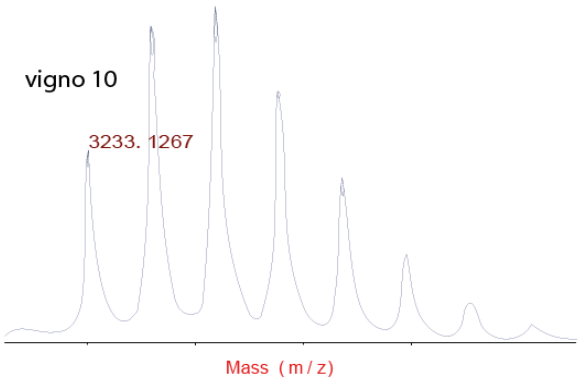
vigno 10
3233. 1267
Mass (m/z)

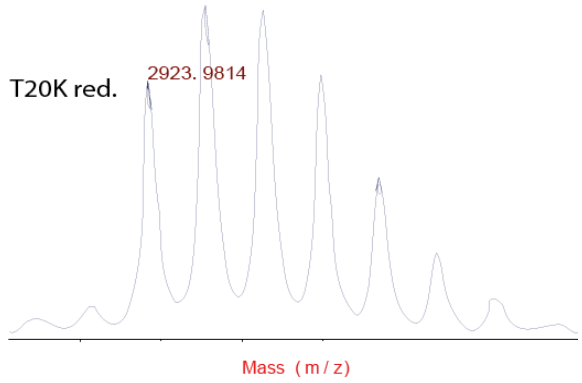
T20K red.
2923. 9814
Mass (m/z)

2.) Oxidative folding of cyclotides

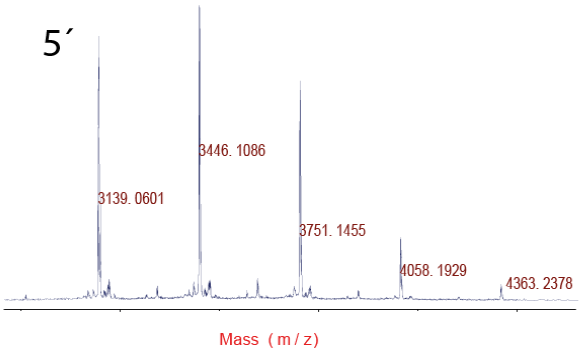

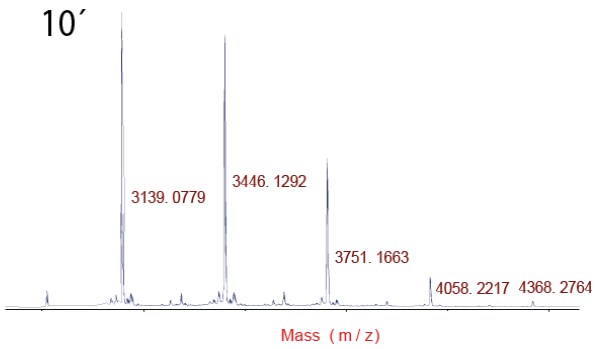

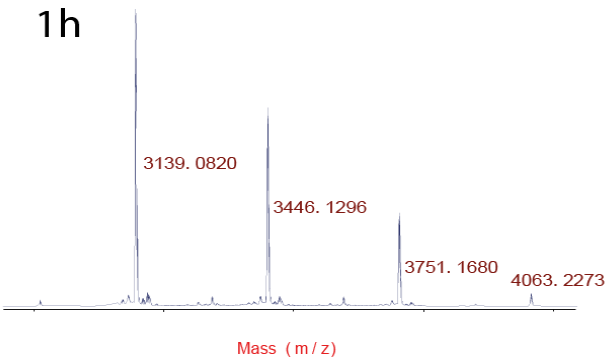

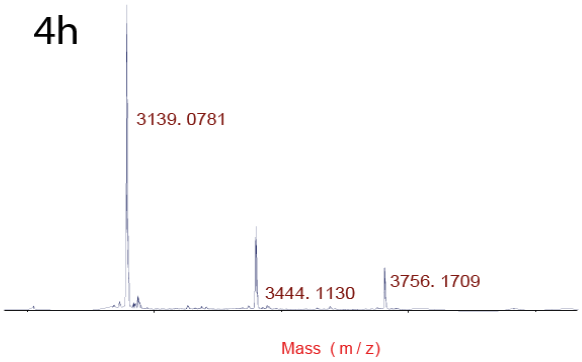

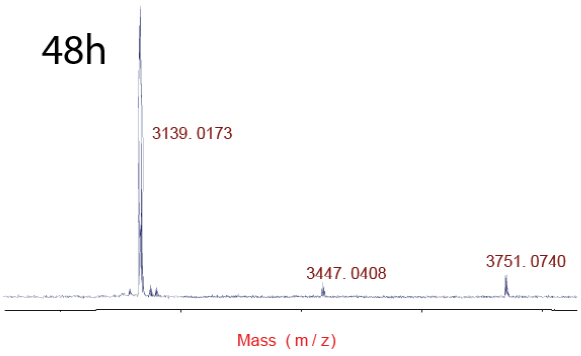

3. Final yields of the folding of cyclotides.

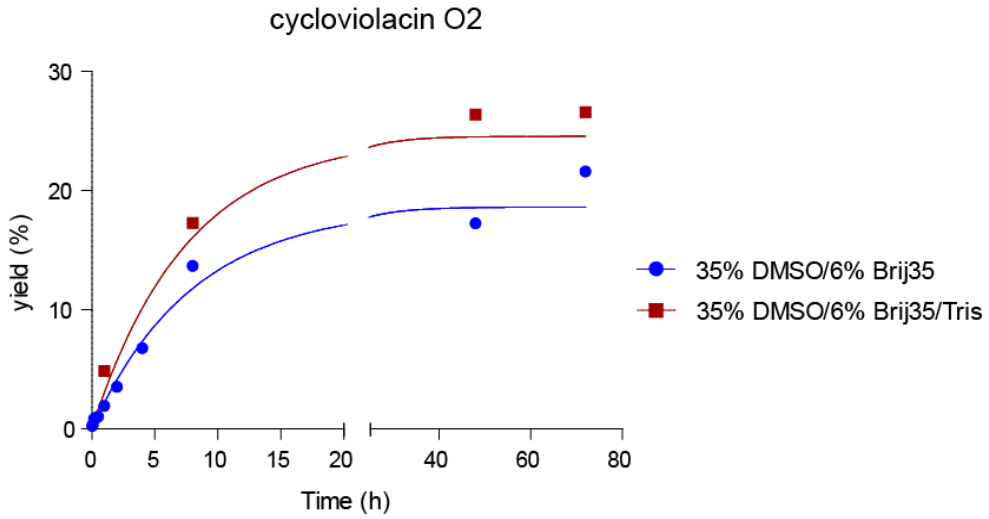

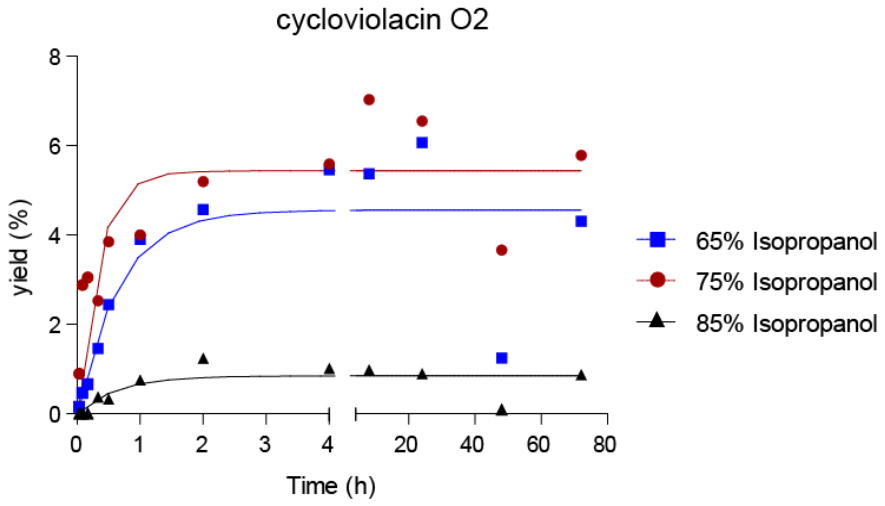

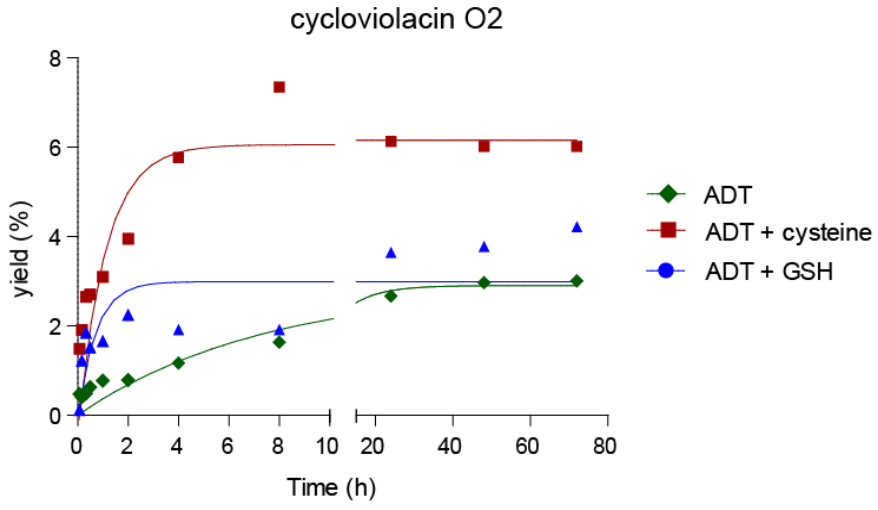

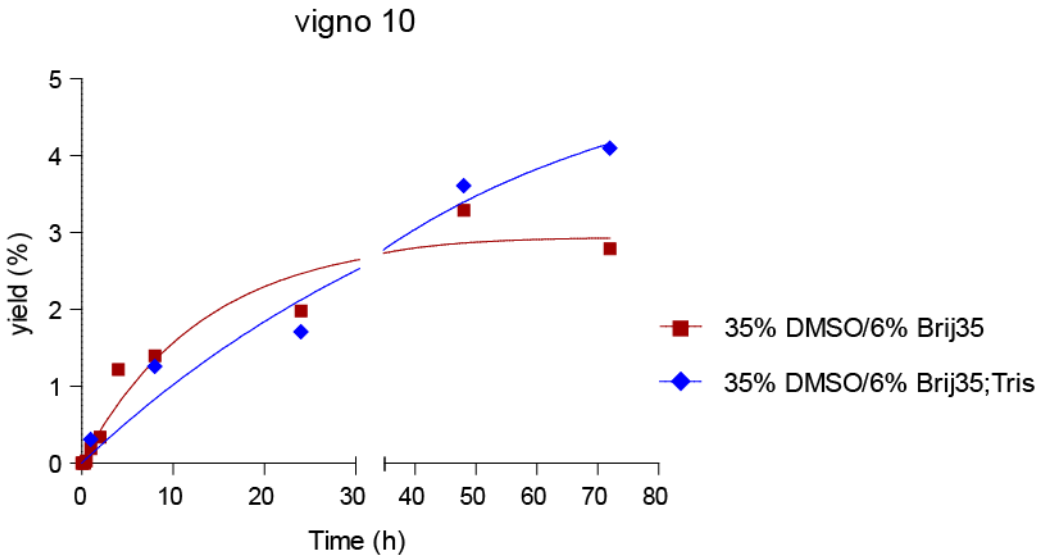
vigno 10
yield (%)
Time (h)
35% DMSO/6% Brij35
35% DMSO/6% Brij35;Tris

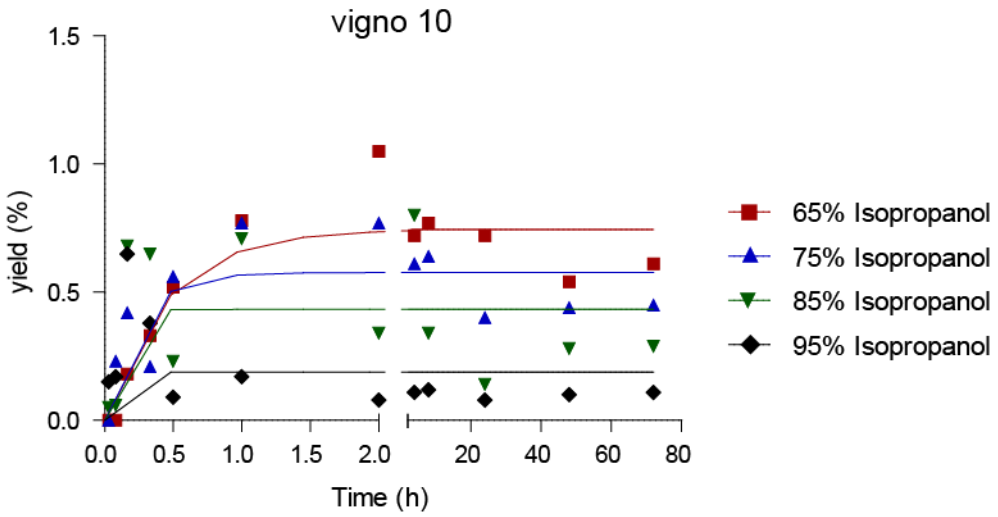
vigno 10
yield (%)
Time (h)
65% Isopropanol
75% Isopropanol
85% Isopropanol
95% Isopropanol

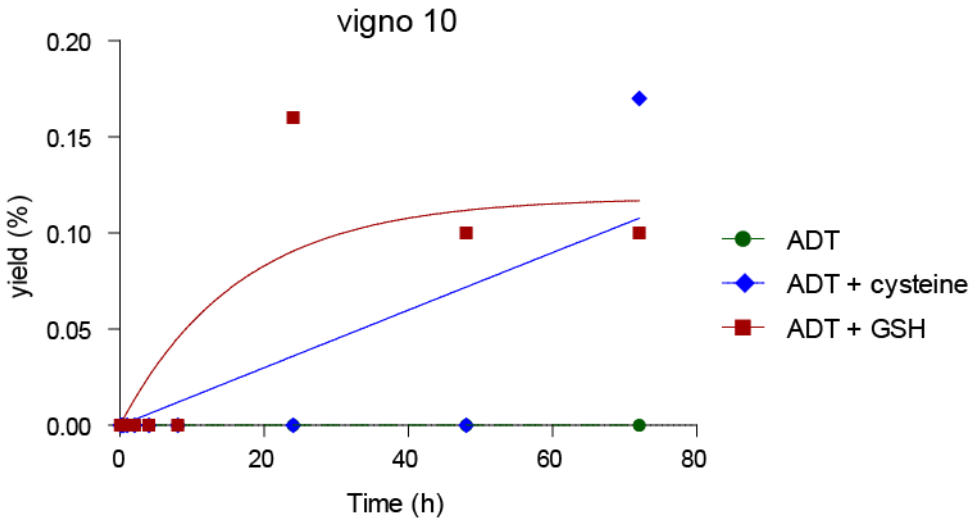
vigno 10
yield (%)
Time (h)
ADT
ADT + cysteine
ADT + GSH

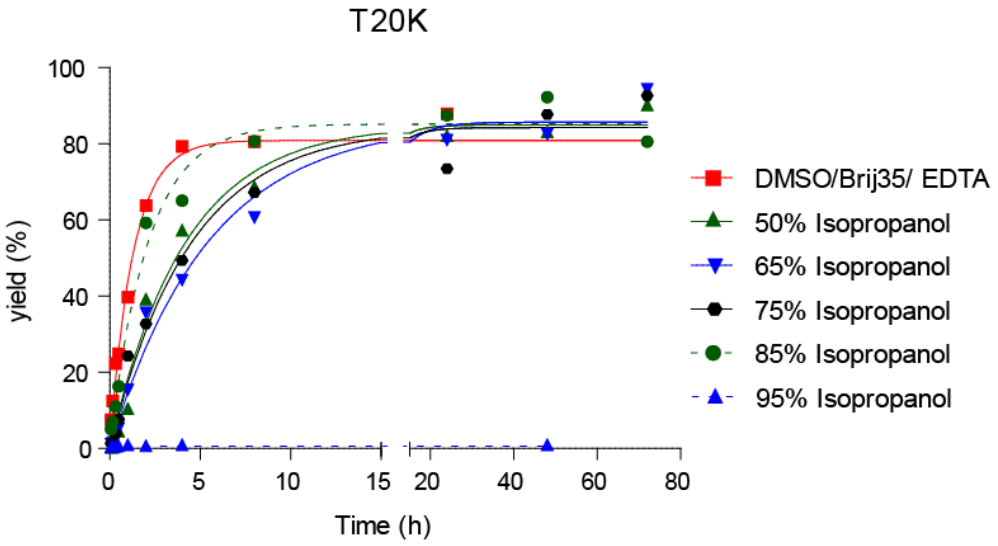

4. Table with disulfide species at certain time points.

cyclotide	condition	reaction time	Observed MW	Disulfid species
cO2	native		3139,14	3SS
	reduced		3145,28	0SS
	35% DMSO/6% Brij 35	2´	3139.10	3SS
		10´	3139.05	3SS
		1h	3138.99	3SS
		2h	3139.00	3SS
		4h	3139.03	3SS
		24h	3138.93	3SS
		48h	3138.96	3SS
		72h	-	-
	65% Isopropanol	2´	3139.07; 3141.08; 3143.08	1SS;2SS;3SS
		10´	3139.04; 3141.05	2SS; 3SS
		1h	3139.01; 3141.06	2SS; 3SS
		2h	3139.01; 3141,03	2SS; 3SS
		4h	3139.02; 3141,03	2SS; 3SS
		24h	3139.02; 3141.02	2SS; 3SS
		48h	3138.99; 3140.99	2SS; 3SS
		72h	3138.96	3SS
	75% Isopropanol	2´	3139.03; 3141.04	2SS; 3SS
		1h	3139.00; 3141.08	2SS; 3SS
		2h	3139.01; 3141.05	2SS; 3SS
		4h	3139.03; 3141.04	2SS; 3SS
		24h	3139.03; 3141.04	2SS; 3SS
		48h	3139.01; 3141.02	2SS; 3SS

		72h	3139.01; 3141.01	2SS; 3SS
	85% Isopropanol	10´	3139.10; 3141.11	2SS; 3SS
		1h	3139.13; 3141.14	2SS; 3SS
		4h	3139.06; 3141,07	2SS; 3SS
		48h	3139.05; 3141.05	2SS; 3SS
		72h	3139.05; 3141.06	2SS; 3SS
	AcN/TFE/DMSO/1M Gu*HCl	10´	3139.11; 3141.12	2SS; 3SS
		1h	3139.08; 3141.09	2SS; 3SS
		2h	3139.04; 3141.05	2SS; 3SS
		4h	3139.01; 3141.01	2SS; 3SS
		24h	3139.00	3SS
		48h	3139.21	3SS
		72h	3138.95	3SS
		7d	3139.16	3SS
	AcN/TFE/DMSO/1M Gu*HCl	5´	3139.06; 3141.07	2SS; 3SS
	GSH/GSSG	10´	3139.07; 3141.09	2SS; 3SS
		1h	3139.08	3SS
		2h	3139.11	3SS
		4h	3139.08	3SS
		24h	3139.05	3SS
		48h	3139.01	3SS
		72h	3139.04	3SS
		7d	3139.07	3SS
	AcN/TFE/DMSO/1M Gu*HCl	5´	3139.05	3SS
	Cystein/Cystin	10´	3139.06	3SS
		1h	3139.06	3SS
		2h	3139.08	3SS
		4h	3139.05	3SS
		24h	3139.09	3SS
		48h	3139.04	3SS
		72h	3138.99	3SS
		7d	3138.96	3SS
vigno 10	native		3227.10	3SS
	reduced		3233.13	0SS
	35% DMSO/6% Brij 35	2´	-	-
		10´	-	-
		1h	-	-
		8h	-	-
		24h	3226.87	3SS
		48h	-	-

	72h	3226.82	3SS
65% Isopropanol	2´	3228.98; 3230.98	1SS; 2SS
	10´	3226.98; 3228.97	2SS; 3SS
	1h	3226.97; 3228.98	2SS; 3SS
	2h	3226.95; 3228.97	2SS; 3SS
	4h	3226.98; 3228.97	2SS; 3SS
	24h	3226.97; 3228.98	2SS; 3SS
	48h	3226.97; 3228.98	2SS; 3SS
	72h	3226.96; 3228,97	2SS; 3SS
75% Isopropanol	2´	3227.27; 3229,28	2SS; 3SS
	10´	3227.19; 3229.19	2SS; 3SS
	1h	3227.18; 3229.18	2SS; 3SS
	2h	3227.16; 3229.17	2SS; 3SS
	4h	3227.18; 3229.18	2SS; 3SS
	24h	3227.12; 3229.13	2SS; 3SS
	48h	3227.10; 3229.11	2SS; 3SS
	72h	3227.05; 3229.06	2SS; 3SS
85% Isopropanol	10´	3229.08;	2SS
	1h	3227.08; 3229.09	2SS; 3SS
	24h	3227.05; 3229.06	2SS; 3SS
	48h	3227.08; 3229.09	2SS; 3SS
	72h	3227.09; 3229.11	2SS; 3SS
95% Isopropanol	48h	3227.04; 3229.05	2SS; 3SS
	72h	3227.04; 3229.04	2SS; 3SS
AcN/TFE/DMSO/1M Gu*HCl	5´	3227.54; 3229.55	2SS; 3SS
	10´	3227.43; 3229.44	2SS; 3SS
	1h	3227.39; 3229.40	2SS; 3SS
	2h	3227.34; 3229.35	2SS; 3SS
	4h	3227.30; 3229.31	2SS; 3SS
	24h	3227.22; 3229.20	2SS; 3SS
	48h	3227.20; 3227.13	2SS; 3SS
	72h	3227.14;	3SS
	7d	3227.12	3SS
AcN/TFE/DMSO/1M Gu*HCl GSH/GSSG	5´	3227.12; 3229.12	2SS; 3SS
	10´	3227.12; 3229.12	2SS; 3SS
	1h	3227.11; 3229.12	2SS; 3SS
	2h	3227.13; 3229.14	2SS; 3SS
	4h	3227.11; 3229.09	2SS; 3SS
	24h	3227.09	3SS
	48h	3227.08	3SS
	72h	3227.10	3SS
	7d	3227.07	3SS

	AcN/TFE/DMSO/1M Gu*HCl	5´	3227.05	-
	Cystein/Cystin	10´	3227.01	3SS
		1h	3227.11	3SS
		2h	3227.11	3SS
		4h	3227.12	3SS
		24h	3227.12	3SS
		48h	3227.13	3SS
		72h	3227.11	3SS
		7d	3227.09	3SS
T20K	native		2917.25	3SS
	reduced		2923.98	0SS
	35% DMSO/6% Brij 35/1mM EDTA	5´	-	-
		10´	-	-
		1h	-	-
		2h	2917.93	3SS
		4h	-	-
		24h	2917.89	3SS
		48h	2917.89	3SS
		72h	-	-
	50% Isopropanol	5´	2919.90; 2921.90	1SS; 2SS
		10´	2919.89; 2921.89	1SS; 2SS
		1h	2917.87; 2919.88	2SS; 3SS
		2h	2917.86; 2919.86	2SS; 3SS
		4h	2917.86	3SS
		24h	2917.85	3SS
		48h	2917,85	3SS
		72h	2917.84	3SS
	65% Isopropanol	2´	2917.84; 2919.85; 2922.03	1SS; 2SS; 3SS
		10´	2917.85; 2919.85	2SS; 3SS
		1h	2917.83; 2919;84	2SS; 3SS
		2h	2917.83; 2919.83	2SS; 3SS
		4h	2917.81; 2919.81	2SS; 3SS
		24h	2917.84	3SS
		48h	2917.81	3SS
		72h	2917.80	3SS
	75% Isopropanol	2´	2917.84; 2919.84; 2921.95	1SS; 2SS; 3SS
		10´	2917.81; 2919.82	2SS; 3SS
		1h	2917.80; 2919.81	2SS; 3SS
		2h	2917.80; 2919.80	2SS; 3SS
		4h	2917.79	3SS

	24h	2917.79	3SS
	48h	2917.80	3SS
	72h	2917.83	3SS
85% Isopropanol	2´	2917.80; 2919.81	2SS; 3SS
	10´	2917.82; 2919.83	2SS; 3SS
	1h	-	-
	2h	2917.80; 2919.80	2SS; 3SS
	4h	2917.82; 2919.83	2SS; 3SS
	24h	2917.82	3SS
	48h	2917.82	3SS
	72h	2917.81	3SS
95% Isopropanol	2´	2917.86; 2919.85; 2921.86	1SS; 2SS; 3SS
	10´	2919.81; 2921.82	1SS; 2SS
	1h	2919.81; 2921.82	1SS; 2SS
	2h	2919.82; 2921.82	1SS; 2SS
	4h	2919.81; 2921.82	1SS; 2SS
	24h	2917.83; 2919.83; 2921.83	1SS; 2SS; 3SS
	48h	2917.83; 2919.82; 2921.82	1SS; 2SS; 3SS
	72h	2917.81; 2919.82; 2921.81	1SS; 2SS; 3SS

9.2 Abstract

Cyclotides are an abundant class of plant peptides containing a head – to –tail cyclic backbone and three highly conserved disulfide bonds, together known as cyclic cystine-knot (CCK) motif. The CCK motif confers them with remarkable stability. Compared to linear peptides they are stable against high temperatures and proteolytic degradation resulting in good bioavailability. The typically comprise about 28-31 amino acids in size, which leads to a typical mass range of 2500-4000 Da. Furthermore they are rather hydrophobic which results in the typically late elution from a RP-HPLC column. Mainly two subfamilies of cyclotides have been described in the literature so far, Möbius and bracelet – type peptides. Almost 2/3 of the known cyclotides belongs to the subfamily of the bracelets cyclotides.

The discovery of cyclotides based on the ethno botanical investigations of Lorents Gran on the plant *Oldenlandia affinis* 40 years ago. This plant was used from indigenous woman to induce labor. As active compound, kalata B1 was identified, hence it was the first and so far the best analysed cyclotide. So far, 36 species in the Violaceae, Rubiaceae, Apocynaceae, Cucurbitaceae and Fabaceae have been discovered. For several cyclotides different bioactivities are reported such as, anti-HIV, antitumor, insecticidal, antimicrobial, haemolytic and immunosuppressive.

Since the availability of the cyclotides is limited and dependent the extraction from native plant material, the development of efficient strategies for chemical synthesis and oxidative folding of cyclotides will be very crucial. Whereas the folding of Möbius cyclotides is far advanced, it is possible to achieve yields >90%, the folding of bracelet cyclotides remains still difficult and complex. The aim of this study was to optimize the folding conditions for the bracelet cyclotides cycloviolacin O2 and vigno 10 as well as the Möbius cyclotide kalata B1 mutant [T20K]kalata B1. Although different folding conditions were tried, it was not possible to fold cO2 and vigno10 with a satisfying yield. The highest yield which was achieved for cO2 was ~27% native peptide and for vigno 10 ~4%. The Möbius cyclotide [T20K]kalata B1 was successfully folded with a yield of 95%.

In a previous study it was shown that the kalata B1 mutant [T20K]kalata B1 has an immunosuppressive effect, but the exactly mechanism remain unclear. (Gründemann et al., 2013) Another study figured out that an structural related peptide which shows also an immunosuppressive effect, blocks the voltage gated potassium channel Kv1.3 which plays a crucial role in the activation and hence the proliferation of T cells. The second aim of this

study was to determine if the cyclotide [T20K]kalata B1 can block the potassium channel Kv1.3. Unfortunately, several measurements showed that [T20K]kalata B1 doesn´t interact with the Kv1.3 channel. Furthermore it was shown that 4µM [T20K]kalata B1 is cell toxic and leads to a slowly disruption of the cell membrane.

9.3 Zusammenfassung

Cyclotide sind cyclische Pflanzenpeptide welche im Pflanzenreich sehr weit verbreitet sind. Sie besitzen eine charakteristische 3D Struktur welche durch drei hoch konservierte disulfid Brücken hervorgerufen wird. Diese drei disulfid Brücken werden auch „cyclic cystine – knot (CCK)“ genannt und verleihen den Cyclotiden besondere Stabilität. Im Vergleich zu linearen Peptiden sind Sie zum Beispiel stabil gegen hohe Temperaturen und proteolytischen Verdau welche in einer guten oralen Bioverfügbarkeit resultieren. Typischer weise bestehen Sie aus 28 – 31 Aminosäuren und haben ein Molekulargewicht zwischen 2500 – 4000 Da. Weiters sind Sie eher hydrophob wodurch sie an einer RP-HPLC Säule relativ spät eluieren. Grundsätzlich unterscheidet man Cyclotide in 2 Untergruppen, Bracelets Cyclotide und Möbius Cyclotide. Rund 2/3 der bekannten Cyclotide gehören zur Untergruppe der Bracelets.

Entdeckt wurden Cyclotide vor ca. 40 Jahren durch ethnobotanische Untersuchungen an der Pflanze Oldenlandia affinis, welche im Kongo von Eingeborenen benutzt wurde um Wehen einzuleiten. Als Wirkstoff in dieser Pflanze wurde das cyclische Peptid kalata B1 identifiziert, welches das Erste und bis heute am Meisten untersuchte Cyclotid ist. Bis jetzt wurden Cyclotide in 36 Spezies in den Violaceae, Rubiaceae, Apocynaceae, Cucurbitaceae und Fabaceae entdeckt. Viele dieser Peptide zeichnen sich durch ihre Bioaktivität aus, wie z.B.: anti-HIV, anticancer, insektizid, antimikrobiell, haemolytisch und immunsuppressive.

Die Gewinnung dieser Peptide ist bis jetzt durch die Zeit und arbeitsintensive Isolierung und Aufreinigung aus den entsprechenden Pflanzen limitiert. Obwohl es auch möglich ist, Cyclotide chemisch zu synthetisieren, ist diese Synthese durch die anschließende Faltung in die native Struktur limitiert. Während die oxidative Faltung von Möbius Cyclotiden schon sehr fortgeschritten ist und man eine sehr hohe Ausbeute (>90%) an nativem Peptide erreicht, ist die Faltung von Bracelet Cyclotiden sehr komplex und schwierig. Ziel dieser Arbeit war es die Faltungsbedingungen für die beiden Bracelet Cyclotide cycloviolacin O2 und vigno 10 sowie für das Möbius Cyclotide kalata B1 Mutante [T20K]kalata B1 zu optimieren. Obwohl verschiedene Faltungsbedingungen analysiert wurden, ist es nicht gelungen cO2 und vigno 10 mit zufriedenstellenden Ausbeuten zu falten. Die höchste erzielte Ausbeute für cO2 betrug ~27% natives Peptide und für vigno 10 ~4%. Das Möbius Cyclotide [T20K]kalata B1 konnte allerdings mit einer Ausbeute von 95% erfolgreich gefalten werden.

Die kalata B1 Mutante [T20K]kalata B1 zeigte in vorangegangenen Studien eine immunsuppressive Wirkung, der genaue Mechanismus der dieser Wirkung zu Grunde liegt ist

bis heute unbekannt (Gründemann et al., 2013). Eine weitere Studie fand heraus, dass ein strukturell ähnliches Peptid, welches auch eine immunsuppressive Wirkung aufweist, den Spannungs-regulierten Kaliumkanal Kv1.3 blockiert (Gurrola et al., 2012). Dieser spielt eine wichtige Rolle in der Aktivierung und dadurch der Proliferation von T – Lymphozyten. Ein weiteres Ziel dieser Arbeit war es daher zu untersuchen ob das immunsuppressive Cyclotide [T20K]kalata B1 den Kaliumkanal Kv1.3 inhibieren kann und dadurch die Proliferation der T – Lymphozyten inhibiert. Mehrere Messungen haben aber leider ergeben, dass dieses Peptid nicht mit dem Kv1.3 interagiert. Viel mehr hat sich gezeigt, dass es ab einer Konzentration von 4µM zelltoxisch wirkt und zu einer langsamen Auflösung der Zellmembran führt.

9.4 Curriculum vitae

Martin Auer

Schulgasse 35/2/10

1180 Wien

Tel.: +43 (0) 6603404553

Email: martin.auer3@gmx.at

Education and Training:

Since 10/2011: Master study in biological chemistry at the University of Vienna

09/2012 – 12/2012: Erasmus internship at King´s College London, Institute of Pharmaceutical Science

09/2008 – 07/2011: Bachelor study in molecular biotechnology at the University of Applied Science FH Campus Wien

2002 – 2007: HTL (Höhere Technische Lehranstalt) for food technology

Work Experience:

Since 01/2013: Master thesis in the Group of Dr. Gruber at the Institute of Pharmacology at the Medical University of Vienna.

Since 05/2011: marginal employee at Life Science Karriere Service

01/2011 – 05/2011: Bachelor Thesis at the AGES - Austrian Agency for Health and Food safety. Topic: Method comparison of RT-PCR with Primers and HRM on the example of the investigation of the variability of genetically modified canola and adh1-alleles.